NEUTRON MODERATION IN SUPERCRITICAL WATER - THEORY AND EXPERIMENTAL DESIGN

A Thesis submitted to the
University of London for the Degree of
Doctor of Philosophy in the
Faculty of Science

by

Peter Rainey, B.Sc.

Nuclear Power Section
Mechanical Engineering Department
Imperial College of Science and Technology

September 1969

ABSTRACT

The experimental design of a project to investigate the temperature dependence of the thermal neutron parameters in water into the supercritical region has been carried out based on the pulsed neutron method. The decay of the neutron flux in a volume of the material under study is measured and from the decay rate the neutron parameters can be inferred.

A method has been developed for the direct comparison of the experimental data with theoretical predictions using the minimum of assumptions. This is based on the Discrete Ordinate Method of solution for use on computors and does not use the Buckling concept and the assumptions it implies which have normally been used in analyses.

The equipment to carry out the experiments was designed and manufactured and the main parameters are given in Appendix 1. The basic design limits were 450°C (842°F) and 3500psia and employed a vessel of internal dimensions of 3 ft. diameter and 3 ft. high and had a weight of 6½ tons.

Acknowledgments

The author wishes to thank his supervisor, Professor P.J. Grant, for his guidance, encouragement and help throughout the project. He would also like to thank all the staff of the Nuclear Power Section for their guidance, especially Dr. A.J.H. Goddard for his help and fruitful discussions. He is indebted to Mr. G. Slater and the Section technical staff and the Mechanical Engineering workshop personnel for their help in many ways. The author would also like to thank the Science Research Council, Imperial College and Rolls-Royce and Associates for support during the project. Finally but not least, Miss L. Pitt for having typed the thesis.

CONTENTS

TITLE		1
ABSTRACT		2
ACKNOWLEDGEMENTS		3
CONTENTS		4
NOTATION		6
CHAPTER 1	INTRODUCTION	7
CHAPTER 2	BASIC SPECIFICATION	20
2.1	Project Specification	20
2.2	Choice of Experimental Method	24
2.3	Basic Theory of the Pulsed Neutron Method	28
2.4	Limitations due to Experimental Method	32
PART I	THEORETICAL CALCULATIONS	39
CHAPTER 3	NEUTRON SCATTERING THEORY	46
3.1	General Neutron Scattering Theory	47
3.2	Scattering Models	50
3.3	Scattering Law and Diffusion Length Calculations	56
3.4	Cross Section Compilations	62
CHAPTER 4	DECAY CALCULATIONS	65
4.1	Derivations of the Difference Equations	68
4.2	Method of Solution	77
4.3	Decay Programme Trand	85
4.4	Theoretical Results	90

PART II EXPERIMENTAL DESIGN

CHAPTER 5	EXPERIMENTAL DESIGN	99
5.1	Basic Vessel Design	102
5.2	Vessel Safety Limitations and Requirements	108
5.3	Stud and Seal Design	117
5.4	Pressure Circuit	126
5.5	Vessel Support and Movement	130
5.6	Dump Tank Design	136
CHAPTER 6	HEATING AND COOLING	141
6.1	Internal Heaters	142
6.2	External Heaters	144
6.3	Insulation	152
6.4	Heater Control	153
6.5	Cooling	161
CHAPTER 7	NUCLEAR EQUIPMENT AND DESIGN	167
7.1	Neutron Source	168
7.2	Thermal Neutron Cylinders	176
7.3	Counting Equipment	188
CHAPTER 8	EXPERIMENTS	198
8.1	VESSEL WALL EFFECT	198
8.2	PULSE PICKUP TESTING	200
8.3	DECAY EXPERIMENTS	203
CHAPTER 9	CONCLUSIONS AND RECOMMENDATIONS	219
REFERENCES		220
APPENDIX 1	MAIN VESSEL PARAMETERS	222
DRG.1	Pressure Vessel General Assembly	Back Pocket

Notation

Standard notation has been used as far as possible throughout the thesis. The neutron physics notation is based on that given in Grant (1966). The units used have been those in common usage for the particular field. This has meant that British units have been used in the mechanical design and reactor units in the theoretical section.

To avoid possible confusion between the macroscopic cross sections and the summation sign the following convention has been used

Σ macroscopic cross sections

$\sum_{g}$ or $\sum_{g' \neq g}$ summation where the first is the summation over g and the second over g' except for g' = g.

1. INTRODUCTION

The project was set up to construct and carry out experiments extending previous work by Besant and Grant (1966) done at Imperial College on the effect of temperature on the nuclear parameters of water. The results obtained were to be compared with theoretically calculated parameters enabling a check on the suitability of the theoretical models and the methods of analysis employed especially at the higher conditions. This thesis was concerned with the design and installation of the equipment for carrying out the experiments and the development of methods for the theoretical calculations over the range of conditions to be covered.

The accuracy of theoretical reactor calculations and the confidence that can be put in the results is limited not solely by the accuracy of the analysis but also the accuracy of the data used in the calculations. The models used to represent water are based on room temperature measurements and the accuracy of the high temperature data is very much in doubt. This is important for calculations on reactors using water for cooling especially if steam is formed in which the change of state would be expected to complicate the issue. Some of the previous results on the diffusion length of water at varying temperatures are shown in Fig. 1.1 and comprehensive reviews have been carried out by Cokinos (1968) and Beckhurts (1965). While the results are in reasonable

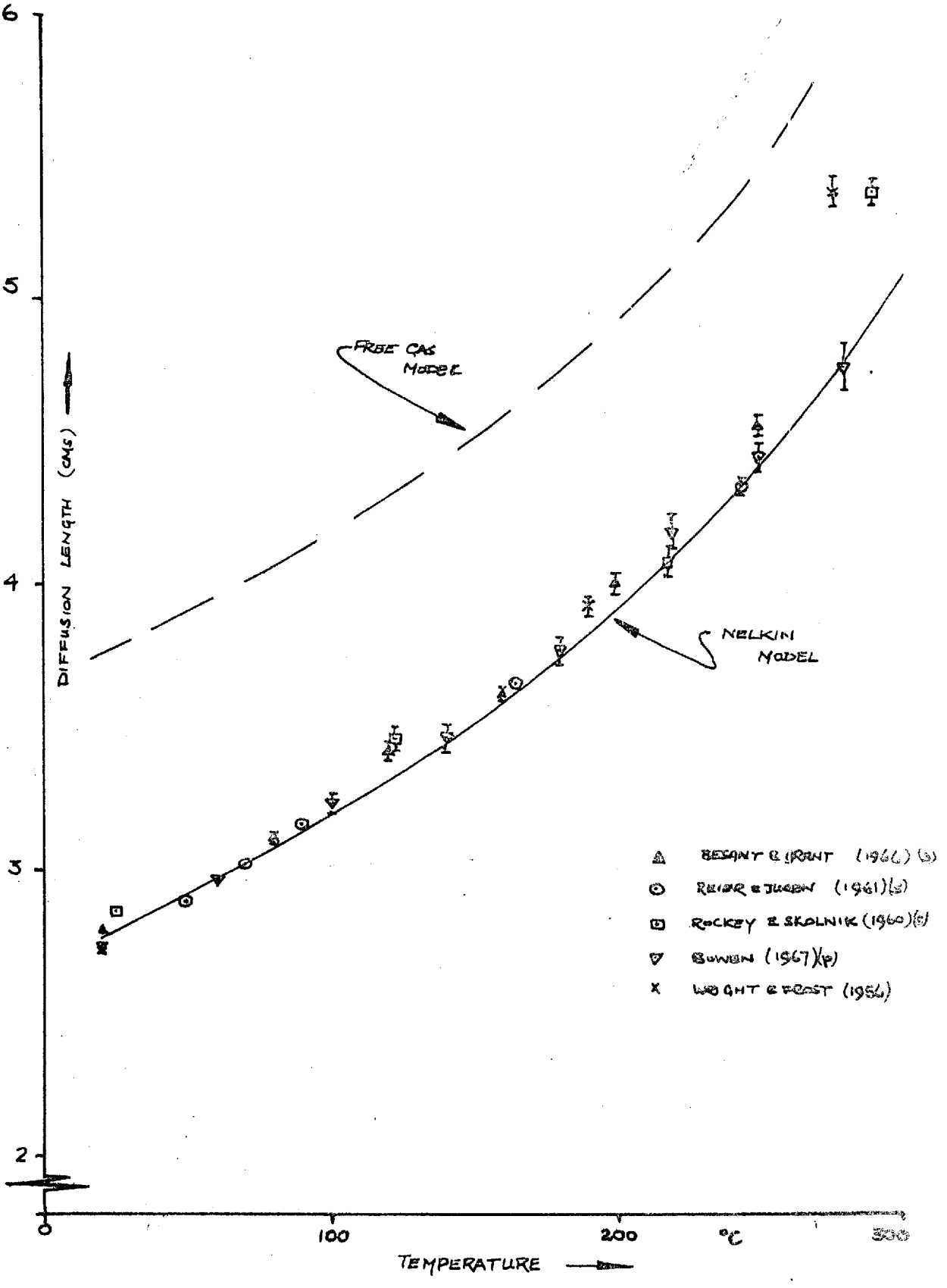

FIG 1.1 TEMPERATURE VARIATION OF THE NEUTRON DIFFUSION LENGTH IN WATER.

agreement up to 240°C above this very little can be inferred due to the large scatter on the small amount of data available. The clarification of the data about 300°C being an early experimental requirement. The theoretical curves are for two theoretical predictions, one being based on the Free Gas Model which makes no allowance for the molecules chemical binding and the Nelkin model which makes simple allowance for the binding effects.

The density changes covered have been limited to 30% but the extension of the experiments to supercritical conditions (374°C, 3206 psia) would enable far greater density changes to be covered as well as involving a change of state. This should enable the importance of the hindered rotations in the liquid state on the nuclear parameters to be studied. From the temperature/density relationships little can be gained by increasing the temperature above 450°C which would cover the widest possible density range.

To obtain this temperature without having two phase conditions in the vessel the design pressure had to be sufficiently above the critical pressure but an excessive margin could increase the vessel thickness, cost and complexity and a working pressure of 3500 psia was chosen being 10% above the critical pressure.

The experimental method chosen for the project was the pulsed neutron method in which a burst of fast

neutrons are injected into the volume under study and the decay of thermal neutron flux produced by leakage and absorption is measured. The decay rate is usually analysed using the normal notation by

$$\lambda = \nu\Sigma_a + D_o B^2 - CB^4 \qquad 1.1$$

This method had some practical advantages over the steady state method which could have been used for the investigation. The main was the need in the steady state method of a high temperature-pressure moving seal. The pulsed neutron method implies the use of varying volumes of water, through the geometric buckling term, and a single cylinder was considered too limited to cover the changes over the temperature range. It was decided to use a large pressure vessel with non-pressure vessels, defining the required volumes of water, suspended inside it.

A policy decision was taken to obtain a cylindrical pressure vessel of 3 ft. diameter and 3 ft. high internally. This enabled not only a wide range of possible moderator experiments but also the extension of the projects to cover sub-critical experiments which would spread the capital cost of the facility over several projects. A smaller vessel suitable only for the pulsed neutron experiments could have been obtained but this would only have been useful for the one project.

The thesis has been split into two parts, the first considering the theoretical aspects of neutron moderation at high temperatures with special reference to the pulsed neutron method used in the experimental investigations. The usual analysis is carried out using equation 1.1 using the buckling concept. This is based on the actual physical dimensions of the volume under study and an extrapolation distance dependent on the material in the volume. This concept introduces assumptions which are not valid over all the volume and the errors introduced into the analysis would be more important at the high temperature conditions because of the lower density and lack of any experimental data for checking. An analysis which did not use this concept has been developed to allow the direct comparison with the experimental results as well as a check on the errors of the Buckling assumptions. This would be necessary if worthwhile conclusions on the models used to represent the nuclear properties of the water were to be made.

The use of an analysis dependent on the actual physical dimensions of the volume and not including the extrapolation distance implies the direct solution of the Boltzman Transport Equation. This was carried out using a much modified form of the Discrete Ordinate Method (DSN) of solution as commonly used in reactor cell calculations., This method has not been used

previously for the analysis of the experiments mainly due to the large differences in the control of the calculation required and the increased importance of an accurate analysis for this project. The method is used on a large fast computor and the variables of the neutron flux, such as energy, space and direction are split into regions and averaged values used in these regions and a repetitive solution of the derived differences equation carried out. If sufficient regions have been used then the averaged values would approximate to the continuous functions.

The theoretical calculations were based on cross sections derived from proposed models used to describe the interactions of neutrons with the atoms in the water molecule. There are models of varying complexity and refinement and the comparison of the experiment results with the predicted values should enable a reasonable assessment of the usefulness of the various models over the large density range. In particular the importance of the hindered rotations on the scattering process would be of interest, as by neglecting them a better representation of the steam condition should be obtained.

The calculation of the cross sections from the models used to describe the water molecule and the theoretical decay calculations using the cross sections are described in the first part of the thesis and are

split into two chapters as this represents the calculational procedure.

The second part of the thesis was concerned with the design and manufacture of the equipment to carry out the experiments required. This was mainly concerned with the engineering limitations on the design imposed by the operating conditions which were more important generally than the experimental limitations. There were some novel problems which had to be solved that were not met in previous experiments, the major one being the material for the thermal neutron cylinders in the pressure vessel. The link between this part and the theoretical calculations was not carried out due to lack of time to carry out the experiments and in the analysis and comparisons of the theoretical and these experimental results. This would require at least two years before reasonable conclusions could be reached and would form the basis for another thesis.

The vessel manufacturer's, Babcock and Wilcox Ltd., general assembly drawing is enclosed at the back of the thesis and the main parameters of the equipment are given in Appendix 1 and the values will not in general be repeated in the introduction. The vessel was made of a low alloy steel and clad on the inside with Stainless Steel weld deposited for reasons of cost as a vessel made of Stainless Steel would have been very much more expensive. A full width opening was provided with a flat cover using an integral flanged joint and a metal O ring.

SECTION AA

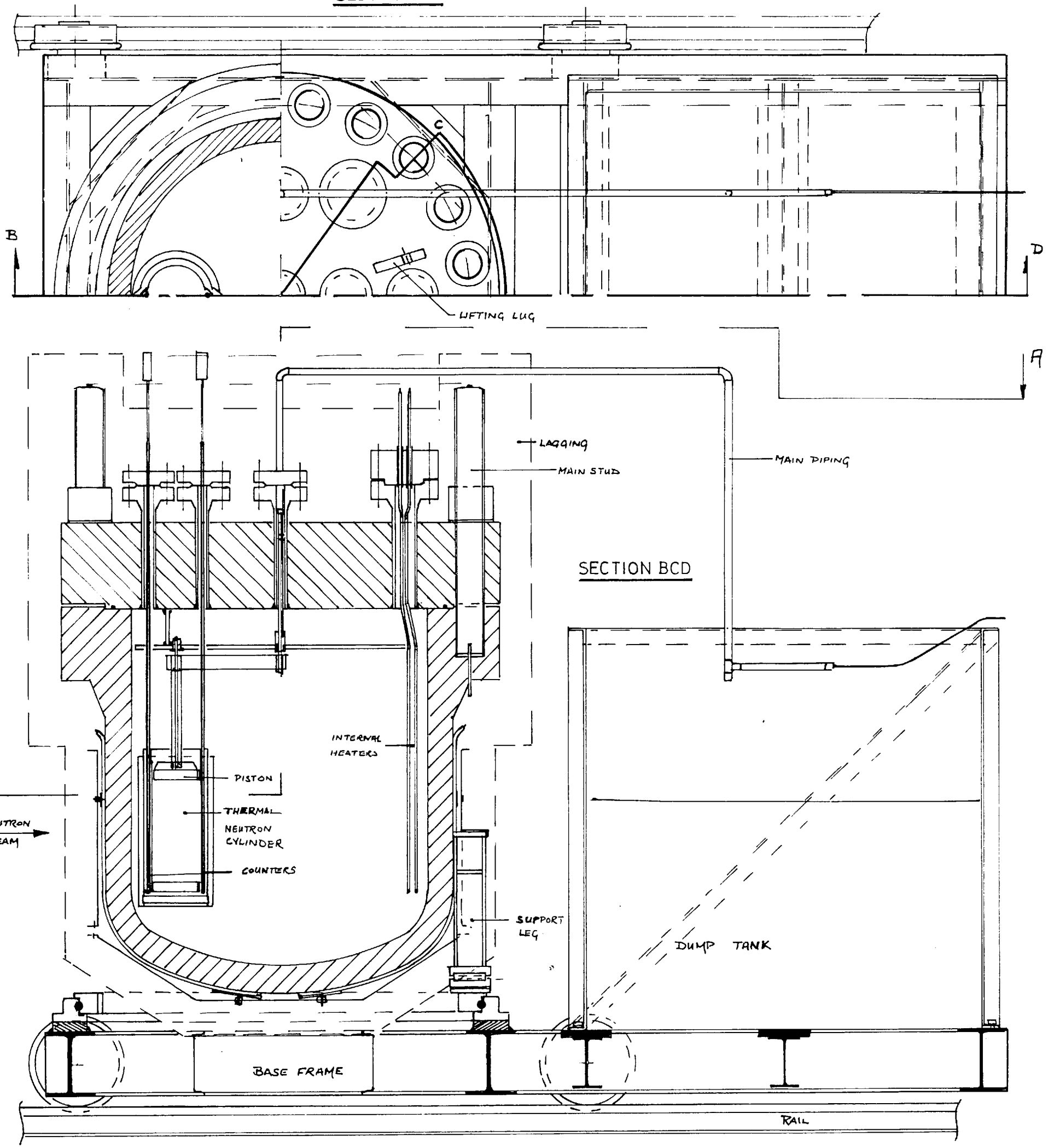

FIG 1.2 PRESSURE VESSEL ARRANGEMENT (CUTAWAY)

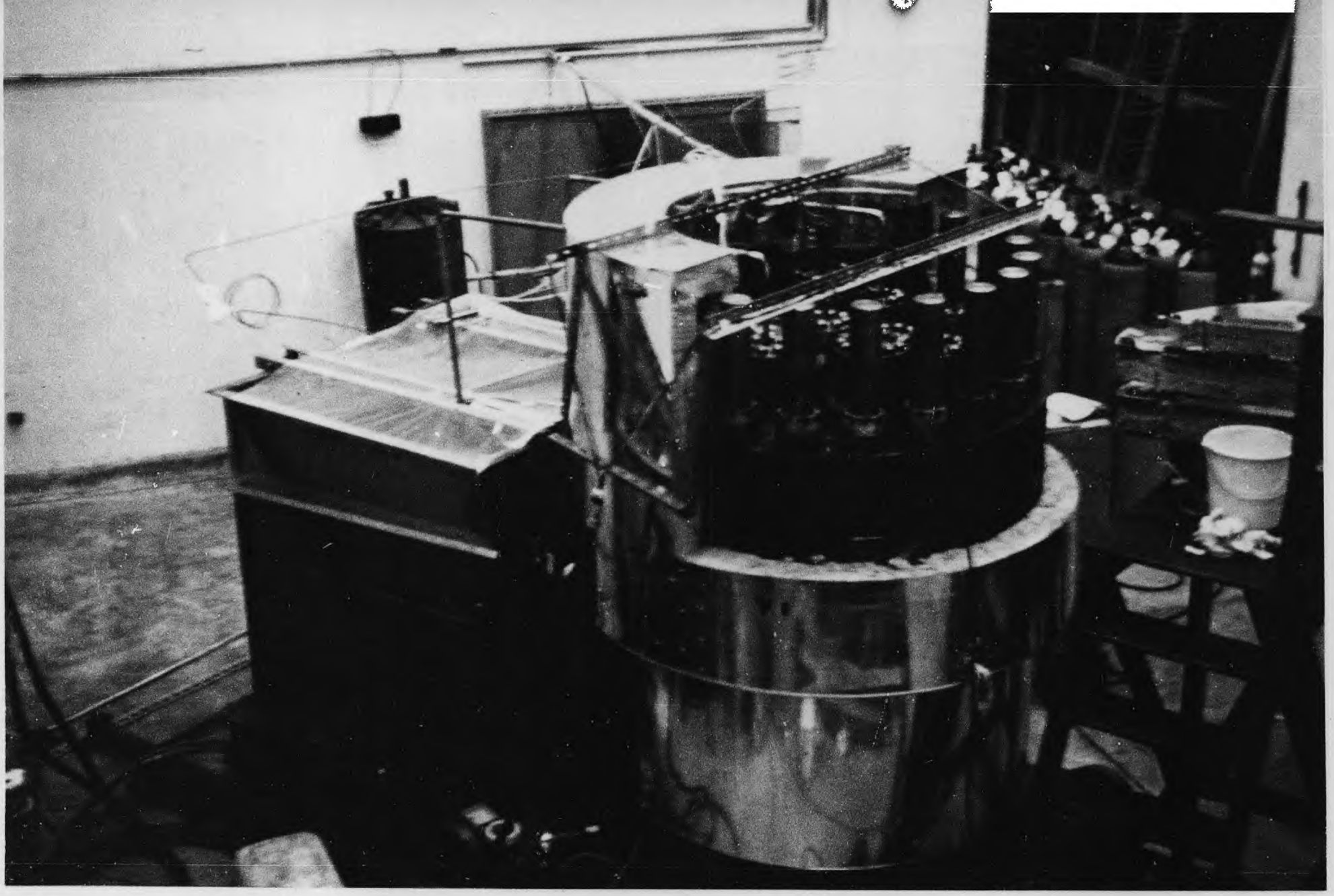

FIG 1.3 PRESSURE VESSEL LAYOUT

Fig. 1.2 is a diagrammatic cutaway of the vessel and its immediate surroundings and Fig. 1.3 shows the actual vessel arrangement with some of the lagging removed from the head. The design of the vessel and its equipment are fully described in the thesis in which the various factors on the design such as safety, weight and operating conditions are discussed and only a brief outline of some of the major limits and the more interesting problems will be given here.

The main problems were concerned with the reliability and safety of the equipment at the high temperature and pressure conditions always being restricted by cost and manufacturing considerations. To obtain a leak-tight seal on the main flange a hollow silver plated O ring was used. This was used as it had good sealing properties and required a very low seating force reducing the closure forces and the main studs size. Even so these main studs, $3\frac{1}{2}$" diameter, were beyond the limit where torque wrenches can be used, and a method using "Pilgrim Nuts" was used for stud tensioning in which hydrostatic force was used to stretch a stud to obtain the prestressing required. Problems with the Nuts considerably delayed the delivery of the vessel but after they had been developed they functioned simply and accurately. Access to the interior of the vessel was obtained by various 1" bore nozzles passing through the head closed by bolted flanges. which had the various piping connections for the control

and safety valves. These positions were arranged for the counters used to measure the rates of neutron decay in the cylinders in the vessel. The counters were placed in re-entrant tubes welded into two of the flanges and could be arranged to suit the experimental arrangement.

The vessel was supported by three legs welded to the body and to reduce any loadings due to the thermal expansion of vessel linear bearings were used under each leg. To reduce the heat losses and as the linear bearings temperature rating was limited a 1" thick insulating block was incorporated between the legs and the bearing pads. The pads were fixed to a slewing ring for reasons that will be described later but it greatly eased the stud tensioning. As the vessel was beyond the capacity of the cranes in the experimental area a base frame was provided which ran on a rail system laid on the laboratory floor.

The vessel was self pressurising and heated by a total of 44 kW of electrical heaters and insulated with a 4" thick layer of rock wool. Immersion type heaters having 14 kW capacity were used to heat the water and used the four $2\frac{3}{4}$" bore nozzles in the head. The rest of the heaters were clamped on the outside of the vessel body and arranged so hot spots were eliminated reducing problems of temperature differentials. The cooling arrangement was designed to use air as the cooling medium for reasons of simplicity.

The control of the equipment had to be by remote operation because of the accelerator neutron safety requirements and this had a great effect on the experimental design and operation especially under all the fault conditions that had to be considered.

The thermal neutron boundaries are normally made of Cadmium but as this melts at 321°C it was not suitable. The boundary material used in the experiment consisted of 30% of Boron Carbide in an Aluminium matrix. This was clad with Stainless Steel sheet to reduce the corrosion. The cylinders were supported from the head and used a movable piston. As the cylinders were not pressure vessels adequate passages for pressure equalisation had to be left but carefully designed to reduce any possible neutron leakage into the cylinder down the passages. To also ensure adequate isolation of the volume under investigation at the same time the cylinders were surrounded by a double wall of absorbing material. The design of the piston movement was governed by problems of ease of operation and reliability as the removal of the head to correct a fault would be a lengthy and expensive process.

The counter positions and the cylinder design were closely related by engineering limitations and the reasons for the decisions made will be given later but two counters in line with the neutron beam were used. The choice of the counter type was severely limited by the temperature and reliability requirements and increased

sensitivity fission counters were used with standard Harwell 2000 series equipment. The analyser was arranged to count the two counters seperately but simultaneously The start pulse was obtained from a pulse pickup near the accelerator target based on an A.W.R.E. Aldermaston design the accelerator being pre-acceleration deflected to reduce background problems.

2. BASIC SPECIFICATION

2.1 PROJECT SPECIFICATION

The basic project specification was to extend the measurement of the diffusion parameters of thermal neutrons in water to higher temperatures than have been previously carried out.

The previous experiments have been limited to results at temperatures below 300°C by a number of difficulties but even at these conditions there is a large scatter on the small amount of data available. These have been extensively reviewed by Cokinos (1966) and Beckhurts (1962 and 1965) giving an overall position of the research on the thermal neutron parameters of moderators including water and a summary of the relevant results is given in Fig. 1.1.

If the temperature is increased above 300°C increasingly higher pressures are required for a small increase in the temperature range as shown by the saturated liquid line in Fig. 2.1. Very little is gained unless the temperature range is extended beyond the critical temperature for water of 374°C and this would also allow a very wide density range to be covered which would be useful in trying to seperate temperature and density dependent effects as previous work only covered a 30% density change and this was dependent on the temperature. From the density curve

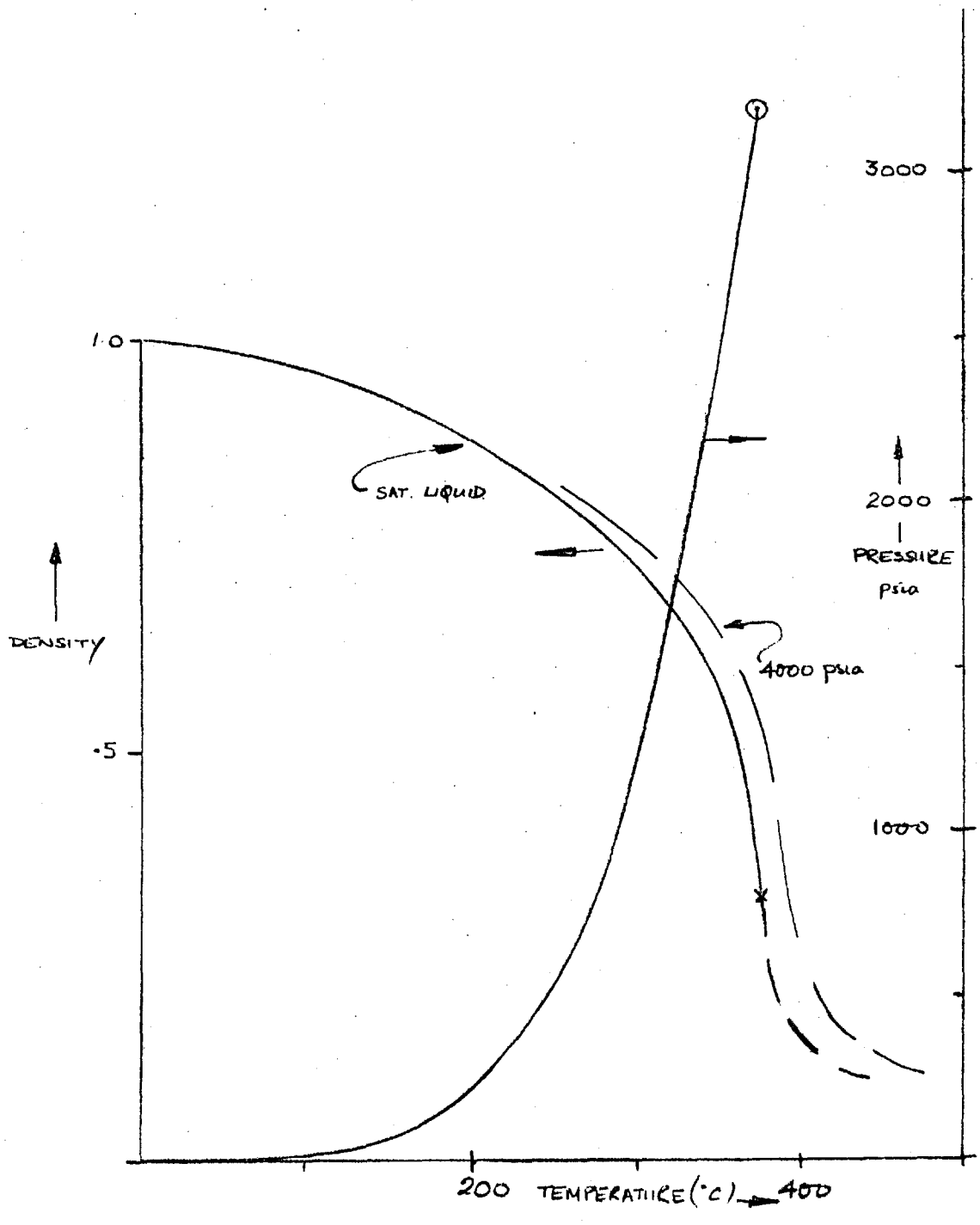

FIG 2.1 DENSITY & PRESSURE TEMPERATURE RELATIONSHIPS

in Fig. 2.1 it can be seen that the gains by going above 450°C are small and this was taken as the high temperature limit for the project and vessel design. By keeping this limit low cheaper more easily available materials could be used for the vessel and studs as even a small increase in the temperature above this limit would require the use of more expensive materials.

To obtain the minimum weight and size of the vessel the high pressure condition was chosen to be as low as operationally possible. This limit was governed by the requirement that the supercritical region was to be reached without entering the two phase region. The working pressure was chosen to be about 10% above the critical pressure of water (3206 psia) to satisfy this.

The basic physical limits on the vessel are shown in Table 2.1.

Table 2.1 Physical Limitations

Working Temperature	450°C (842°F)
Working Pressure	3500 psia
Design Pressure	3850 psia

For the pulsed neutron method a vessel diameter of 18" would suffice with an 18" length for measurements while the steady state would preferably require a length of greater than 5 ft. over which measurements would have to be taken and even with this length corrections would

have to be made for the finiteness of the system though these corrections would not be a major limitation. For the reasons which will be discussed in the next section the pulsed neutron method was chosen as the experimental procedure.

A policy decision was taken to obtain a vessel with an internal diameter of 3 ft. and internal height of 3 ft. which was larger than required. This was decided on because although a smaller vessel would have been sufficient for this project it would have had limited use afterwards while a large vessel would enable other projects such as ones on sub-critical assemblies to be carried out spreading the increased costs. The size decision was however dependent on the method of carrying out the pulsed neutron experiment and the vessel would act basically as a high temperature facility for pulsed or steady neutron experiments using the accelerator. The increased size of the vessel had however a large effect on the weight and complexity not only of the vessel itself but also the associated equipment and is best demonstrated in the problems of stud tensioning and movement of the vessel. The problems and limitations on the vessel design and the methods of meeting them are discussed in Chapter 5. The safety limitations on the project other than those laid down by the design codes were mainly governed by the neutron safety requirements to be met by the accelerator and these were supplemented as required by those specific to the vessel and are outlined as relevant in the design.

The vessel was obtained from Babcock and Wilcox Ltd. who were responsible for the vessel design and manufacture to the requirements of the insurers and the specification set by the College to enable the proposed project to be carried out. Their responsilibity was best outlined by the Vessel General Assembly Drawing (4337/A/301F) enclosed at the back of the thesis though many parts on it were designed to a detailed requirement. The author's responsibility was the specification of the vessel design and the design,installation and working of the required associated equipment for the vessel and that needed to carry out the pulsed neutron experiments but excluding the Accelerator except for the pickup and target assembly.

This gives a brief outline of the basic specification and the chosen limits on the vessel design but many other limitations are dependent on the experimental method used to obtain the required data. The reasons for the choice of the pulsed neutron method and the basic theory of it will now be given followed by the limitations it imposes on the design.

2.2 CHOICE OF EXPERIMENTAL METHOD

There are two commonly used methods for the determination of the diffusion parameters of a material, the steady state and the pulsed neutron method. In the steady state method a flux plot is done for various

distances from a preferably low energy neutron source and the diffusion length obtained. The pulsed neutron method relies on measuring the rate of decay, by leakage and absorption, of a burst of neutrons in a volume of the material under study.

The steady state method implies moving the counter relative to the source at the required condition. The volume of the vessel proposed would be big enough for the experiments but would limit the accuracy obtainable at the high energy condition. The source has to be placed inside the vessel and no source was readily available for operation at the maximum conditions and so it would have to be specially manufactured increasing the cost of the experiment and would probably cause a long time delay. The increased size would have meant that the source would have deviated even more from the theoretical point source wanted than in previous experiments. Unless measurements were done for one source-counter spacing over the range of temperatures and the process repeated for the required number of positions then the counter or source would have to be moved during an experiment.

The first method suffers from the need to reproduce vessel conditions accurately a large number of times as Cadmium measurements would be necessary for the fast neutron corrections and the long term counter drift between counts would have to be considered. The second method

implies the use of a moving seal and would have been an attractive method but no moving seals were available which would be leaktight at the maximum conditions. It must also be noted that both of these methods would suffer from the problem that the Cadmium would melt before reaching the high temperature condition. The counters in this experiment would cause a much greater perturbation than in previous work as the increased pressure loading would require a much thicker wall and could cause an increased error in the results.

To obtain as much information as is possible from the pulsed neutron method the water is poisoned with a $\frac{1}{v}$ absorber, usually Boron, and the variation of $\frac{1}{L^2}$ against the added poison analysed. The possible seperation of the poison from the water in the supercritical region would have to be resolved and could be a large source of uncertainty and error in the method as well as increasing the time required for the experiments as several poison concentrations would have to be used.

The pulsed neutron method is carried out by injecting a burst of fast neutrons into the volume under investigation and measuring the decay of the resultant thermal neutron flux. The neutron diffusion parameters are obtained by plotting the rate of decay against the volume's Buckling - a parameter dependent on the volume of the material. Time has to be allowed for the fast neutrons to be thermalised and the harmonic flux

distributions to die away before the measurements are carried out or errors can be introduced. This problem of harmonics will be referred to later on as a clash of engineering and experimental requirements occurs due to the possible counter positrons.

The major problems with the method are concerned with reducing the background to very low levels so the required part of the decay curve is not swamped. If any neutrons were produced during the off period then a time dependent source could be introduced and would be very difficult to detect and correct for. High energy neutrons can be scattered from the surroundings into the volumes under study though this effect can be reduced by surrounding it with moderating material so these are thermalised before reaching the volume. This requires that the two volumes are seperated by a boundary sufficiently black to thermal neutrons. The normal forms of background counts have to be considered especially the possibility of spurious counts due to the gamma sensitivity of counters.

The pulsed neutron method was chosen mainly because of the lack of a moving seal for the steady state method which would probably otherwise have been an easier method of measuring the diffusion parameters but the other way of carrying out the steady state method would have created large problems of vessel control and reproduceability. The basic theory of the pulse neutron method will be outlined but this will be discussed more fully later in the theoretical analysis.

2.3 BASIC THEORY OF THE PULSED NEUTRON METHOD

The interaction of neutrons with matter can be expressed by the Boltzman Transport equation in which the change in the neutron density can be equated to gains and losses in the system and can be written

$$\left(\frac{1}{v}\frac{\partial}{\partial t} + \underline{\Omega}.\nabla + \Sigma_T\right) \phi\,(\underline{r},\ v,\ \underline{\Omega},\ t) \;=\; S(r,\ v,\ \underline{\Omega},\ t) \qquad 2.1$$

in the notation given and the source term contains the scattering source. This equation is not soluble in the general case but analytical solutions can be obtained in certain cases. Nornally simplifying assumptions have to be made to enable calculations to be carried out, the usefulness of the results being bounded by the assumptions made.

The first analysis was based on Diffusion Theory in which space and time seperability and Ficks Law are assumed to hold and for monoenergetic neutrons we can write

$$\left.\begin{aligned} \Omega.\nabla\phi(\underline{r},t) &= D\nabla^2\phi(\underline{r},t) \\ \text{and}\qquad \phi(\underline{r},t) &= \phi(\underline{r}).\,T(t) \end{aligned}\right\} \qquad 2.2$$

rewriting equation 2.1 incorporating these

$$D\nabla^2.\phi(\underline{r})/\phi(\underline{r}) \;-\; \Sigma a \;=\; \frac{1}{v}\,T(t)\,\frac{\partial T(t)}{\partial t} \qquad 2.3$$

This is an eigenvalue equation and using

$$\nabla^2.\phi(r)/\phi(\underline{r}) \;=\; -B_L{}^2 \qquad 2.4$$

we can write

$$T_L(t) = Ae^{-(v\Sigma a + Dv\, B_L^2)t} \qquad 2.5$$

or if $T_L(t) = Ae^{-\lambda_L t}$

then $$\lambda_L = v\Sigma a + vD\, B_L 2 \qquad 2.6$$

The permissable values of B_L^2 are eigenvalues of equation 2.4 and depend on the boundary conditions of a particular problem. The boundary conditions used are that in the system the flux must be continuous and non zero and the flux would equal zero at the extrapolated boundaries of the system. This is the physical dimension plus an extrapolation distance dependent on the material in the system. The values of B_L^2 are termed "Bucklings" of the spatial mode L and are unique for a given system. For a finite cylinder of radius R and height H and an extra-polation distance (d) then

$$B_{nm}^2 = \left(\frac{\gamma n}{R+d}\right)^2 + \left(\frac{m\pi}{H+2d}\right)^2 \qquad 2.7$$

where γn is the root of the Bessell function of the first kind, that is, for which $J_n(\alpha_n) = 0$.

The fundamental mode (n = m = 1) is the one having the longest decay so if the higher modes have decayed and only the fundamental was present when the decay rate (λ) was measured then a plot of λ v B^2 would from equation 2.6 be a straight line such as curve A

in Fig. 2.2

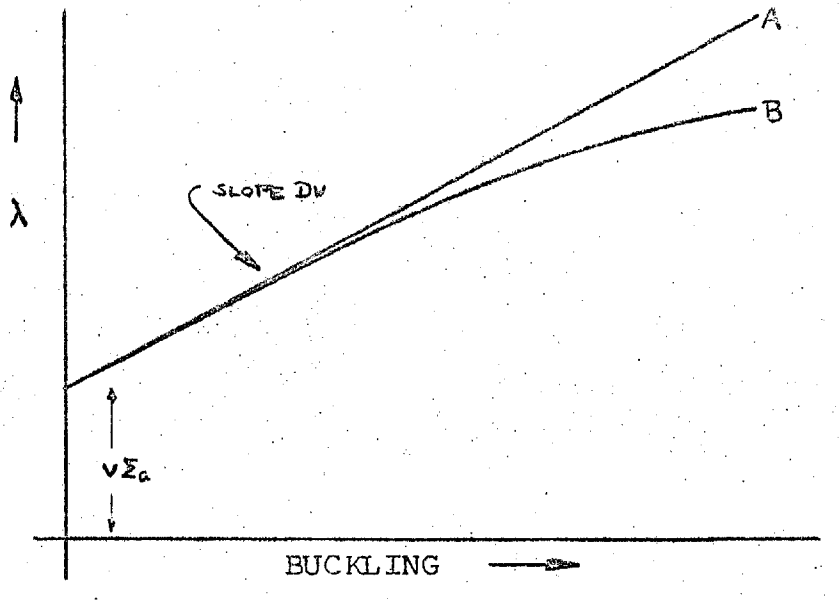

FIG.2.2 Decay Constant Variation with Buckling

enabling one to find $\nu\Sigma a$ and D for the material. This is not the case and a curve similar to B is produced. This is because the assumptions made in the analysis are not valid over the whole range of bucklings. Diffusion Theory is not valid near the boundaries and this volume increases in proportion to the total volume as system gets smaller and for a 7 cms. cube ($B^2 \simeq .5$) at $20^{\circ}C$ over 50% of the volume can be considered to be in this invalid region so there is uncertainty in the validity of what is being measured.

The assumption that all the neutrons have the same energy would not be bad if the neutron spectrum was constant for all bucklings as correctly averaged

values could be used in equation 2.6. The material properties are not constant and this is most noticeable when considering the diffusion coefficient D as this increases with energy for most moderators. This means that higher energy neutrons leak preferentially from the system and for small systems, where leakage becomes more significant, the neutron spectrum is distorted and has a lower average value than that in an infinite medium. This effect is called Diffusion Cooling and is a measure of the distortion.

More rigorous analyses have been carried out on the Fourier Transformed transport equation which gives an expression for λ in even powers of B^2 which can be written as

$$\lambda = v\Sigma a + D_o B^2 - CB^4 - FB^6 \qquad 2.8$$

where the diffusion constant $D_o = v D$. Usually only three terms are retained as the other terms are small and the errors in these terms are large though they can have a small effect on the fitted values. The C term, or diffusion cooling constant takes into account the transport effects as well as the diffusion cooling but the variations in the experimental results are large.

All these analyses depend on the buckling concept to describe the spatial mode of the neutron flux and use not only the physical dimensions of the system but also

,as shown in equation 2.7,on the extrapolation distance.

In this project the accuracy of this distance has to be carefully considered as even a large cylinder (small buckling) at the high temperature would be equivalent to a small cylinder at room temperature if the distances were measured in mean free paths of the material. The extrapolation distance is not only temperature or material dependent but also depends on the buckling through the preferential leakage which complicates the analysis.

Thus it can be seen that many of the errors present in the pulsed neutron theory are dependent on the use of the buckling concept and an analysis independent of it and only using the physical dimensions would be useful not only to enable direct comparison with experimental decay results but also to check the relevance of the buckling concept. This is expanded in the next two chapters but the limits on the design due to pulsed neutron methods will now be outlined.

2.4 LIMITATIONS DUE TO THE EXPERIMENTAL METHOD

The limits on the project due to the choice of pulsed neutron method were mainly concerned with the choice of counter positions for measuring the neutron decays as these defined the cylinder sizes that could be used in the experiments. The pulsed neutron method implies the use of varying volumes of material and in

this work it was felt that a single diameter vessel would be too limited considering the range of parameters that the project covers. It was decided to use a large pressure vessel and define the smaller volume in this by thermal neutron absorbing material which would not form pressure vessels and could be changed.

The positions of the penetrations and flanges on the head were dependent on the cylinders in the vessel and the counter position in the cylinders. The first limit on the design was that there were to be no penetrations in the body so if later experiments could not be accommodated by the present arrangement only the head would require modifying or replacing.

Using a vertical cylinder with a moveable piston the counters had to be vertical as they passed through the head and flux plots across a diameter could not be carried out. Cranking a counter would not be possible due to the engineering design of the nozzle and would not be helpful. To remove the need for the counters to resist the pressure loading it was decided that they could be placed in re-entrant tubes welded into two small flanges. This would enable the counters to be moved vertically aligning them with the flight tube and reducing harmonic effects in the decay curve.

The positioning of the counters relative to cylinders was governed by two limitations, the piston

movement, and the re-entrant pressure tubes. As the piston would rotate in the larger cylinders when its height was being changed the positions were limited to either the centre or the sides of the cylinder. These re-entrant tubes had an overall diameter of .540" and a wall thickness of .119" so that if they were placed in the volume they would have a large perturbing effect as well as making the piston movement design very difficult. Due to the physical size of these tubes they were housed in pockets let into the cylinder sides as not only would they otherwise obstruct the piston rotation but also have made the calculation of the buckling more difficult.

Usually the counters are placed on a diameter perpendicular to the neutron beam as the induced harmonics are least in this direction. This would mean that a large number of flanges would be needed to cover the cylinder sizes required but the available space on the head was severely limited as heater flanges had to be positioned near the edge and also lifting lugs had to be accommodated. If the flanges were used for more than one cylinder size then the utilisation of the available space would be increased. This could be done if the counters are placed in line with the neutron beam and accepting the increase in the harmonic contamination of the measured decays. To reduce this effect two counters were used and the decay curves from them could

be measured seperately and then analysed as carried out by Bach (1961). The use of the two counters did not increase the number of flanges required as the second counters were placed in the intermediate positions for other cylinders, at the flanges provided for moving the piston.

The largest designed cylinder had a 32" nominal size, this length being the distance between the counter centre lines and will be used as the defining size. The actual cylinder diameter is about $\frac{11}{16}$" less than this. By placing a flange at the centre of the head for moving the piston of this 32" cylinder then the counter positions for 16" cylinders were provided and by repeating this process an 8" cylinder can be incorporated. An intermediate flange could not however be provided for this size cylinder because of the size of the flanges and the piston would have to be moved indirectly from the central flange. Support arms would transmit the vertical movement and would have to miss the counter tubes and the cylinder supports. The flanges had an overall diameter of $6\frac{1}{8}$" and the smallest counter spacing designed was $6\frac{1}{2}$" and this was placed diametrically opposite the 8" position. These decisions provided only five small flanges and a minimum of six were required for various connections. The available space was limited to a diameter at 90° to the line of flanges and to provide the maximum of possible sizes

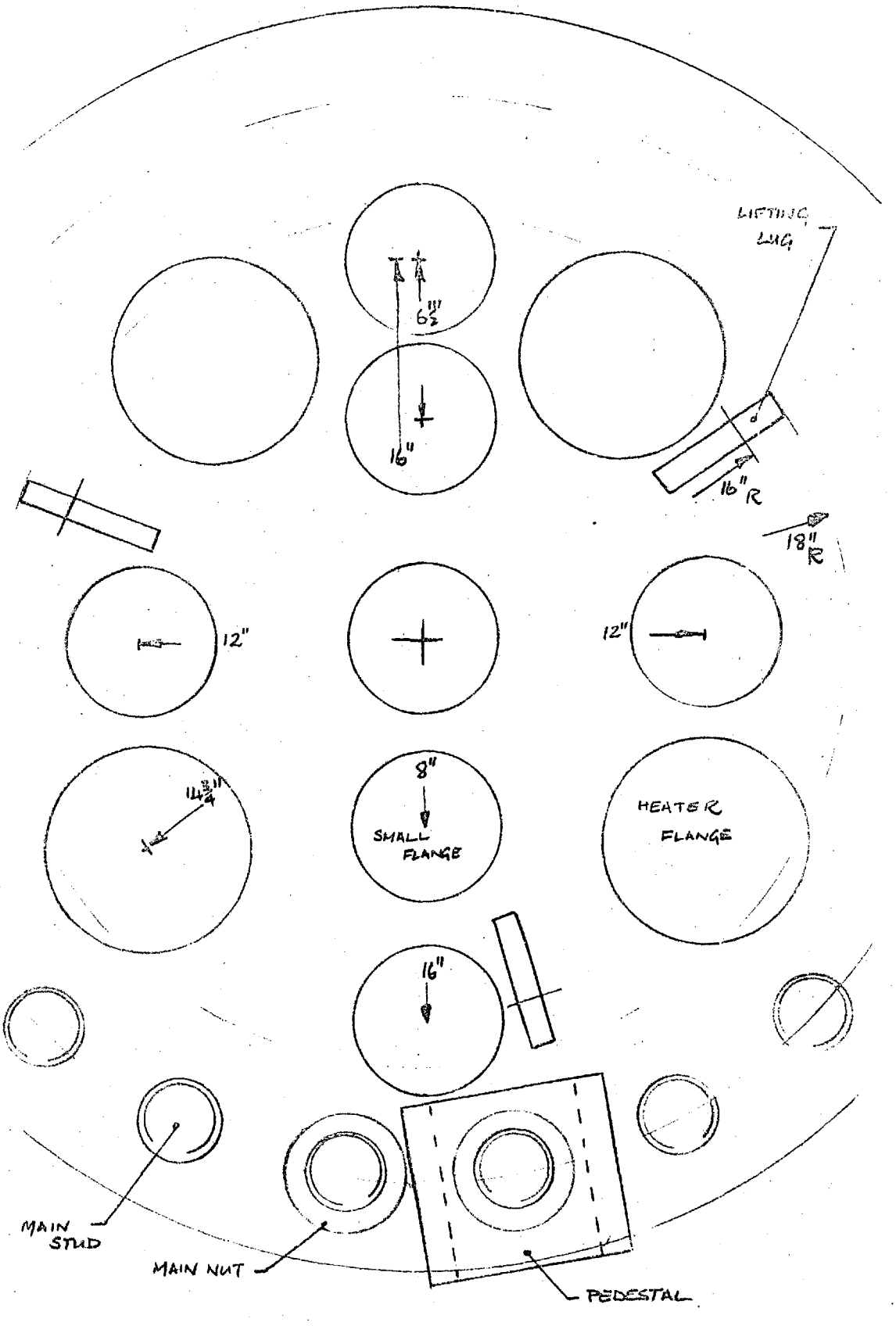

FIG 2.3 FLANGE POSITIONS

two flanges were arranged 12" from the centre giving another two sizes 12" and 24" if required. The flange layout is shown in Fig. 2.3 and the actual arrangement can be seen in Fig. 5.2 showing the various flanges.

These considerations fixed the small flange positions but the heater flanges positions were also fixed by these considerations. These had to clear the largest cylinder and meant they were placed as far from the centre as possible without fouling the stud tensioning arrangement but even so the heaters had to be cranked. This was possible but limited by nozzle design and is more fully outlined in Chapter 7.

It should also be noted that in this project not only will the temperature have to be measured accurately but also the pressure. This is especially important when operating near the critical point where a small pressure change can cause a large density change. This compressability effect seems to have been neglected by previous experimenters using overpressure systems to stop boiling occuring. The effect of a 500 psi over pressure at 300^{o}C would cause an increase in density of over 1% and would be significant. This becomes increasingly important as the temperature nears the critical point.

The theoretical analysis derived to represent the pulsed neutron experiment and the models used to

describe the scattering of thermal neutrons by the water molecules will be now explained. The design of the equipment to carry out the experiments is described in the second part of the thesis.

P A R T 1

THEORETICAL CALCULATIONS

The purpose of the theoretical calculations was to carry out an accurate analysis of the pulse neutron experiment using the minimum of assumptions reducing any errors implicit in the method of analysis. There were two main problems involved, the accurate representation of the interaction of neutrons with the medium and the accurate calculation of the flux distribution in the volume of material under study both within the computational facilities available.

The first requires a full knowledge of the dynamics of the scatterer's motion so reasonable simplifying assumptions can be made so manageable representations, or models, can be set up. These can be checked against experimental data and discrepancies between the two can be used to refine the models as well as giving a better insight into the interactions. The collision of neutrons with atoms cannot be described solely by the laws of elastic collisions since the thermal motion of the atoms themselves and even nearby molecules can have an effect. As the temperature of the material rises one would expect any intermolecular forces to be reduced in effect until in the gaseous state they could be considered negligible.

The calculation of the required cross sections and the checks carried out to show the significance of any errors in the numerical methods are outlined in Chapter 3. The relationship between the proposed models

representing the dynamic motion of the atoms and the scattering cross sections is shown and then various models used in reactor calculations are described. The method of calculating the cross sections from the models is outlined in the latter part of the chapter. A model has been proposed to represent steam in which the hindered rotation was neglected and this will be described later.

The calculation of the decay constants depends on the required cross sections and some dimensions. In the experiment these are the actual physical dimensions of the volume of material but previous analyses have however been based on the buckling concept as mentioned in Chapter 2. Most of these methods, which are reviewed by Cokinos (1966), such as done by Nelkin (1960) have been based on the solution of the Fourier Transformed Transport equation. This can be written for isotropic scattering in the slab system with no fission or fixed sources as

$$(\Sigma_T + \frac{\lambda}{v} + iB\mu)\ \phi(B,\mu,E) = \int_{-1}^{1}\int_{0}^{\infty} \Sigma_s(E'\mu' \rightarrow E\mu)\ \phi(B,\mu,E')dE'd\mu \qquad 3.1$$

where space time seperability has been assumed and also again the buckling concept, that the flux vanishes at the same extrapolation end point for all neutron energies. In this method the decay constant can be expressed as

infinite series in powers of B^2 and can be related to the usual decay constant equation. Irrespective of the actual refinement of the calculation procedure the method is limited by the validity of the buckling concept.

The extrapolation distance (d) can be shown to be, using monoenergetic diffusion theory for an infinite slab,

$$\left.\begin{aligned} d &= 2D = \frac{2Do}{v} \\ d &= 2.13D \end{aligned}\right\} \qquad 3.2$$

using transport theory. Since D varies with energy some averaged value has to be used and Gelbard and Davis (1962) have calculated a value of 2.28. This averaging procedure would not be a problem if the spectrum was constant for all volumes but as mentioned previously the smaller systems have a colder spectrum than the large ones due to the preferential leakage of higher energy neutrons so the extrapolation distance itself is dependent on the physical size of the system. This has been theoretically investigated by Gelbard and Davis amongst others, who have calculated the variation with buckling using Diffusion Theory and Spherical Harmonics methods. They found that the dependance varied for the three basic geometries as well as with the buckling.

There is also more importantly uncertainty in the correctness of using one quantity, the buckling, for all geometric shapes and it has been shown by Hall and Scott (1962) that cubic and cylindrical volumes of the

same nominal bucklings gave different decay constants. This has also been noted by Beckhursts (1962) comparing the data of Lopez and Beyster with that of Kulche. In these the D_o term differed by 5% throwing doubt on the usefulness of this concept. This difference is much greater than could be explained by the variation of the extrapolation distances and seems to be dependent on the physical shape. This is not surprising as in a cubic system alarger proportion of the volume is in an area where diffusion theory is not valid. Work by Gon (1965) and Elkert (1968) on spherical samples has found that the results agree better with the data from cylindrical assemblies of Kulche which would be expected.

In this project very large density and transport length changes will occur, therefore any errors in the extrapolation distance would be of greater importance than in previous experiments. Over the experimental range to be covered the buckling of a 30 cms. slab would change by about 20% taking into account the buckling dependence so errors would have a greater effect. The extrapolation distance would not only be buckling dependent but this relationship would also change with the temperature and pressure changes. For these reasons it would be very useful to carry out calculations dependent only on the physical dimensions enabling a direct comparison with experiments to be carried out, and also enable a check on the buckling concept to be carried

out. This would be especially useful when dealing with small volumes at the high temperature condition.

To carry out a calculation based on the physical dimensions a direct solution of the transport equation would be required. The spherical harmonics method is basically an analytic solution and to represent accurately the vacuum boundary condition a high order calculation would be required. Collision Probability Methods which basically solve the integral transport equation whilst being useful for small complex systems are less accurate and more time consuming for larger moderating systems. These two methods also both suffer from difficulty in accurately representing the source term.

A method of analysis often used in reactor cell calculation is the Discrete Ordinate Method (DSN) first proposed as an SN Method by Carlson (1958). In this method which was developed to make the best use of the large fast computers the neutron balance in a volume is solved assuming linear variation over the volume and repeating the calculation over the regions of interest. As the size is reduced by using more volumes the averaged values should tend to the actual continuous functions. A large amount of effort has been spent checking the method and improving its accuracy and convergance. Previous DSN codes have all required either a fixed or fission source for normalisation of the calculations to obtain convergance

but in this problem neither was present, only the scattering source which meant that the convergance control had to be completely changed. The problem was worsened by the presence of upscatter which is not present in fast calculations and causes difficulty in scaling.

The theory of the DSN method and the programme written to solve the problem will be described in Chapter 4 with the results obtained with the versions used after the cross section calculations have been outlined.

3. NEUTRON SCATTERING THEORY

In this chapter the models used to represent the dynamic motion of the water molecule are outlined after the relationship between the models and the scattering cross sections has been shown. The models predict the frequency distributions of the hydrogen atoms and vary considerably in the data used and the complexity in describing the effects of the chemical and intermolecular forces on the scattering process. The general trend has been that the development of larger, faster computors and better data has enabled more realistic models to be prepared and used.

The Free Gas Model was the first and simplest model proposed whilst the Nelkin Model was the first to incorporate the binding effects being based on physics data with very little neutron scattering data due to the lack of any at the time of formulation. Some attempts have been made to improve this model mainly by taking into account the anisotropy of the molecule. The Haywood Model was based on a large series of experiments carried out at Chalk River and Harwell and is the reduction of this data into a useable form.

The calculation of the decay constant required the computation of group averaged cross sections as input. This computation was split into two parts. The first was concerned with the compilation of the scattering law for the model from the frequency distributions. The cross sections were calculated from the scattering laws by a

second programme and were output in a form suitable for the decay calculation programme. The effect of the oxygen scattering was incorporated as a free gas of mass 18. The error in doing this is very small as its bound atom cross section is under 3% of the combined hydrogen value so any errors are correspondingly reduced.

At the same time the spatial eigenvalue calculation could be carried out and was used as a check on the calculational procedure.

3.1 GENERAL NEUTRON SCATTERING THEORY

In this section only a rough outline will be given, the formulation being mainly based on work done in Eglestaff (1965) which covers the relevant work. The probability of a neutron being scattered, the scattering cross section, depends on two factors, one is a function of the neutron properties and the other on the sample. These are assumed to be seperable and are treated independently, the work being developed from the neutron/atom correlation functions developed by Van Hore (1954). The first factor, dependent only on the neutron can be written as

$$\frac{\sigma_b}{4\pi} \cdot \frac{k'}{k} \qquad 3.3$$

where σ_b is the bound atom scattering cross section and k' and k the wave numbers before and after the interaction.

The sample only gains and looses a certain amount of energy (Q) and momentum (w) during an interaction,

assuming no change of state occurs and the relationship between them is called the Scattering law for the sample $S'(w,Q)$.

The scattering cross section for a neutron undergoing certain energy change and deflection or the double differential cross section as it is termed can be written as

$$\frac{d^2\sigma}{dEd\Omega} = \sigma(k',k) = \frac{\sigma_b}{4\pi} \cdot \frac{k'}{k} \cdot S'(w,Q) \qquad 3.4$$

This can be integrated over angle and energy to give the required cross sections. It is often preferable to use non-dimensional units or units in common usage and the use of the first allows a condensation of the data. By letting the momentum transfer (α) and the energy transfer (β) be defined by

$$\alpha = \frac{\hbar^2 Q^2}{2mkT} = \frac{E' + E - 2(EE')^{\frac{1}{2}}\cos\theta}{mkT}$$

$$\beta = \frac{\hbar w}{kT} = \frac{E' - E}{kT} \qquad 3.5$$

then equation 3.4 can be written as

$$\frac{d^2\sigma}{d\Omega dE} = \frac{\sigma_b}{4\pi} \frac{1}{kT}\left(\frac{E'}{E}\right)^{\frac{1}{2}} S'(\alpha,\beta) \qquad 3.6$$

The detailed balance criteria can be incorporated implicitly into the scattering law if use is made of the relationship

$$S'(\alpha, \beta) = e^{-\frac{\beta}{2}} S(\alpha, \beta) = S'(-\alpha, -\beta) \qquad 3.7$$

giving

$$\frac{d^2\sigma}{d\Omega dE} = \frac{\sigma_b}{4\pi} \frac{1}{kT} \left(\frac{E'}{E}\right)^{\frac{1}{2}} e^{-\frac{\beta}{2}} S(\alpha,\beta) \qquad 3.8$$

The scattering law is made up of two parts, the major part in the case of fluids being the incoherent or self scattering function $S_s(\alpha,\beta)$. The coherent or distinct part $S_d(\alpha,\beta)$ can be considered as an interference term. This term being neglected for fluids as only of significance for low α's and β's to which the neutron spectrum is not sensitive.and its effect was considered by Haywood (1964) to under 3% and mainly tends to modulate the incoherent part. It does however have an important effect on the calculational procedure in deriving the haywood Model.

The Self scattering term is the time transform of the intermediate scattering function $I_s(\alpha,t)$

$$S_s(\alpha,\beta) = \tfrac{1}{2}\pi \int I_s(\alpha,t)\, e^{i\beta t}\, dt \qquad 3.9$$

this function being the Fourier transform of the self correlation function $G_s(r,t)$ which is normally assumed to a guassian function of position. If this assumption is made then it can be shown that

$$I_s(\alpha,t) = \exp\{-\alpha \int \frac{\rho(\beta)}{\beta \sinh\frac{\beta}{2}} [\cosh\frac{\beta}{2} - \cos\beta t]\, d\beta\} \qquad 3.10$$

where $\rho(\beta)$ is the generalised frequency distribution describing the scatterer's motion, this being the basis of the models and the use of the relationships shown enables the cross sections to be calculated from a given frequency distribution. The frequency distributions for the various models now being outlined.

3.2 SCATTERING MODELS

3.2.1. Free Gas Model

The Free Gas model, first proposed by Wigner and Wilkins (1944), neglects the molecular binding effects completely and assumes the hydrogen atoms to be completely free, having a motion dependent only on the water temperauure. In the frequency distribution $\rho(\beta)$ consists of a delta function at $\beta = o$ and $S(\alpha,\beta)$ can be analytically expressed as

$$S(\alpha,\beta) = \frac{1}{2(\pi\alpha)^{\frac{1}{2}}} \exp - (\alpha^2 + \beta^2) /4\alpha \qquad 3.11$$

Due to the possibility of obtaining analytic solutions this model was the basis of much early work with and without the use of computers. Whilst this is a crude model the techniques available at the time were limited and it enables the importance of the binding effects on the scattering process to be seen and for this reason was incorporated.

3.2.2 Nelkin Model

This is a commonly used bound atom approach for cross section calculations due to ease of computation and the reasonableness of the results.

Nelkin (1960b) proposed a model in which the binding forces were taken into account by assuming that the effects could be represented by delta functions in $\rho(\beta)$. The possible vibrations of the water molecule are shown in Fig. 3.1. From infra-red spectroscopy the stretching vibrations were shown to correspond to frequencies about ·48ev and the bending frequency to ·2ev. This model assumed that these frequencies were the same in the liquid as in the vapour state. It has been shown that the hindered rotations have a band of frequencies being the torsional oscillations of the molecule under the influence of the dipole moments of the surrounding molecules. This motion was reqresented by Nelkin in the model by a delta function at ·06ev. All the oscillations are assumed to be isotropic and the translations of the molecule to be free. From mass tensor considerations the vibrational modes have a total weight of ·5 assigned to them being split as shown in Fig. 3.2 showing the frequency distribution for the model, the two high energy vibrations being considered degenerate.

An improvement to this model has been incorporated by Koppel and Young (1964). They assumed as before that the bending and torsional vibrations were isotropic but

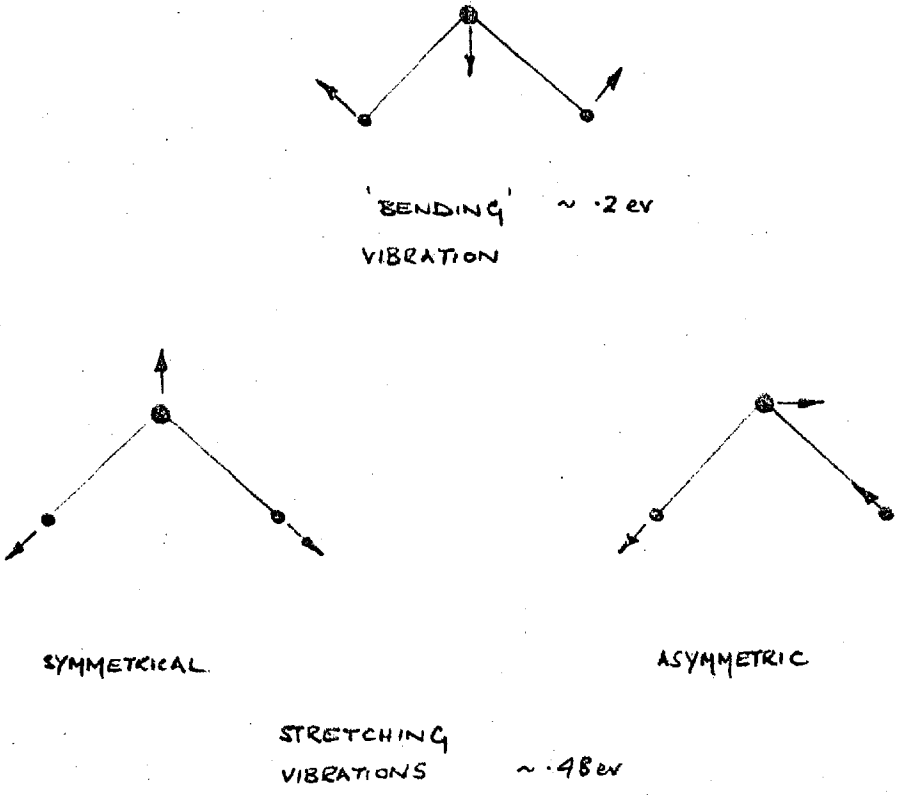

FIG 3.1 NORMAL MODES OF VIBRATION OF THE WATER MOLECULE

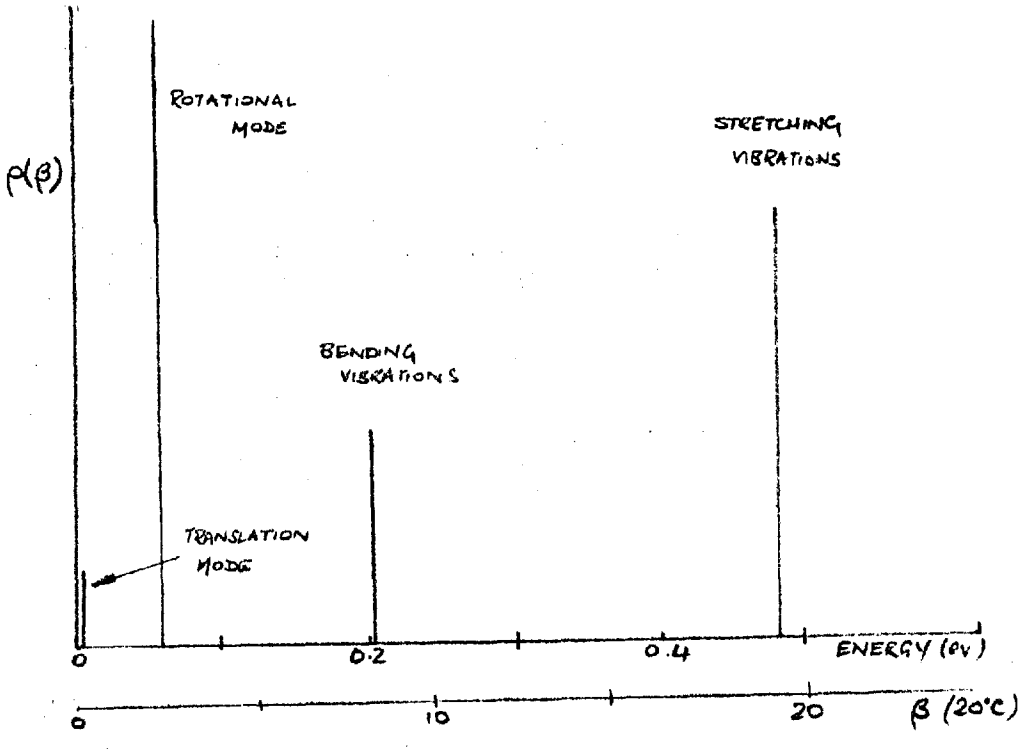

FIG 3.2 NELKIN MODEL FREQUENCY DISTRIBUTION

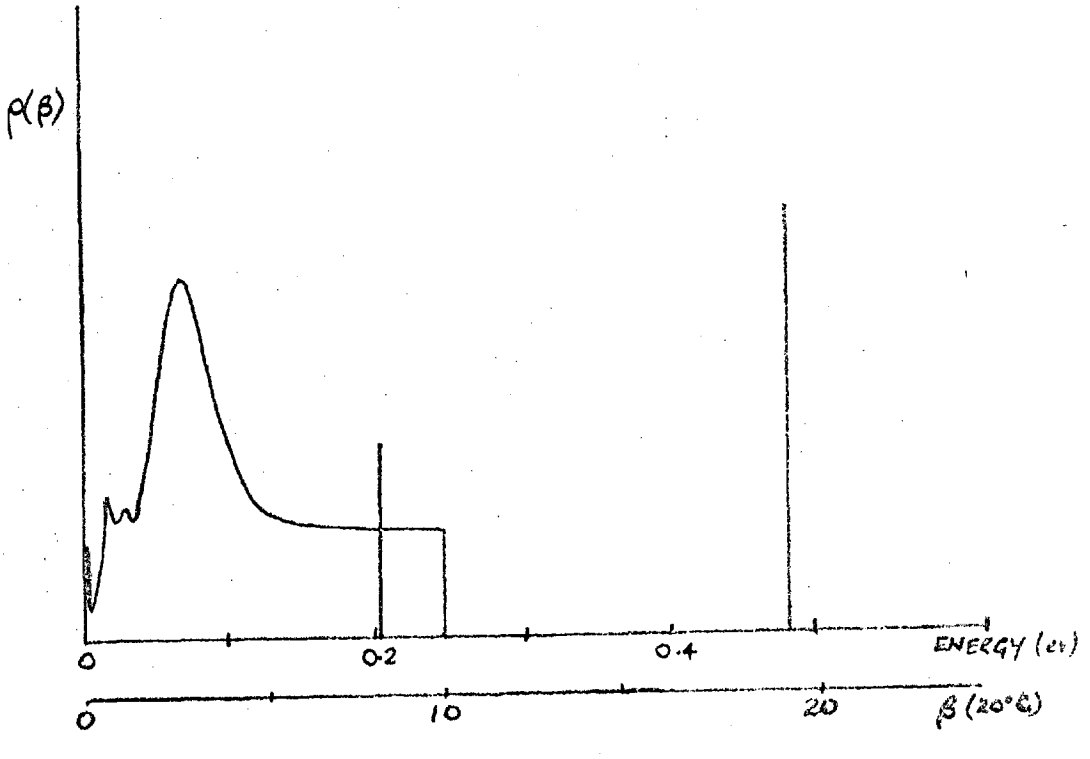

FIG 3.3 HAYWOOD MODEL FREQUENCY DISTRIBUTION

the stretching vibrations act only along the bond. This has led to an improvement in the agreement between calculated and experimental integral cross section data. This model has not been used in this project though it could be incorporated into the programme used to generate the $S(\alpha,\beta)$.

3.2.3 Free Rotator

When water becomes a vapour the rotations of the molecule are not so hindered due to the greater intermolecular spacing and proton energy. A model has been proposed by Goddard and Besant (1965) in which the hindered rotational mode was neglected and an effective translational mass of 2.06 was used giving the correct vibrational masses. In the computational work the hindered rotational mode could not be completely neglected so a rotational mass of 200 was used with a translational mass of 2.076. The differences between diffusion lengths calculated using masses of 100 and 200 were less than .1% so this assumption was assumed to have a negligible effect on the results.

The differences between this model and the Nelkin enables the effect of the hindered rotations to be seen and should enable interesting comparisons to be made with data in steam, when these are available, as this would seem a more representative model of the water molecule at supercritical conditions.

3.2.4 Haywood Model

The weaknesses of the Nelkin Model lie in the lack of neutron scattering data incorporated and the replacement of the rotational mode by a discrete mode. Haywood (1967) and (1964) used a large amount of neutron scattering data to produce a frequency distribution based on the experimental results as far as they extended completing the model by extrapolation and the use of physical data as carried out in the Nelkin Model

Haywood converted the experimental determined partial scattering cross sections to a scattering law. He then used the extrapolation technique of Eglestaff and Schofield (1962) to generate the frequency distribution. This was based on the relationship between the scattering law and the frequency distribution which, assuming the guassian approximation, can be written as

$$\rho(\beta) = \beta^2 \lim_{\alpha \to o} \frac{1}{\alpha} S(\alpha,\beta) \qquad 3.12$$

However as mentioned, as α decreases the coherent scattering becomes increasingly important and causes this relationship to become invalid as α decreases so care had to be taken in the evaluation of the scattering law. The results obtained were iterated on so agreement was increased and the second modification of the fifth iteration as recommended was used. This frequency distribution is shown in Fig. 3.3 in which it can be seen that the chemical binding is treated in the same

way as in the Nelkin Model but the low energy modes are replaced by a continuous spectrum. This was used with a Debye Waller factor of .719 to allow for the diffusive motion.

The extension of this area was carried out to achieve the correct weighting as mentioned in the above reference.

Haywood had also at the same time compiled scattering law at 250°C and for intermediate temperatures has suggested linear interpolation, but no data is available at a greater temperature than this and extrapolation would be uncertain.

3.3 SCATTERING LAW AND DIFFUSION LENGTH CALCULATIONS

The Scattering Laws for the various models were calculated for a given set of α,β mesh values and were used later to calculate the required group averaged cross sections. The mesh used in the calculations must be fine enough so interpolation errors in the numerical procedure are negligible. Because of the wide temperature range of the project the modes in the models varied in β value, the Nelkin Model high energy vibration mode changed its dimensionless value from 19.0 at 20°C to 7.7 at 450°C but had a constant value of .48ev. Bunching the mesh points where

the greatest changes occur in the scattering law would reduce the interpolation errors in a calculation for a given number of mesh points, the number of points being limited by computer storage and computational time. The greatest changes occur near the modes of vibrations of the models and the points were bunched about these. In this project a basic electron volt mesh has been set up for the 20°C calculation the points being bunched in both the α and β meshes. These ev values have been used to define the mesh for all the temperature calculations and the actual dimensionless units used in the calculation were generated from the ev values input into the program with the temperature which ensured that the relative positioning of the mesh points about the models was preserved.

For all the models, except the Haywood Model, the Scattering Laws were generated by a program DIST, a modified version of DIS programmed by Johnson (1966) which used the Nelkin type models as modified by Frederici and Goldman (1962). This program could not only calculate the scattering law but also carry out a point cross section and diffusion length calculation. The programme was first checked out for the scattering law calculation which had not been carried out and the programming errors corrected before a series of modifications were incorporated, Rainey (1969a), enabling the extended use of the programme while retaining all the original facilities.

The first was to allow the input of the α,β mesh values in ev or in dimensionless units for the reasons stated. The large amount of data generated needing to be stored, each temperature for each model being a 40 x 40 matrix, meant that the use of magnetic tape was preferable to output onto cards. The scattering law could be written onto a binary magnetic tape with the necessary titles and identifiers in a format suitable for input to the cross section program. This modification caused the program to exceed the available computer storage so subroutine overlay was used in which only the required part of the program remained in the core, the rest being stored on disc and special shorter tape subroutines incorporated.

The program could form the point cross sections either from the internally coded models or from an input $S(\alpha,\beta)$ and these used to solve the transport equation for the fundamental space eigenvalue using the B_L method proposed by Honeck (1962) giving the diffusion length for the model. The input was generalised so all mesh orderings could be read in as the original program only accepted meshes using increasing α and β value meshes. As a further modification the scattering law on tape could also be read in so a check on all the scattering laws calculated could be carried out.

The program does not treat all the modes exactly when calculating the cross section but uses approximations

which greatly eased the computations, the theory being described by Johnson. The scattering law calculated by this method was compared with one calculated by a programme Addelt written by Madatchie and described in Goddard (1969) which treats all the modes exactly for all incident energies. To reduce the calculational time required the diffusion lengths were done using a 32 energy mesh and the B_1 approximation but these were checked against 64 Group and B_2 calculations the differences being under 1% and ·1% respectively.

The Haywood Model used was calculated by Goddard (1969) and is fully described in that reference and used the Addelt program in its compilation.

A check was carried out on the α,β meshes by calculating the 20°C Diffusion lengths for water and comparing them with that calculated using internally calculated cross sections. These were calculated as required whereas those from the scattering law entailed interpolation in the scattering law matrix and would indicate the errors involved in using the scattering law. The scattering law was in fact input as $e^{\frac{\beta}{2}} S(\alpha,\beta)$ reducing interpolation errors, and the constants used were

Table 3.1 Calculation Constants

		Hydrogen	Oxygen
Free atom Scattering Cross section	σ_t	20.37b	3.76b
Absorption Cross Section	σ_a	.332b	0.0b

and the oxygen scattering was incorporated by a Free Gas of mass 16 calculation. The diffusion lengths calculated are shown in Table 3.2.

Table 3.2 20°C Diffusion Lengths

Model and Mesh	Diffusion Length cms.	Errors %
DIST Internal	2.7978	
ADDELT (41,39)	2.7785	- .7
DIST (41,39)	2.7907	- .25
DIST (40,40)	2.7946	- .11
DIST (55,55)	2.7960	- .07
HAYWOOD (51,60)	2.6077	
FREE ROTATOR	2.9549	
FREE GAS	3.7862	

The differences between the Addelt and Dis calculation using the same meshes, less than ½%, could be attributed to error in DIST in the calculation of the scattering law due to the approximations it it. This mesh was coarse over the region of interest as it covered a much greater α,β range than was required in this project as it was developed for use in reactor calculations. The use of a bunched (40,40) mesh halved the error with the internally calculated value, but the use of an even finer mesh did not greatly increase the accuracy but involved much longer calculational time and the (40,40) mesh was used in the scattering law calculations.

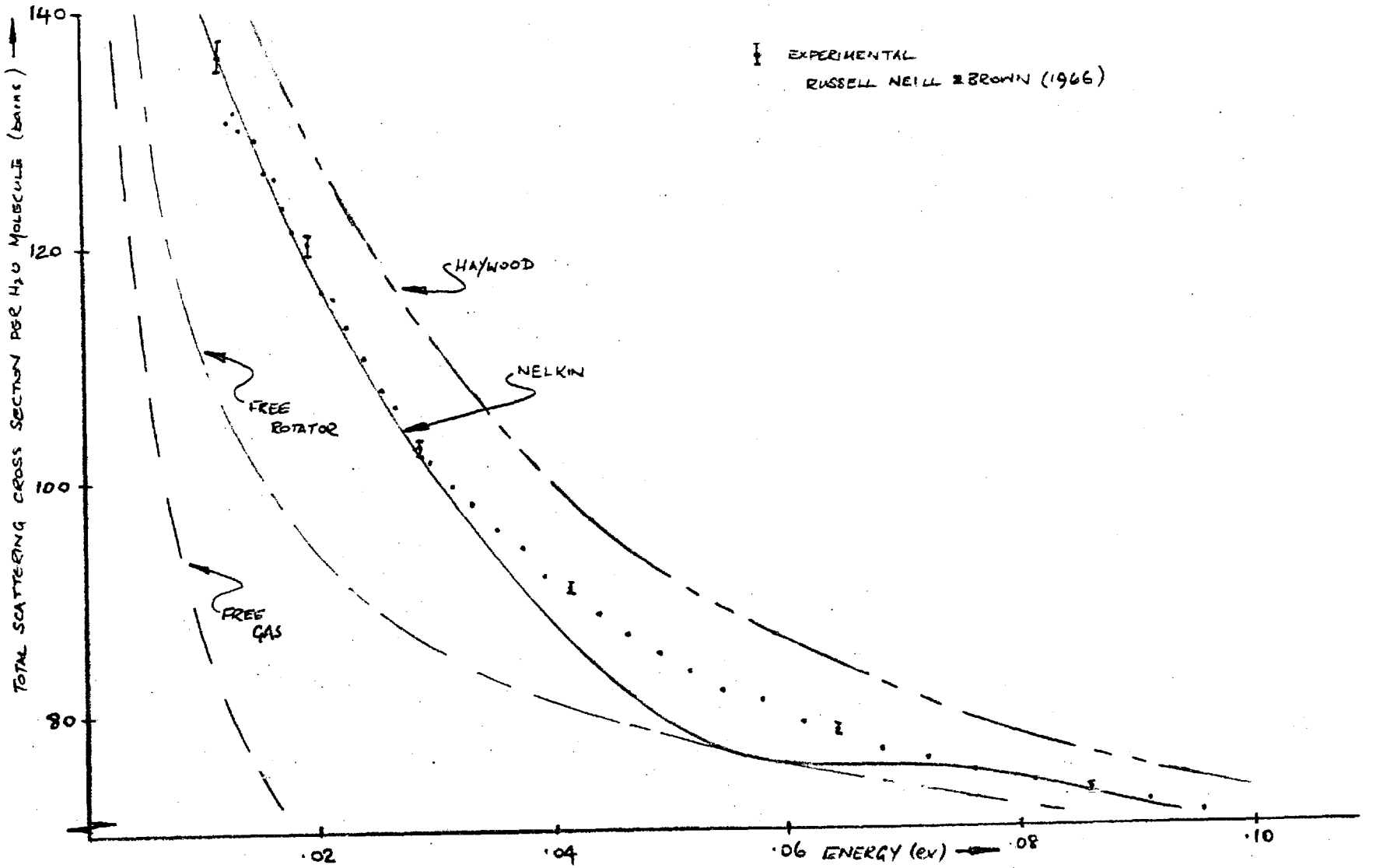

Fig 3.4 TOTAL SCATTERING CROSS SECTIONS FOR WATER.

The total scattering cross sections calculated are shown in Fig. 3.4 for the various models with the experimental data of Russell, Neill and Brown (1966) and the effect of the discrete mode representation of the Nelkin Model can clearly be seen and the curves are positioned as would be expected from the diffusion length calculations.

The temperature dependence of the diffusion length for the Nelkin Model has been calculated and the results are plotted in Fig. 1.1 with the experimental results and the Free Gas calculations giving an indication of the errors involved in neglecting the binding forces.

3.4 CROSS SECTION COMPILATION

The group averaged cross sections were calculated from the scattering law using a program TRIXSE(4), Rainey (1969b) based on PIXSE written by Macdougall (1963). This was modified to suit the particular problem being solved and the edit and output sections have been completely rewritten. The scattering law could be read from cards or from the tape written by DIST and the matrix used to calculate the required cross sections these being averaged over the energy group.

As the calculations in this project were concerned with water one of the control parameters (INXTC) was changed so that after carrying out a bound hydrogen calculation the oxygen scattering was automatically calculated using the built in Free Gas Model and the results combined and stored before editing. This meant that the problems of data handling and the sources of error inherent in it were greatly reduced.

The method of calculation was based on the relationship of the differential scattering cross section and the scattering law defined by equation 3.8 and the group averaged cross section defined by

$$\sigma_{ng'g} = \int_{\Delta E}\int_{\Delta E'} \sigma_n(E'\rightarrow E)\phi(\frac{E'}{KT})dE'dE \Big/ \int_{\Delta E'} \phi(\frac{E'}{KT})dE \qquad 3.14$$

where

$$\sigma_n\ (E'\rightarrow E) = \int_{-1}^{+1} \mu^n\, \sigma(E'\rightarrow E,\mu)\, d\mu \qquad 3.15$$

These integrals over the angles and energy ranges were evaluated by Gauss quadrature, the orders 3, 5 and 7 being built into the program. The weighting flux spectrum was a Maxwellian at the moderator temperature. The σ_n matrices could be calculated to the required order but as the decay calculation was limited to isotropic scatter the transport correction to the σ_o matrix was carried out. This is a correction to allow for anisotropic scattering in the isotropic cross sections while preserving the correct diffusion coefficient by

modifying the elastic cross sections.

$$\sigma_{Tgg} = \sigma_{ogg} - g' \sum \sigma_{1\, g'g} \qquad 3.16$$

The edit and output sections were written to suit the project requirements as the original form provided output for the DSN code written by Askew and Brissenden (1963) which used a condensed cross section matrix compilation and was not relevant or useful. The group averaged absorption cross sections were calculated in a similar manner to the scattering cross sections assuming a $\frac{1}{v}$ variation and by incorporating these the total cross sections were compiled. At the same time the $\frac{1}{vg}$ terms were calculated as they were required in the decay calculation. By using a consistent method of calculation any errors in the method would be systematic for all the values reducing the overall effect.

The whole matrix with title could be written onto tape or punched onto cards for input to the decay calculation program. A full investigation needs to be carried out to check the inaccuracies in the program and the best compromise for the angular and energy quadratures considering the accuracy required and the running time. In the calculations carried out a fifth order quadrature was used for both integrations, the computer time setting the main limit. The checks done on the program are mentioned in Section 4.4.

4. DECAY CALCULATIONS

The Discrete Ordinate Method is based on splitting the variables of the directional neutron flux into regions and considering neutron balances in the cells formed assuming usually only linear variation of variables over the cell. The solution is obtained by repeating the cell solution over all the regions of interest in a systematic way and finding overall balance. The correct solution has been obtained when the system is in balance and is usually considered to have been achieved when the parameter being calculated changes by less than a required tolerance.

Before the difference equation, which is used to carry out the chain like solution of the cells, can be obtained the required form of the transport equation has to be derived. After forming the difference equations the methods of solution used to obtain the required convergance and balance are outlined, the problem being complicated by the prescence of a source only dependent on the calculated fluxes. This will be followed by a description of the program used in the calculations.

The program used was purpose written as there were large differences between previously written DSN codes and the one necessary to perform this decay calculation mainly due to method of scaling used to obtain overall neutron balance. Previous codes have all required the use of either fixed or fission sources and the method of solution has been to normalise to these, the parameter

value required being the one that achieves neutron balance in the system. This cannot be done in this case as the only source is the scattering source and is dependent on the calculation. Many facilities often written into transport codes such as critical radius calculations also will not be wanted and also material cross sections libuaries and identifiers will not be required meaning that core storage requirements could be greatly eased, simplifying the coding complexity. With these advantages and the specialised requirements the writing of a special code was carried out and the opportunity taken to set up the code so repeat calculations could be carried out with the minimum of setting up. The programme will be described in section 4.3.

Using the transport equation as written in Chapter 2 assuming space time seperability we obtain

$$\left(\frac{1}{v}\frac{\partial}{\partial t} + \underline{\Omega}\cdot\nabla + \Sigma_T\right) N(\underline{r}, \underline{\Omega}, v, t) = S(\underline{r}, \Omega, v, t) \qquad 4.1$$

The problem to be solved is the decay of a neutron pulse in a one dimensional purely moderating homogeneous assembly and the interest based in thermal systems where upscatter is great but the theory applies as well to fast systems. If it is assumed that the transient response has decayed and only the fundamental decay mode is present then one can write

$$N(\underline{r}, t) = N(\underline{r})\, e^{-\lambda t} \qquad 4.2$$

where λ is the decay constant.

The problem can be converted from a time dependent one to a steady state problem by saying that the neutron decay rate can be considered as the source required to maintain the system in a steady state condition and equation 4.1 becomes

$$(\underline{\Omega}.\nabla + \Sigma_T)\, N(\underline{r}, \underline{\Omega}, v) = S(\underline{r}, \Omega, v) + \frac{\lambda}{vg} N(\underline{r}, \underline{\Omega}, v) \qquad 4.3$$

in which the neutron decay is considered as a source of neutrons to the system.

In the one dimensional case if μ is the cosine of the angle $\underline{\Omega}$ then the geometric terms become

$$\left.\begin{aligned} \underline{\Omega}.\nabla &= \mu\frac{\partial}{\partial x} \quad \text{for a slab} \\ \underline{\Omega}.\nabla &= \mu\frac{\partial}{\partial r} + \frac{(1-\mu^2)}{r}\frac{\partial}{\partial \mu} \quad \text{for a sphere} \\ \underline{\Omega}.\nabla &= \eta\cos\theta\frac{\partial}{\partial r} + \frac{\eta\sin\theta}{r}\frac{\partial}{\partial \theta} \quad \text{for a cylinder} \end{aligned}\right\} \qquad 4.4$$

using the cylindrical angular representation in Fig. 4.1.

The incorporation of these terms gives the form of the transport equation for which the difference equations will now be formed.

4.1 DERIVATION OF THE DIFFERENCE EQUATIONS

The derivation of the difference equation is based on the work of Carlson (1963) and Askew and Brissenden (1963). The equations for a one dimensional system have been used and the derivation for the cylindrical case, the most complicated, will be given the differences between this and the slab and spherical cases being noted where appropriate.

The neutron energy will be split into a number of groups (NG) giving a multigroup representation. In a group g of width ΔE_g all the neutrons are considered to have the same velocity v_g and the material properties are assumed constant over the group this following from the monoenergetic neutron assumption. The averaging of the material properties has been described in section 4.3 but it must be noted that because the neutron spectrum could be easily predicted and the problem was fairly insensitive to any errors in it the averaging procedure was more complex than assuming linear approximations which reduced the number of groups required for a given accuracy in the cross sections. This greatly eased the core storage requirements and the computing time for a problem. In this multigroup representation for a group g the transport equation 4.3 becomes

$$(\underline{\Omega}.\nabla + \Sigma_{Tg})\, N_g(\underline{r}, \underline{\Omega}) = S_g(\underline{r}, \underline{\Omega}) + \frac{\lambda}{v_g} N_g(\underline{r}, \underline{\Omega}) \qquad 4.5$$

and considering the cylindrical system this can be written

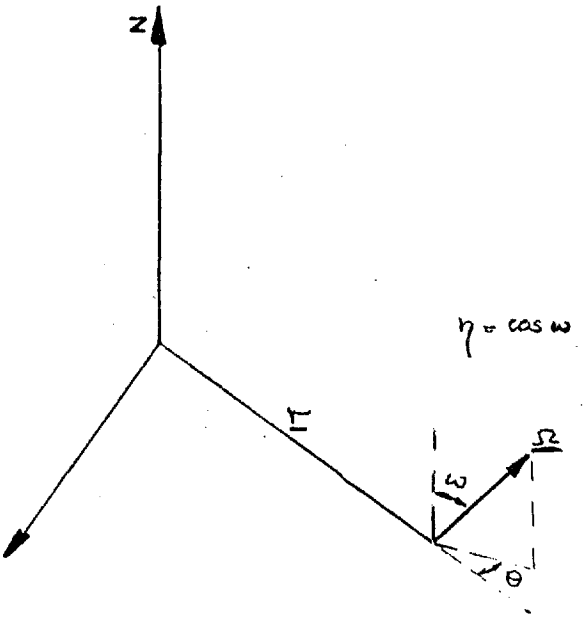

FIG 4.1 CYLINDRICAL REPRESENTATION

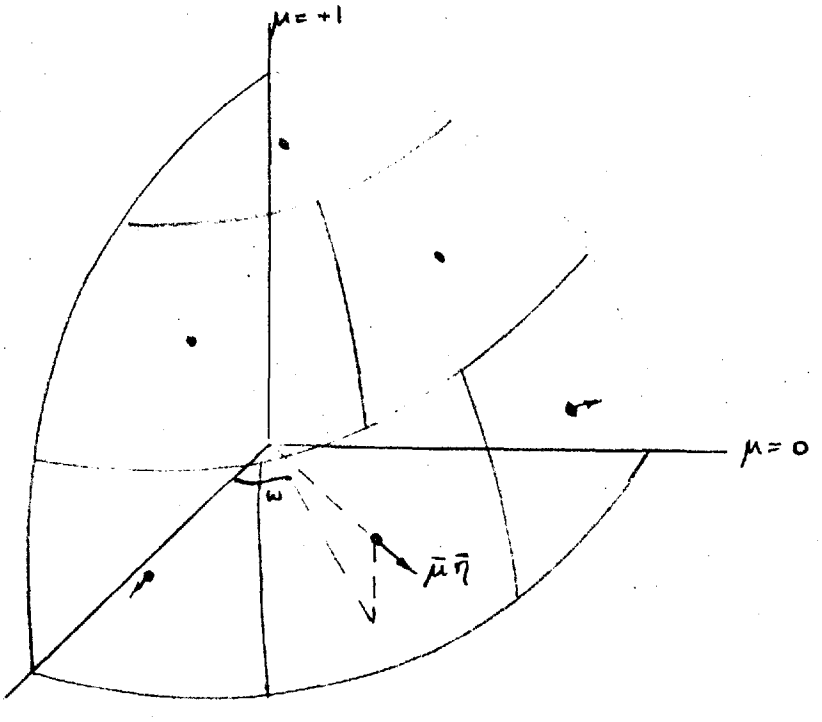

FIG 4.2 S6 MESH FOR CYLINDER

$$(\eta\cos\theta + \frac{\eta\sin\theta}{r}\frac{\partial}{\partial\theta} + \Sigma_{Tg})\, Ng(r,\eta,\mu) = Sg(r,\eta,\mu) + \frac{\lambda}{vg} Ng(r,\eta,\mu) \quad 4.6$$

To obtain the angular variation in a spherical or slab system the quadrant defining $\underline{\Omega}$ is divided into n areas (where n is the order of the DSN approximation) each having an average $\overline{\mu}_n$ and weight w_n associated with it. For the cylinder the octant defining (η, θ), or (η, μ) where $\mu = \cos\theta$, is divided into $\frac{n}{2}$ layers, or levels, each level j having been divided into j equal areas giving a total of $\frac{n}{4}(\frac{n}{2} + 1)$ areas each having an average $\overline{\eta}_j$ $\overline{\mu}_{ji}$ and weight w_{ji} associated with it. The choice of these average values will be discussed later but the layout for a n = 6 calculation is shown in Fig. 4.2. For each j level a mesh is constructed having i=2j intervals one way the mesh extending from $\mu = -1$ to $\mu = +1$ and r (where r = number of radial zones) the other, so in cylindrical geometry there are $\frac{n}{2}$ meshes but for slabs and spheres there is one n x r mesh the set up for 10 region S6 slab calculation being shown in Fig. 4.3. The fluxes in a cell mesh are defined as shown in Fig. 4.4 and the local average $\overline{N}$ is assumed to be, using the diamond difference or linear interpolation method, related to the fluxes of the edges of the cell by

$$\overline{N}_{jir} = \tfrac{1}{2}(N_{ji} + N_{ji-1}) = \tfrac{1}{2}(N_r + N_{r-1}) \quad 4.7$$

This is related to the scaler flux $\phi(r)$

$$\phi(r) = \sum_{ji} \overline{w}_{ji}\, \overline{N}_{ji} \quad 4.8$$

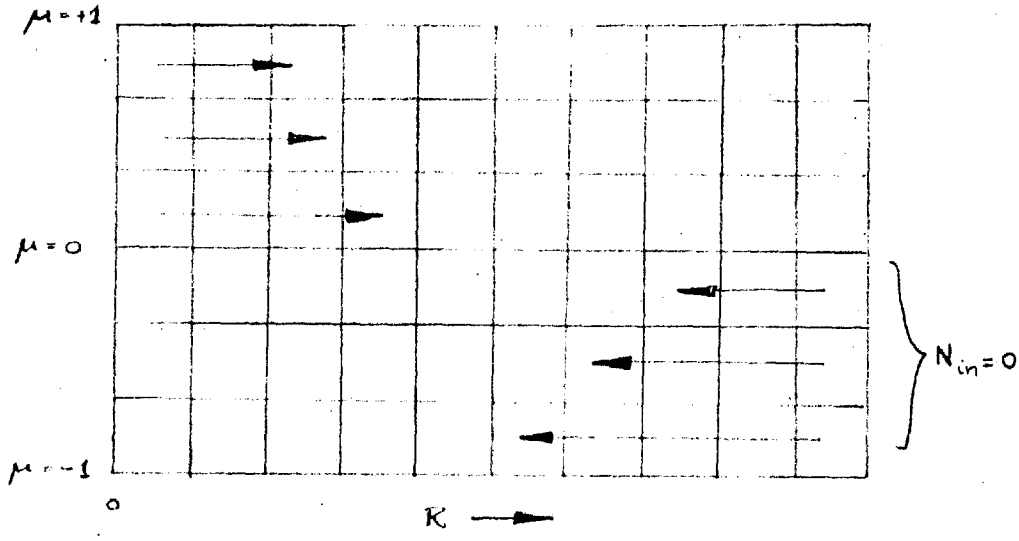

FIG 4.3 SLAB MESH FOR S6 10 REGION CALCULATION

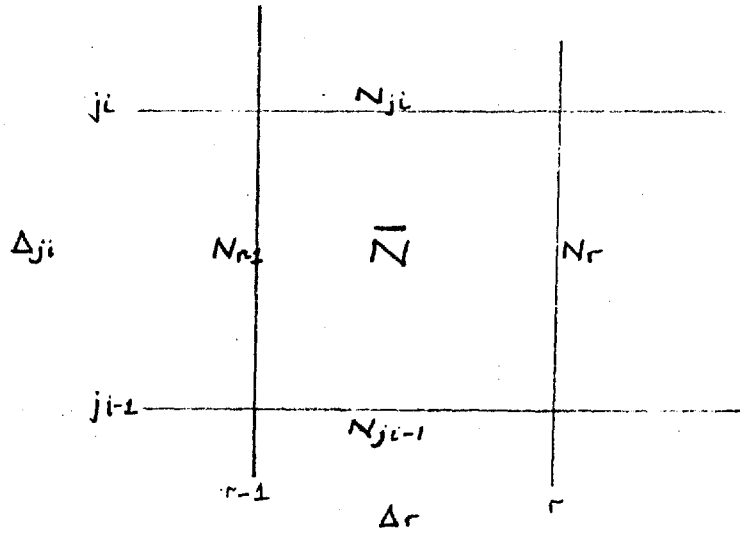

FIG 4.4 CELL FLUX REPRESENTATION

and in a group the flux level $\psi g(r)$ can be written

$$\psi g(r) = \phi g(r) / \Delta Eg \qquad 4.9$$

The source term contains not only the scattering into a group from other groups but also the self scatter source within the group and all sources in this derivation will be assumed to be isotropic so the source term in equation 4.6 now can be written

$$Sg(r, \eta, \mu) = Sg(r) + \Sigma gg \, \phi g(r) \qquad 4.10$$

where $$Sg(r) = \sum_{g' \neq g} \Sigma g'g \, \phi g'(r) \qquad 4.11$$

This splitting of the source is done because of the method of obtaining neutron balance in the group.

The difference equation equation has to be formed for the following equation

$$\left(\eta \cos\theta \frac{\partial}{\partial r} + \frac{\eta \sin\theta}{r} \frac{\partial}{\partial \theta} + \Sigma_{rg}\right) N(r, \eta, \mu) =$$

$$Sg(r) + \Sigma gg \, \phi g(r) + \frac{\lambda}{vg} N(r, \eta, \mu) \qquad 4.12$$

and in all the following derivation only the immediately relevant subscripts will be included for clarity. Each term of equation 4.12 will be taken in turn and its difference form for the cell derived assuming linear variations as defined by 4.7, this implying the acceptance of second order errors, but if the mesh size is small enough then these errors will be negligible. The difference equation is formed by the summation of these terms.

The first term can be written

$$\eta\mu \frac{\partial N}{\partial r} = \bar{\eta}_j \bar{\mu}_{ji} \frac{(Nr - N_{r-1})}{\Delta r} \qquad 4.13$$

The second term which represents the angluar redistribution term will be written

$$\frac{\eta \sin\theta}{r} \frac{\partial N}{\partial \theta} = \frac{\eta \cos\theta}{r} N - \frac{\eta}{r} \left(\frac{\partial}{\partial \theta} N \sin\theta\right)_{\Delta\theta} \qquad 4.14$$

and we would like to put this term into the form

$$\frac{\bar{\eta}}{2} \frac{b_{ji}}{r} (N_{ji} - N_{ji-1}) \qquad 4.15$$

so it is similar to the other terms. Equating these

$$\frac{\bar{\eta}_j}{2} \frac{b_{ji}}{r} (N_{ji} - N_{ji-1}) = \frac{\bar{\eta}_j \bar{\mu}_{ji}}{2r} (N_{ji} + N_{ji-1}) - \frac{\eta_j}{r} (\sin\theta_{ji} N_{ji} - \sin\theta_{ji-1} N_{ji-1})/\Delta\theta_{ji} \qquad 4.16$$

or

$$b_{ji}(N_{ji} - N_{ji-1}) = \bar{\mu}_{ji}(N_{ji} - N_{ji-1}) - 2(\sin\theta_{ji} N_{ji} - \sin\theta_{ji-1} N_{ji-1})/\Delta\theta_{ji} + 2\bar{\mu}_{ji} N_{ji-1} \qquad 4.17$$

and using the transformations

$$\left.\begin{aligned} \sin\theta_{ji} &= i\sum \bar{\mu}_{ji} \Delta\theta_{ji} = i\sum \\ \text{or} \quad \sin\theta_{ji} - \sin\theta_{ji-1} &= \bar{\mu}_{ji} \Delta\theta_{ji} \end{aligned}\right) \qquad 4.18$$

then 4.17 becomes

$$b_{ji}(N_{ji} - N_{ji-1}) = \bar{\mu}_{ji}(N_{ji} - N_{ji-1}) - \frac{2\sum_{i}}{\Delta\theta_{ji}}(N_{ji} - N_{ji-1})$$

$$- \frac{2(\sum_{i} - \sum_{i-1})}{\Delta\theta_{ji}} N_{ji-1} + 2\bar{\mu}_{ji} N_{ji} \qquad 4.19$$

$$= \bar{\mu}_{ji}(N_{ji} - N_{ji-1}) - \frac{2\sum_{i}}{\Delta\theta_{ji}}(N_{ji} - N_{ji-1}) \qquad 4.20$$

$$\therefore \; b_{ji} = \bar{\mu}_{ji} - \frac{2}{\Delta\theta_{ji}} \sum_{i} \bar{\mu}_{ji} \Delta\theta_{ji} \qquad 4.21$$

or if $\Delta\theta_{ji}$ are equal

$$b_{ji} - b_{ji-1} = -(\mu_{ji} + \mu_{ji-1}) \qquad 4.22$$

this relationship is used in the calculation of the b_{ji}'s. The derivation of other terms is straightforward and the transport equation can be written.

$$\bar{\eta}_j \bar{\mu}_{ji} \frac{(N_r - N_{r-1})}{\Delta r} + \frac{\eta_j b_{ji}}{2\bar{r}}(N_{ji} - N_{ji-1}) + \frac{\Sigma_T}{\Delta_r}(N_r + N_{r-1})$$

$$= S_g(r) + \Sigma_{gg}\phi_g(r) + \frac{\lambda}{\bar{v}_g}\phi(r) \qquad 4.23$$

or rearranging and using

$$N_{ji} = N_r + N_{r-1} - N_{ji-1} \quad \text{from 4.7}$$

it becomes

$$\left\{\eta_j\mu_{ji} + \frac{\eta_j b_{ji}\,\Delta r}{2\bar{r}} + \frac{\Sigma_{Tg}}{2}\right\} Nr + \left\{-\bar{\eta}_j\bar{\mu}_{ji} + \frac{\bar{\eta}_j b_{ji}\,\Delta r}{2\bar{r}} + \frac{\Sigma_{Tg}}{2}\right\} Nr-1$$

$$- \eta_j b_{ji} N_{ji-1} = \Delta r\, S_g(r) + \Delta r(\Sigma_{gg} + \frac{\lambda}{\bar{v}_g})\phi_g(r) \qquad 4.24$$

This is a three-point scheme, the original SN code using a four point, which can be used to calculate the third flux if the other two are known enabling all the fluxes in the cell to be predicted, using 4.7. If a negative flux is calculated, this being physically impossible, the offending fluxes are set to zero and the calculation then proceeds as before. In these calculations however, the presence of a negative flux signified an error in the calculation and if it occured during a final iteration a message was printed giving the number of times the negative flux fix up had to be used.

The choice of the average values of the angles and the weights to be used in the calculation is restricted by certain conditions which have to be fulfilled, two being

$$\sum_{ji} w_{ji} = 1 \qquad \sum_{ji} w_{ji} \bar{\eta}_j \bar{\mu}_{ji} = 0 \qquad 4.25$$

where the summation is carried out over a quadrant of the sphere. These are firstly the usual normalisation requirement and secondly the requirement that the quadrature set is symmetric so the solution is independent of the problem orientation which was not the case with some of the original sets. The weights are assumed to be the same so the weight for an area in a cylindrical system is given by

$$w_{ji} = \frac{8}{n(n+2)} \qquad 4.26$$

We would also like the problem to satisfy the diffusion theory condition which if n = 2 means that the transport equation should become the diffusion equation. This is satisfied if

$$\sum_{ji} w(\overline{\eta}_j \overline{\mu}_{ji})^2 = 1/3 \qquad 4.27$$

As the problem is concerned with the black boundary (or current) condition an accurate representation of this would reduce any errors due to the calculational procedure. If the flux is isotropic in a hemisphere adjacent to a black boundary the current into the absorber is

$$J_{in} = \sum_{in} \overline{w}_{ji}\, \overline{\eta}_j\, \overline{\mu}_{ji}\, \overline{N}_{ji} \qquad 4.27$$

$$= W\, \overline{N} \sum \overline{\eta}_j\, \overline{\mu}_{ji} \qquad 4.28$$

but the current $J_{in} = \overline{N}/_2$ so the condition to be satisfied by the set is

$$\sum_{in} w_{ji}\, \overline{\eta}_j\, \overline{\mu}_{ji} = \tfrac{1}{2} \qquad 4.29$$

Whilst the first three conditions are generally met, quadrature sets often do not satisfy this last condition. Carlson (1956) sets are in error even when using an S6 set by over 1% for slabs and over 2% for the cylindrical case.

The choice of angles and weights for the slab and spherical geometrics have been based on work done by Carlson and Lathrop (1965) who have compared various quadrature sets. For slab calculations the $DP_{\frac{n-2}{2}}$ sets

(half range Gauss Legendre) gave very good results due to their angular grouping. In the spherical case, included for completeness, the projection invariant Carlson (1963) set A have been included.

The cylindrical weights and angles used are those derived by Askew and Brissenden (1963) being specifically arranged to accurately represent the boundary conditions in cylindrical geometry and a full derivation will be found in their report.

4.2 METHOD OF SOLUTION

The method of solution was split into two parts one of which was the solution of equation 4.24 for a group over the mesh constructed and the other is how these group solutions are connected and overall balance obtained. The problem depends on the boundary conditions imposed and these were

$$\left.\begin{aligned} N_g(\mu,R) &= 0 \qquad \mu < 0 \\ N_g(\mu,0) &= N_g(-\mu,0) \end{aligned}\right\} \qquad 4.30$$

where R is the outer radius. The first states that there is no incoming flux into the system at the outer boundary and the second states that complementary fluxes at the centre are equal which is the no current condition.

Before a calculation can be carried out a guess

at the fluxes has to be carried out to enable the scattering sources to be calculated. These fluxes are more accurately calculated as the computation proceeds. After the guess fluxes have been calculated and the meshes and cross sections set up the solution of 4.24 for the groups can be carried out.

4.2.1 Inner Iteration

A complete scan through the angular and space mesh for a group is called an inner iterationn Using the guess source of neutrons from other groups the solution is obtained when neutron balance in the group is achieved, the source term being considered fixed during the calculations. At this stage however we have only n-1 equations for n unknowns and another is required to enable the solution to be carried out. This flux must be independent of any other direction and of zero weight. There are two possibilities in the $\mu = -1$ and the $\mu = +1$ directions. The first of these is used as not only does it fit better into the computational procedure in that the boundary conditions are used as starters but also errors in the numerical procedure are reduced. If the solution is carried out in the direction of neutron flow truncation errors do not build up in the calculation.

The method of solution is outlined in Fig. 4.3 in which the black boundary condition is used with the solution in $\mu = -1$ direction to solve the equation from

the outer to the inner boundary till the $\mu = 0$ boundary is reached. By using the second boundary condition the solution is carried out from the inner to the outer boundary, the direction of neutron flow, and the fluxes at the outer boundary give the leakage flow.

The fluxes calculated are the fluxes obtained using the guessed source containing the self scatter and decay term. If the calculated flux is the same as the guess fluxes then the system is in balance and calculation can proceed to the next group. Usually the fluxes do not agree and they must be altered till balance is achieved remembering that the self scatter and decay source terms would also be changed. The out of balance is used to calculate the flux change required.

Considering neutron balance over the mesh then

$$r\sum \Sigma_{Tg}\ \phi_g + \text{Leakage} = r\sum S_g(r) + r\sum(\Sigma_{gg} + \frac{\lambda}{V_g})\ \phi'_g \qquad 4.31$$

where ϕ_g is the calculated scaler flux

ϕ'_g is the previous scaler flux and the summation is over the whole mesh. To obtain balance equation 4.31 is multiplied a factor f and dropping the summation signs and rearranging it becomes

$$f\Sigma_{Tg}\phi_g + fL = S + f(\Sigma_{gg} + \frac{\lambda}{V_g})\phi_g + (1-f)S - f(\Sigma_{gg} + \frac{\lambda}{V_g})\phi_g$$

$$+ f(\Sigma_{gg} + \frac{\lambda}{V_g})\ \phi'_g \qquad 4.32$$

If the out of balance part of this equation is put equal to zero then one obtains that

$$f = \frac{S}{S + (\Sigma_{gg} + \frac{\lambda}{V_g})(\emptyset'_g - \emptyset_g)} \qquad 4.33$$

The fluxes are multiplied by this factor and the mesh calculation repeated using the new in group sources. The solution can be considered to have converged by using one of two possible criteria. One is that if (f-1) is less than a stated tolerance and the other criteria is that the scaler flux in each radial region doss not change by more than a stated tolerance. the latter is stricter in that the flux shape has to have converged as well as the overall level and has been used in the calculations.

This group solution is carried out over each group in turn using the group sources calculated before the first group was solved. The next stage is to calculate the overall out of balance and use it to predict the correct decay constant.

4.2.2 Outer Iteration

As mentioned earlier in the problem being solved there is no fixed or fission source so the numerical procedure had to use the scattering source for the normalisation noting that the source was implicit in the calculation and care had to be taken to avoid

setting up an unstable situation and meant that the methods of accelerated convergance such as used in Askew and Brissenden could not be used.

The method of solution used was to compare the balance between the sources calculated with the latest fluxes and the previous fluxes and its source. Summing over a group we can say as in equation 4.31

$$\Sigma_{Tg}\ \phi_g + \text{Leakage} = S_g + \frac{\lambda^*}{V_g}\ \phi_g + \Sigma_{gg}\ \phi_g \qquad 4.34$$

$$\text{where } S_g = \sum_{g' \neq g} \Sigma_{g'g}\ \phi'_{g'} \qquad 4.35$$

λ^* is the guess value of the decay constant and ϕ_g is the latest and ϕ'_g the previous flux in group g.

If we also say that

$$\text{Leakage} = k_g\ \phi_g \qquad 4.36$$

$$\text{and} \qquad C_g = (\Sigma_{Tg} + k_g - \Sigma_{gg}) \qquad 4.37$$

then equation 4.34 can be written, summing over all groups,

$$\sum_g (C_g \frac{\lambda^*}{V_g})\phi = \sum_g S_g = \sum_g \sum_{g' \neq g} \Sigma_{g'g}\ \phi'_g \qquad 4.38$$

in the balanced case 4.38 can be written

$$\sum_g (C_g - (\frac{\lambda^* - d\lambda}{V_g}))\ \phi'_g = \sum_g S_g \qquad 4.39$$

where the true decay constant $\lambda = \lambda^* - d\lambda$

combining 4.38 and 4.39

$$g\sum\left(C_g - \frac{(\lambda^*-d\lambda)}{V_g}\right)\emptyset'_g = g\sum\left(C_g - \frac{\lambda^*}{V_g}\right)\emptyset_g \qquad 4.40$$

and rearranging

$$d\lambda\ g\sum\frac{\emptyset'_g}{V_g} = g\sum C_g(\emptyset_g - \emptyset'_g) - \lambda^*\ g\sum(\emptyset_g - \emptyset'_g)/V_g \qquad 4.41$$

which is used to calculate the change in the decay constant. The latest fluxes, scaled to give the same total neutron density, are used to calculate the sources for the next set of inner iterations.

It has been assumed that the leakage is proportional to the total neutron flux in the group and the neutron energy spectrum does not change, the flux being only incorrect by a factor. The first is reasonable as the leakage is not a large proportion of the total flux but it does depend on the flux shape which could cause errors. The second is more serious as convergance on the decay constant or the flux shape cannot explicitly be done together. If the spectrum converges while the decay constant is being iterated on then the correct spectrum will be used when the final value of the decay constant is being calculated. If it has not converged it will cause changes in the decay constant. The situation can be compared to the physical situation where the non-asymptotic flux decays to asymptotic flux by the scattering process and is correct when the fundamental mode only is

present.

This convergance scheme does not hovever take into account the implicit change in the source that occurs so a better rate could be obtained if it was allowed for. It is found that after a few of the iterations where the flux shape is settling down (under four if a good flux guess is used) the calculated decay constant converges monatonically to the equilibrium value so the use of convergance acceleration methods based on predicted values may be more efficient. This was not written in but would be useful in reducing times by at least a factor of four for some of the present calculations.

The transport equation has been solved for a one dimensional system but it would be useful to make a correction to represent the leakage that occurs in the other directions in a two or three dimensional system. This correction can be considered as the extra absorption in the one dimensional system which gives the same increase in the decay constant as the extra leakage out of the two dimensional system. Assuming space seperability of the flux and using diffusion theory we modify the total transport cross section in a group for a finite cylinder by,

$$\Sigma'_{Tg} = \Sigma_{Tg} + \frac{\lambda_z}{V_g} \qquad 4.42$$

where $\lambda_z = D_o B^2$

$$\text{or} \quad \Sigma'_{Tg} = \Sigma_{Tg} + \frac{B_{Zg}^2}{3\Sigma_{Tg}} \qquad 4.43$$

where for a slab

$$B_{Zg}^2 = (\pi/(H + d_g))^2 \qquad 4.44$$

The extrapolation distance (d_g) has been shown to be given by

$$d_g = .710466/\Sigma_{Tg} \qquad 4.45$$

for an infinite slab and monoenergetic neutrons. The above relationships are used to calculate the increase in the cross sections and enable an analysis of the usual experimental geometries to be carried out, the buckling terms for the other geometries being similarly formed. The error involved in this approximation is reduced if $B_Z^2 < B_R^2$ which means that the dimension giving the predominant decay should be treated by the transport calculation.

A facility was also written into the programme so the decay constant could be read in. This meant that the decay in the second direction could be calculated using transport theory and this fed into the subsequent calculation. This means only the seperability of the fluxes is assumed and is the nearest approach to a two dimensional code without actually writing one.

4.3 DECAY PROGRAMME - TRAND

To carry out the decay calculations described in the previous sections a programme TRAND was written by the author(1969c) in Fortran IV for the IBM 7094 computer at Imperial College. This was purpose written for the reasons previously stated and consisted of three major sections.

The first part was the setting up procedure assembling the required values to start the calculation. The core of the programme was the solution of equation 4.24 over group mesh. The third part consisted of the outer iteration or decay scaling governing the overall calculation. The flow sheet of the programme is hown in Fig. 4.5.

The overall control of the programme was done by a short subroutine Maniac. This started the setting up and the calculation and at the end of a problem checked whether a new problem or a sub-problem was to be calculated next. The possible sub-problems were the use of finer angular or radial meshes or a new radial mesh using the same cross sections. At the start of the problem control is passed to Gog which governed the setting up and compilation of the required initial values. The first two cards read had the control parameters defining the problem and the tolerance to be met. These problem identifiers were printed out with the titles at the beginning of a

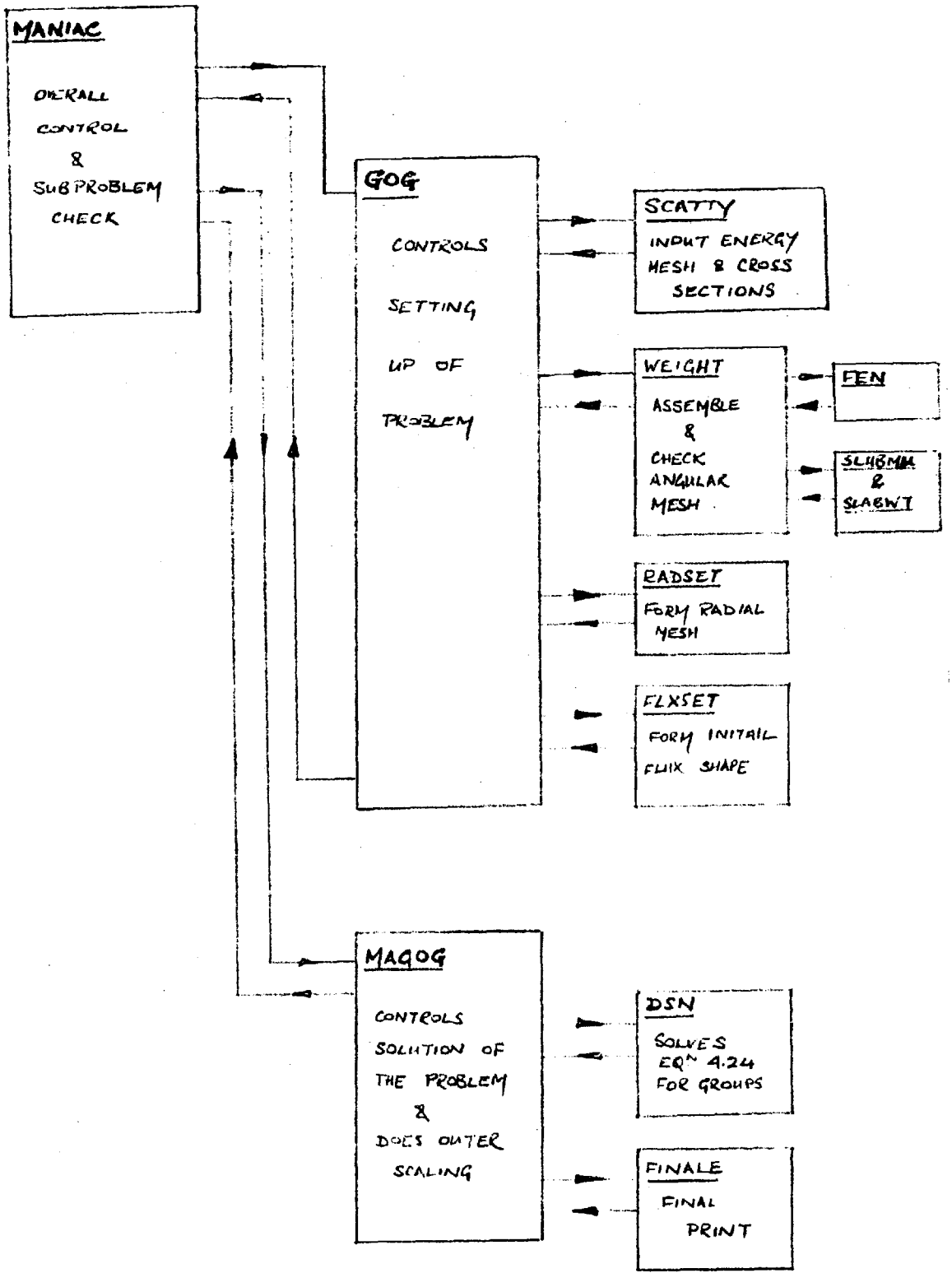

Fig 4.5 TRAND FLOW SHEET

calculation. The subroutine then controlled the assembly of the required data.

Scatty read in the energy boundaries and macroscopic cross sections with a title defining the model and some of the parameters used in their compilation either from cards or the tape written by TRIXSE(4). These input values were output as a check at the beginning of the problem and before each sub-problem. The subroutine Weight calculated the required angles and weights as described in section 4.1 and checked that the conditions of equations 4.25 and 4.27 were met to a tolerance of better than 1 in 10^{-4}. If either of these were not met then an error message was printed out and the calculation stopped. If sets other than those built in were wanted to be used they could be read in by use of the appropriate control parameter. After the radial mesh had been formed in Radset and using the input group energy boundaries the flux distribution was predicted in Flxset. The flux shape could be read in, assumed constant, as well as provision made to predict the values more accurately. The usual method was to assume a Maxwell energy distribution using the mean group energy values. For the radial shape, which is dependent on the geometry, the flux shapes predicted using diffusion theory were used with a simple extrapolation distance. The use of accurate energy flux shape could greatly reduce the computation time but the final result was independent of the initial shape

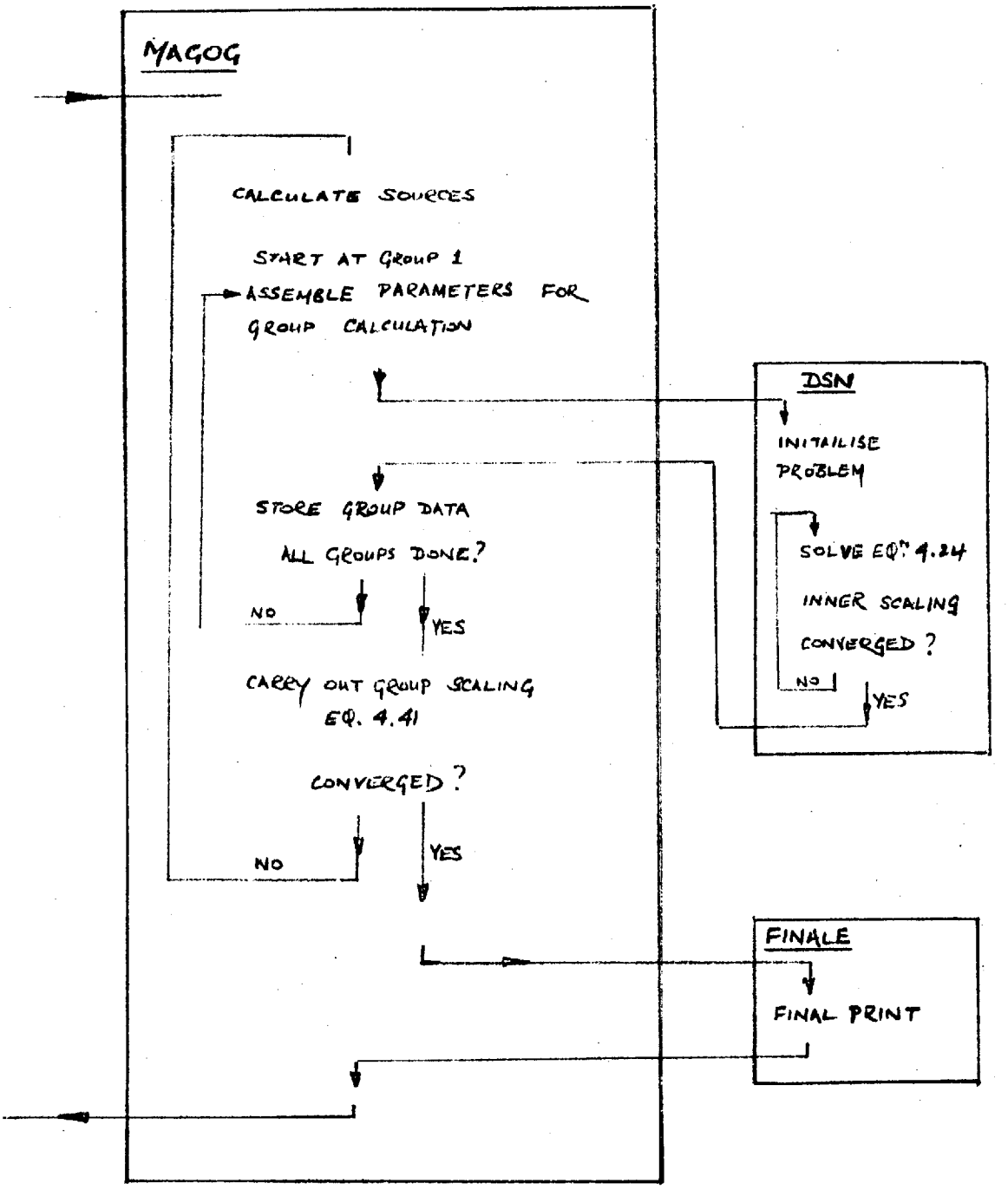

FIG 4.6 MAGOG FLOW SHEET

When the input values had been assembled control was passed to Magog which controlled the outer iterations its flow sheet being given in Fig. 4.6. It first set up the sources for the inner iterations and then assembled the parameters used in equation 4.24 for each group in turn the inner iterations being done by DSN. DSN solved equation 4.24 for a group over the mesh using the inner scaling till group convergance was obtained. After all the groups had been solved the outer scaling as defined in Section 4.2.2 was carried out. The calculation was repeated with the new sources and decay constant until the required tolerance had been met or too many iterations had been done in which case the computation was stopped and an error message was printed out. It was often useful to use the values just calculated as good initial guesses for sub problems and this was controlled by a parameter read off the last card in the set of data, after control had been transferred back to Maniac.

This programme was used to calculate the results shown in the next section on the diffusion parameters of water.

4.4 THEORETICAL RESULTS

The basic calculations used an S16 10 region mesh in Slab geometry with varying group structures. To obtain results for comparison with previous work the decay constants calculated were fitted in the same manner as the experimental results are analysed using

$$\lambda = v\Sigma a + D_o B^2 - CB^4 \qquad 4.46$$

The method of calculating the extrapolation distance (d) was based on work by Gelbard and Davis (1962). From this data the variation of the extrapolation distance with buckling for a slab can be represented by

$$d(B^2) = 2.28D\ (1 - .086B^2) \qquad 4.47$$

This relationship is quite satisfactory where D does not vary very much but because this does not hold in this project this would be a source of error and the use of consistent units would be required and this has been done by using

$$d(B^2) = 2.28D\ (1 - .086B^2\ (\frac{D_t}{D_{20}})^2\ ) \qquad 4.48$$

where D_t is the Diffusion Coefficient at temperature t

D_{20} is the 20^oC Diffusion Coefficient

The method of analysis was to fit a quadratic to the decay constants using guessed constants to calculate the extrapolation distances and the bucklings for the slab sizes. After carrying out a fit the bucklings

were recalculated using the new values. The process was repeated until the bucklings changed by less than a specified tolerance (.005%) and the parameters by less than .001%. The fitting was done using a general least squares programme DECAN and equal weighting was used on each decay point.

As a check on the radial and group meshes a series of calculations were performed for a series of slabs having half thicknesses in the range 4 to 15 cms. corresponding to bucklings of .13 to .01 cm^{-2}. The cross sections were from the 20°C Nelkin Model and the energy meshes were set up to cover the whole temperature range. This meant that the higher energy groups had low neutron flux levels at 20°C but would be required at the higher temperatures and so the energy mesh was effectively coarser than would be indicated by the number of groups.

Table 4.1 Mesh Variations

Mesh		D_o	C
Radial	Group	$cm^{+2}\ sec^{-1}$	$cm^{+4}\ sec^{-1}$
10	6*	27035	1209
10	6	36169	4177
10	12	36477	4478
10	24	36686	4000
20	12	36354	4324

(* These cross sections used σ_o values, all the other cross sections having the transport correction included)

The effect of the good initial guesses was checked against a calculation which assumed a Maxwellian energy guess and the shape appropriate to the geometry with a good decay guess which took eleven outer iterations. A bad decay guess($\lambda = 0$) only required two extra iterations but a constant energy initial guess calculation took fifty-three outer iterations. The differences in the final answers were negligible and from these calculations the major part of the calculation was required to settle the flux shape, and to accelerate the convergance the flux shape must be considered rather than using the decay constant.

The parameters of some of the models using an S16 10 region 12 group mesh at 20°C are given in Table 4.2 with other Nelkin model values.

Table 4.2 20°C Model Values

Model	D_o $cms^2\ sec^{-1}$	C $cms^4\ sec^{-1}$
DIST Nelkin	36477	4479
Addelt Nelkin	36220	5358
Free Gas	68080	18190
Clendenin (1964)	37580*	3380
Koppel and Young (1964)	36350	

* The Clendenin result had to be corrected to 20°C using a variation of 130/°C in D_o.

The cross sections used were calculated by Trixse using a fifth order guassian angular and energy integration procedure and as a check on the accuracy the calculations were repeated with the use of cross sections computed using third and seventh order schemes. The variations in the Diffusion Constants were < ½% but C varied by 20%.

The temperature variations were calculated using the 12 group Nelkin model cross sections but were checked with 24 group calculations and a difference of 10% in the D_o values was found at 300°C, the differences at 20°C being < 1%. The values are given in Table 4.3.

Table 4.3 Temperature Variation

Temp	Groups	D_o $cm^2\ sec^{-1}$	C $cm^4\ sec^{-1}$	d(O) cms.
20°C	24	36686	4000	.342
250	12	68684	18835	.472
"	24	74934	17327	.515
300	12	79737	27555	.524
"	24	88677	25013	.582
350	12	110034	62324	.693
"	24	126342	63334	.795

These results are plotted on Fig. 4.7 and 4.8 with various experimental results and shows the effect of improving the energy mesh. The 24 group diffusion

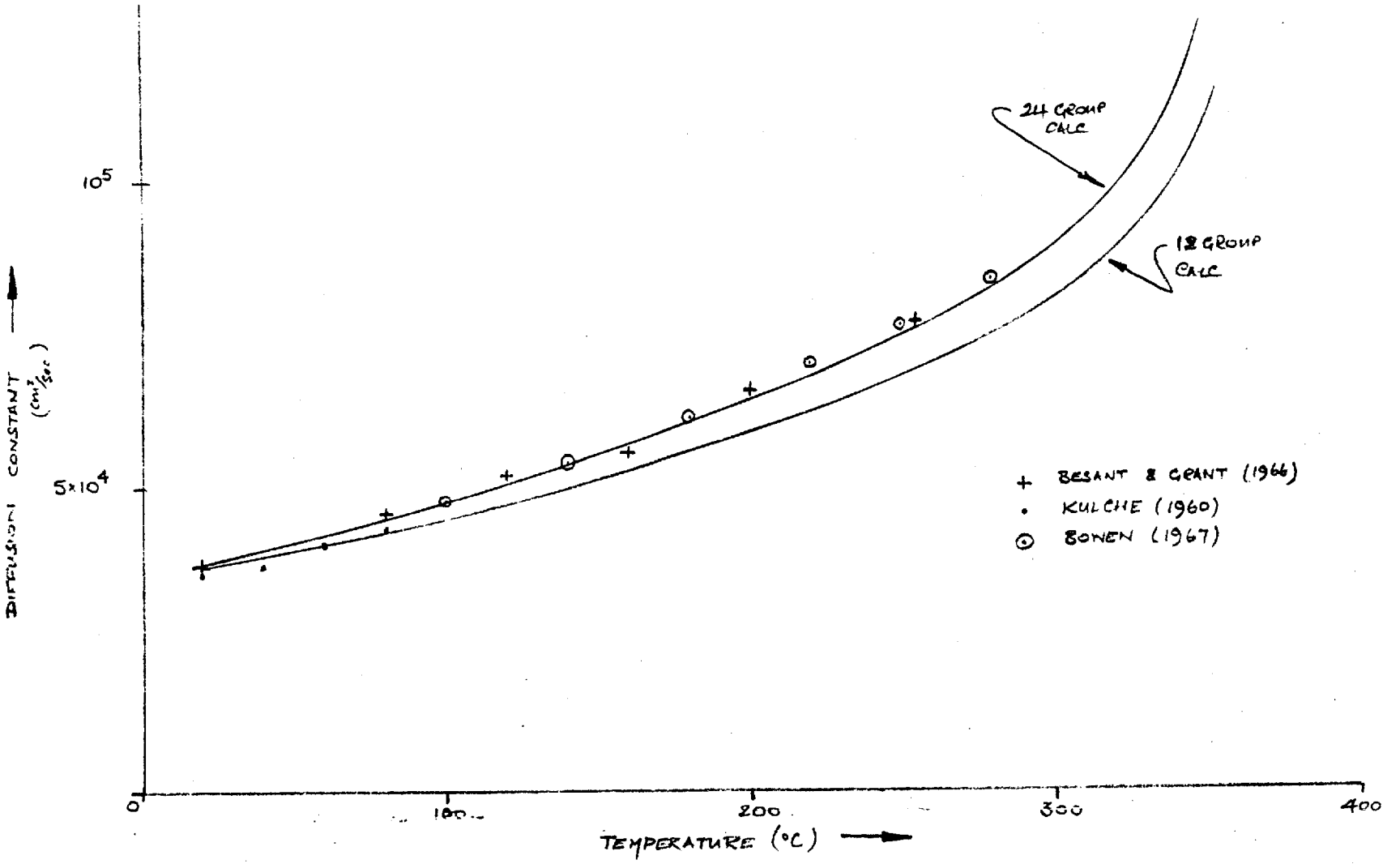

FIG 4.7 VARIATION OF DIFFUSION CONSTANT WITH TEMPERATURE

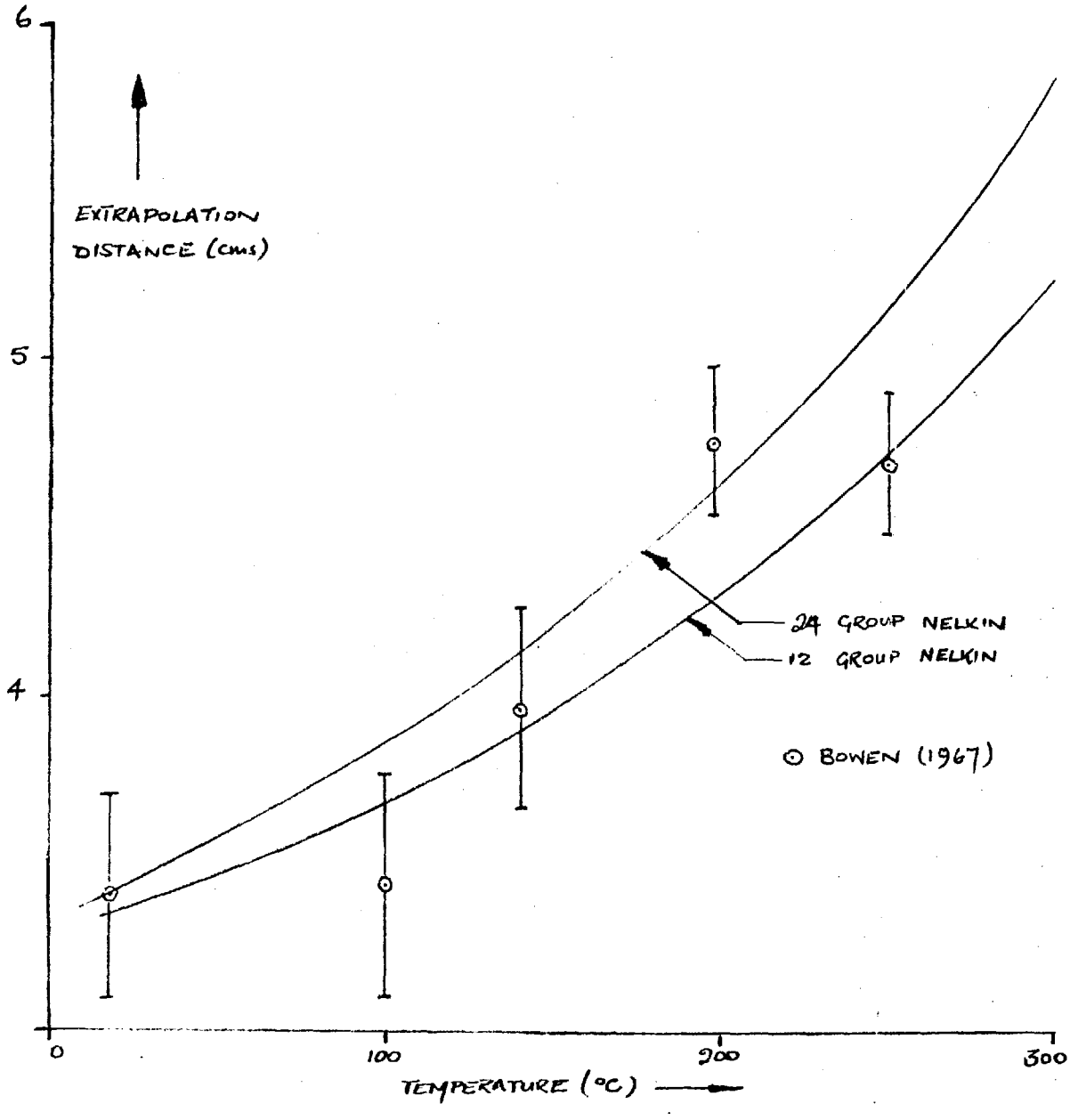

FIG 4.8 TEMPERATURE VARIATION OF EXTRAPOLATION DISTANCE

constants are in very good agreement with those calculated by Clendenin (1964).

The results obtained for the slab geometry have shown the use of this new method of analysis of the pulsed neutron experiment. The results obtained are in good agreement with other theoretical results. It has not been possible, due to the checking required, to carry out the calculations for the other two geometries. The analysis of the results enabling any geometric dependence of the diffusion constant to be calculated will be the subject of a further study.

The main source of error in the programme, neglecting the mesh sizes, which can be varied, was due to not incorporating the anisotropy of the scattering process explicitly in the calculation. This feature can be fairly reasonably incorporated in the programme but to reduce the computing times that would be required it should be carried out after incorporating the accelerated convergance.

A large amount of effort has been spent on the models used to represent water and the basic models modified as carried out by Goddard (1969) and Ardente and Gallus (1968) to improve the agreement of experimental and predicted integral and differential scattering data as shown in Beyster (1968).

The computer analysis of the problem with the change in the computational procedure should show up any limitations in the Fourier Transformed method of analysis as well as resolving the possible shape effect which it has not been possible to analyse before.

The recommendations for future work are given in Chapter 9, but now the design of the equipment to carry out the pulsed neutron experiments will be discussed in the second part of the thesis.

P A R T II

EXPERIMENTAL DESIGN

5. EXPERIMENTAL DESIGN

In this part of the thesis the design of the equipment required to carry out the proposed experiments will be described, the main parameters being assembled in Appendix I. Whilst the basic limitations on the design have already been outlined (Chapter 2) there were others which had to be considered due to the actual physical layout rather than experimental requirements. These were mainly due to safety requirements or to the existing equipment and facilities and these will be mentioned after the outline of this part of the thesis.

The design of the vessel and how the safety limits as laid down in the design codes were complied with will be mentioned after which the possible accidents that could occur and the precautions taken to overcome any hazards involved are mentioned. The detailed design of various major features of the vessel and its associated equipment will then be discussed. Detailed drawings and calculations will not generally be included for reasons of space and bulk but the problems involved in the designs and the methods of solution will be given. The heating and cooling equipment with the control and safety feature incorporated is outlined in Chapter 6 whilst Chapter 7 covers the apparatus required for the pulsed neutron experiment being the accelerator, the neutron cylinders and the counting system.

Throughout the design the conflicting requirements of reliability and sensitivity of the equipment had to be balanced being coupled with the general problems of cost and ease of manufacture. These factors were most apparent in the choice of the neutron detectors to operate under the adverse conditions.

The major physical limitations were the vessel's size and weight. The workshop crane used for unloading the vessel from the lorry and moving it to the well in the experimental area as shown in Fig. 5.1 had a capacity of ten tons setting an overall weight limitation. The width of the well was 6 ft. and was an absolute width limitation, but a narrower limitation was imposed by the existing equipment which blocked the exit from the well whose removal would have been awkward. The cranes in the experimental area had a capacity of three tons governing the maximum allowable weight of the head. As the designed vessel had a total weight of seven tons some form of support frame or trolley had to be provided to move the vessel from the wall to its required position as shown in Fig. 5.1 with the movement required. Means for rotating the vessel when changing the internal cylinder had also to be incorporated into the design.

There was no overall height limitation except for a general vessel stability one but the mid-plane of the neutron cylinder had to be centralised with the target to reduce harmonic generation and this set a height

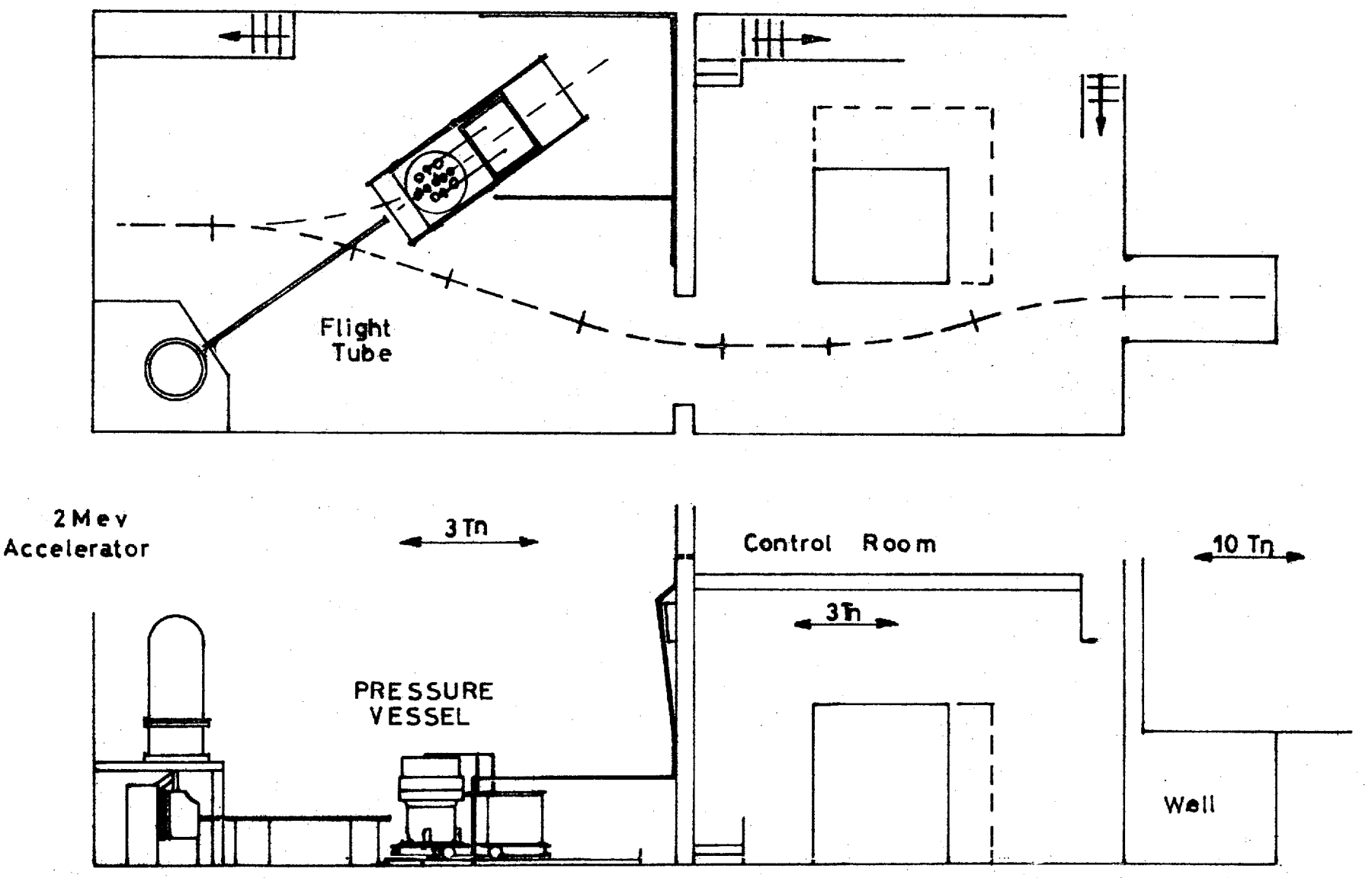

Fig 8.1 GENERAL LAYOUT

limitation on the base frame and the vessel support structure. As the piston defining the top of the cylinder would be raised and lowered to vary the volume under investigation the mid-plane would also vary and the base frame would have to be able to be raised by up to $10\frac{1}{2}$".

The safety limitations will be mentioned as they occur in the design discussion which now follows.

5.1 BASIC VESSEL DESIGN

As mentioned earlier the vessel was manufactured by Babcock and Wilcox (Operations) Ltd., on their contract No. 98/4337 with Imperial College to the College's requirements, the insurers being the Commercial Assurance Co. Ltd.

The vessel was designed to BS 1515 (1965) code except in three sections. All the Stainless Steel components were designed to ASME VIII and the main flange to BS 3915 which was based on the ASME VIII method of calculation. The design of the nozzle/head weld could not be done by BS 1515 and was proved by calculation. Compliance with sections four and five of 1515, the parts dealing with manufacture and inspection were met as applicable except prior certification of the welders was acceptable and the production of test plates was not required.

The vessel was basically a cylinder of 3 ft. internal diameter having a basic wall thickness of 3". The bottom was closed by a semi-ellipsoidal cover also 3" thick welded on and the head was a flat cover $10\frac{3}{8}$" thick giving a full width opening and used a metal O seal with a bolted flange. The General Assembly is shown on the enclosed drawing at the back of the thesis designated DRG. 1. The vessel was made of a low alloy steel Ducol 30W, a brand name of a $1\frac{1}{2}$% Mn $\frac{3}{4}$%Cr $\frac{1}{4}$%Mo $\frac{1}{4}$% Ni ·1% V Steel with ·$1\frac{1}{2}$% C and ·2% Si. The inner surface of the vessel was clad with Type 304 Stainless Steel weld deposited and dye penetrant tested. The flange and the bottom cover were welded together using a backing plate which was removed and back welding carried out. Full X ray radiography of the weld was carried out before the weld area was clad with Stainless Steel as the rest of the vessel and magnetic crack detection was done after the vessel body had been stress relieved.

The head cover could have been made up using a ring flange with a domed central section welded in, which not only would have been much lighter but would also have given more room at the top than a flat cover. It would however have required much more thick plate welding with full radiography and would have been more difficult to manufacture. As flat head was just within the crane capacity the extra expense for the domed head could not be justified. The main flange seal was obtained using a

silver plated hollow O ring vented to the inside of the vessel, the design and method of stud tensioning to obtain the required pretension for the studs being described in section 5.3.

Four nozzles, 2¾" bore, passed through the head and were welded at the inner end to the cladding. This weld arrangement meant that there was a continuous Stainless Steel lining to the vessel as the nozzles were made of Stainless Steel reducing any corrosion effects at the same time allowing for the differing expansions of the nozzle and the head. This weld could only be dye penetrant tested and for this reason such high reliance could not be placed on it as on the other welds which were X rayed as well. The nozzles were closed by a bolted flange seal using a hollow metal O ring similar in construction to the main seal O ring. The seal and tensioning will be described more fully later. These flanges were used for the internal heater which passed through and were brazed into Stainless Steel sleeves welded into the flanges. This was done as the heaters could not be brazed directly into the flanges because of the differing heat capacities. The heater design will be considered in Chapter 7 but they were pressure tested at the College assembled, the arrangement shown on D^{R}G. 1 being used for the pressure test, at the works before delivery.

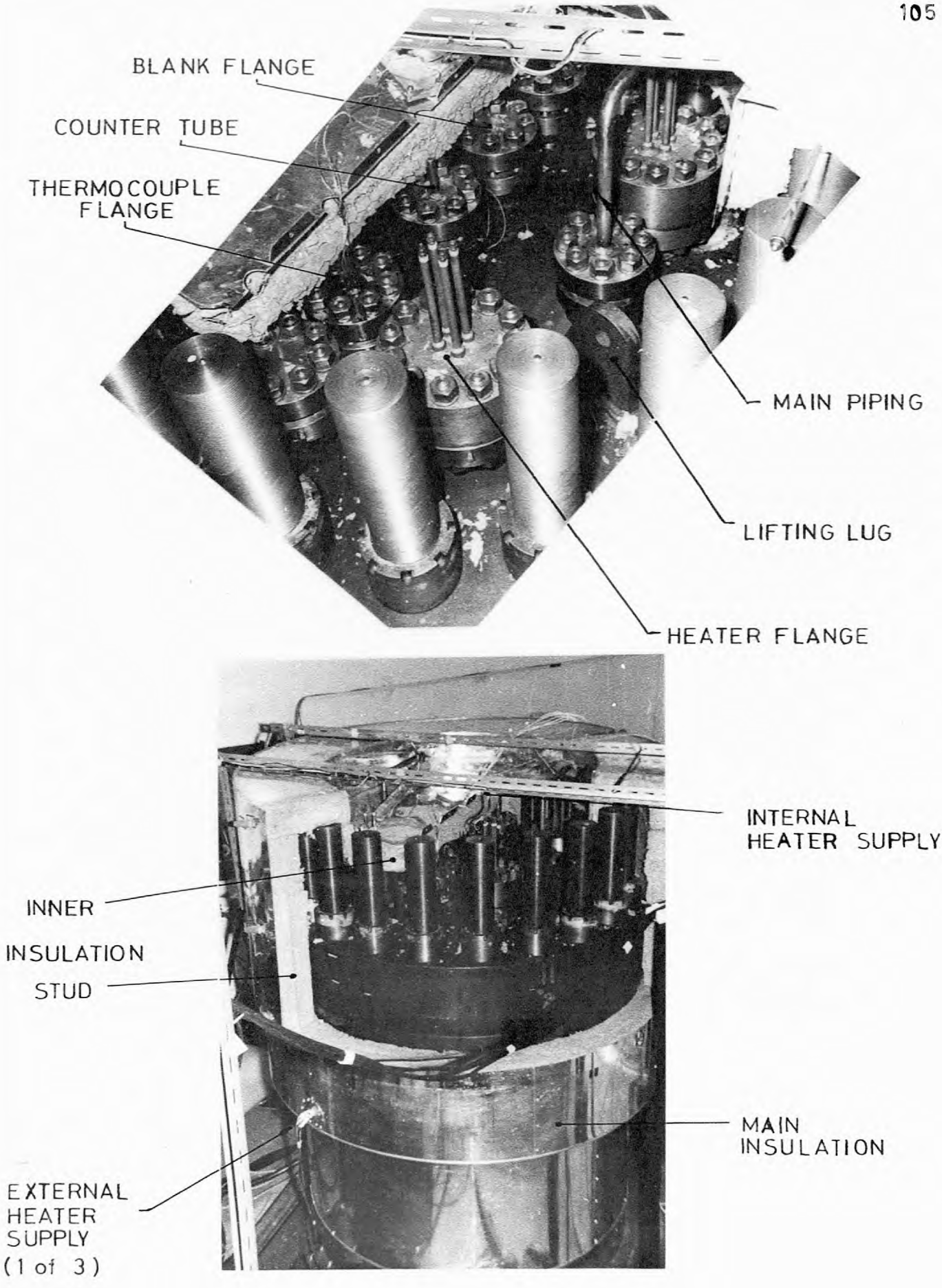

FIG 5.2 HEAD & FLANGE LAYOUT

The position of these can be seen in Fig. 5.2 with some smaller penetrations. These of which there were seven provided 1" bore nozzles through the head. The positioning of these was governed by the counter positions as outlined previously but were also used for thermocouple and pressure connections and at least one had to be kept blank for changing the piston position. The flanges were interchangeable to suit the experimental layout. The penetrations were similar in design to the heater flanges except that the reduced size enabled a re-useable solid Stainless Steel 0 ring requiring higher seating forces to be used due to the reduced hydraulic loads. Two of the flanges had .540"O.D. x .119" wall Stainless Steel tubes welded in which were blanked off at the inner end for the counters. This meant that the counters were moveable in the vertical direction for alignment and also they only had to be designed to take the high temperature condition considerably easing manufacture. Two flanges had the main piping connections welded to them the piping being .840"O.D. x .187 wall. This weld like the nozzle/head weld could not be X rayed and was only dye penetrant tested. The temperatures inside the vessel were measured using Chromel-Alumel thermocouples. These were protected from the steam by a 1 mm O.D. Stainless Steel sheath and high purity Alumina was used as the insulation. To facilitate the installation the thermocouples were supplied with bushings (5 mm O.D.) arc welded on 4' 9" from the hot

junction but even so one of the six thermocouples set on a $\frac{7"}{8}$ PCD on the flange was damaged on welding the bushes into the flange. The thermocouples were connected to extension cable the joints being enclosed in a thick Aluminium box to create an isotherm so thermally induced errors were reduced.

The head was lifted using three lifting lugs made of carbon steel welded onto the head and one can be seen in Fig. 5.2. These were not strong enough however for lifting the whole vessel and when this was required on delivery strops had to be used under the main flange. The only other welding on the head was the cross support frame made from $\frac{1}{2}$" Stainless Steel plate welded 4" below the head to take the internals and will be fully described later.

Due to the requirement of a clean body to the vessel the only welding was for fixing the support legs and a number of $\frac{1}{2}$" Whitworth studs to facilitate the clamping up of the external heaters. These attachments were inspected by magnetic crack detection.

5.2 VESSEL SAFETY LIMITATIONS AND REQUIREMENTS

1) Pressure

The pressure limitation required that the internal pressure should not exceed the working pressure by more than 10% this being the design pressure. Some form of automatic pressure relief had to be incorporated being set to operate at this pressure since the rate of pressure increase was low. This could have been done using a bursting disc assembly but these tend to be insensitive and are thus set to operate at a pressure slightly below the design condition. They also have a tendency for accidental operation at pressure well below the design condition due to fatiguing of the membrane under the cyclic loading which would be very annoying in this project and would cause quite a delay in the experiment.

Due to the high steam conditions the required discharge capacity was very low (<.02 in^2 orifice area) and was below the normal capacity of spring loaded relief valves (S.R.V.). Also a suitably sized valve able to take the high temperature condition was not available but by placing the valve away from the vessel using some piping to connect them the temperature limitation could be relaxed if the spring, which was limiting, was shielded from the steam flow. A larger sized valve than required would be liable, when operating, to hammer

and scoring of the seating to occur especially when using a long piping connection due to the pressure drop along the pipe. This would mean that the seal after operation might not be completely leaktight. Whilst this would be unacceptable in a continuous process vessel in this project it would be undergoing a cyclic form of operation and the disc and nozzle could easily be replaced if required and this was considered an acceptable form of operation.

The safety valve used was made of Type 316 Stainless Steel and had an orifice area of .077 in^2. The temperature limit on the spring made of Tungsten Steel was 750°F but it was shielded from direct steamflow. The valve was connected to the vessel by 8 ft. of main piping but adequate restraint had to be incorporated to reduce any reaction stresses induced in the piping during a blow down, the restraint structures being described in Section 5.6. To limit the pressure rises that occur while heating the vessel an adjustable pressure switch is to be incorporated in the heater control circuit and will be mentioned more fully later, being more for ease of operation rather than any safety requirement.

2. Temperature

The operating temperature of the vessel was 450°C (842°F) and the main safety feature was a controller that on measuring a temperature above the set one would

switch all the heaters off. The failure of the supplies to the controller would cause the heaters to be switched off and a thermocouple going open circuit would cause the controller to effectively see a full scale temperature also shutting the heaters off. The thermocouples and controllers were connected to a common panel so the thermocouples used for control could be easily changed during a run, the layout being outlined later. This would be useful as different control requirements would be important at different times in the experiment.

Temperature differences also had to be checked to see if they were of significance. The possibility of hot spots on the vessel due to the external heaters were eliminated by careful design and were checked by experiment as will be outlined more fully in Chapter 6. No maximum rates of heating or cooling have been specified but BS 1515 Appendix B3.2 recommends the following limitations for vessels where slow rates (not defined) of heating and cooling cannot be employed.

1. During start up or shut down the differences in temperature within a distance equal to twice the thickness of the shell should not exceed 60^{o}C near discontinuities and 150^{o}C at uniform sections.

2. Temperature differences due to temperature transients repeated periodically during service shall be limited to similar levels.

If the maximum temperature differences were found to be less than 60°C (108°F) then the limits are easily met. With all the heaters on the initial temperature rise was 40°F/hr assuming no heat losses, the water taking up most of the heat. To calculate the temperature differences the vessel will be considered to be made up of three effectively thermally independent sections as shown in Fig. 5.3. Except for a small amount of conduction as shown all the heat transfer was by natural convection of the water.

Section 1 is the part of the vessel having the heaters clamped to it. Heat is transferred to section 2, the unheated flange, by conduction (1 kw) along the metal the rest by natural convection of the water heated by section 1. The head cover is heated solely by natural convection and the heating powers required by each section to reach the equilibrium temperature rise are shown on the diagram. The 24.6 kw that had to be conducted through the vessel wall would cause a temperature difference of about 23°F and was one of the reasons for reducing the possibility of any heater hot spots.

Using the natural convection correlation as given in McAdams (1954) equation 7.4a which can be written as

$$N_u = .13\, N_{Gr}^{\frac{1}{3}}\, P_r^{\frac{1}{3}} \quad . \qquad 5.1$$

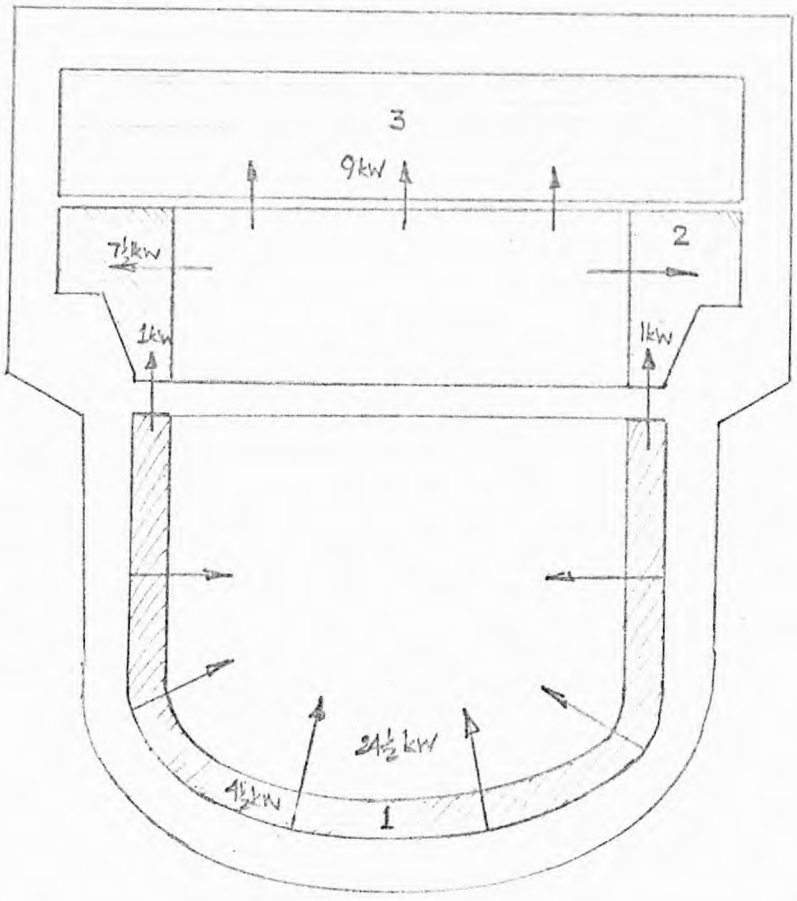

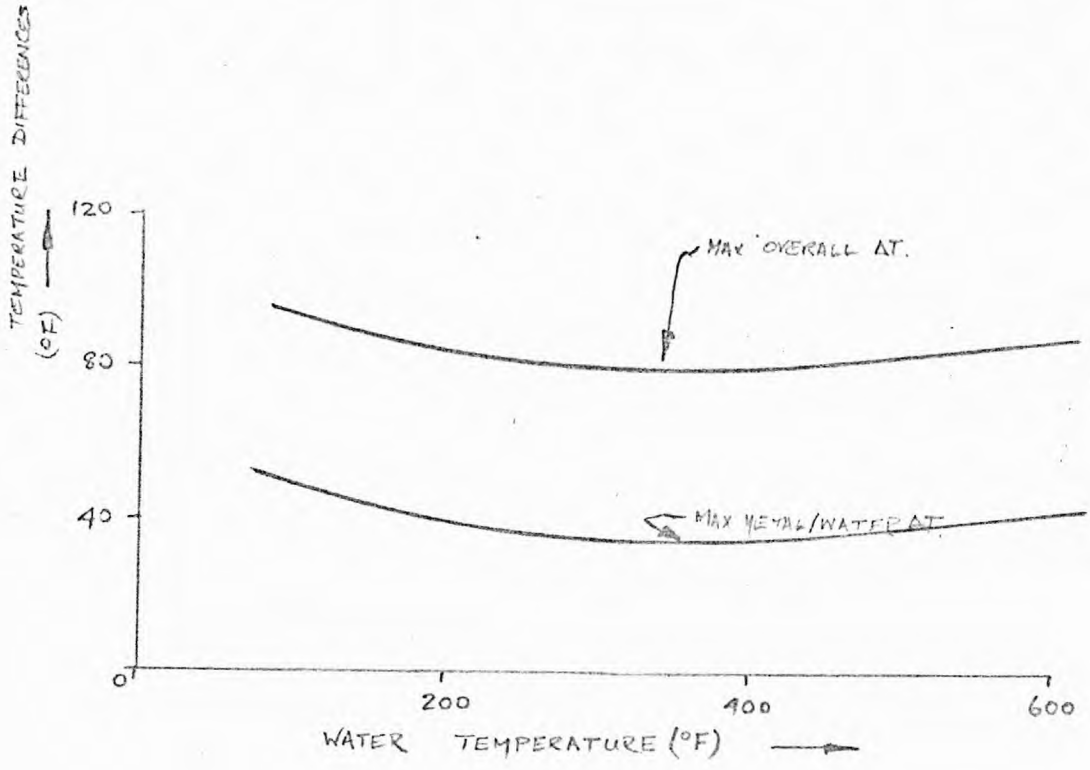

FIG 5.3 NATURAL CONVECTION HEAT TRANSFER

the water/metal temperature differences required to transfer the heat were calculated. These were combined with the calculated temperature differences across the metal and the totals are plotted on Fig. 5.3. These are under 55°F in the region of interest. No coefficients of expansion are quoted for steam but from the density/temperature curve these should cause no problem until very near the high temperature limit in which case this latter limitation would be more limiting on the operation. This was because the outside metal temperature would be near the limit and the power would have to be reduced to keep within the set limit reducing the heater power and the temperature differences. Also the amount of water would be very much less than at the low temperature condition because of the very much lower density, also reducing the heating requirements and the temperature differences. At this condition the external heaters would be used basically to offset the heat losses.

The heat transfer to the unheated flange can be worked out in a very similar manner and although effectively remote for the thermal stress aspect from the heated section and curve B as shown in Fig. 5.3 is obtained. This shows that the worst case is at 100°F where the total temperature difference is under 105°F, within the limits set by BS 1515.

The heat transfer to the head is outside the correlation limits given in McAdams but predicted values

would again give values within those set by BS 1515. This however would be an unrealistic limit as the head is in contact only with the unheated flange whose temperature would be similar and as only the temperature differences in the head itself need to be considered which are well within the limits and so there was no thermal stress problem associated with this part of the vessel.

3. Brittle Fracture

Failure of the vessel due to brittle fracture was removed by the stipulation on operation that the vessel was not to be pressurised at temperatures below 74°F, the pressure test limit being 60°F min.

Neutron irradiation can cause the embrittlement and loss of ductility of steels if the neutrons have sufficient energy (>1 Mev) to cause dislocation and defects in the metal structure and is experienced as an increase in the brittle fracture transition temperature.

This effect is only of significance for integrated fast neutron doses of greater than 10^{17} nvt (fast flux/hr) and this is far above the dose likely to occur in the vessel. Also if the temperature is high the damage caused can anneal out and generally for low alloy steels this becomes effective above 500°F reducing the importance of this effect to very small proportions.

For these reasons a full investigation into the effect of the neutron irradiation was not carried out.

4. Accident Analysis

The normal form of accident that would occur during a maloperation of the vessel would be the blowing of the safety valve discharging into the Dump Tank. The capacity of the tank being considered sufficient if it was half full of water and fitted with splash guards over the top. The safety valve exhaust was not led to atmosphere due to the long length of piping that would have been required to clear the building and that a busy road was nearby. To protect personnel no access to the experimental area was allowed while the vessel was being heated. An interlock to do this will be incorporated when the proposed Van de Graaff safety system is fully operational. The mesh door into the area was closed by a special castle key and it is proposed that this has to be inserted into a lock on the accelerator control panel controlling the belt start circuit. A connection is to be taken from this lock so the key has to be inserted before supply can be fed to the heater control switches.

As limited access to the experimental area was allowed while the vessel was at pressure but not being heated and to protect other equipment, concrete barriers 12" thick could be placed round the vessel as a safeguard from steam jets in the event of an 0 ring leak.

In order to decide on the worst accident to be guarded against one has to consider how failure might occur, bearing in mind the testing and inspection the vessel had undergone. The vessel was pressure tested at the works and in the College. All the welds were fully X rayed, dye penetrant tested, and magnetic crack detection carried out where possible except for the nozzle/head and the main piping/flange welds where X ray inspection was not possible.

These welds were considered weak points not only because of the lack of X ray inspection but also because the nozzle/head weld could be loaded in torsion when bolting up the flanges and the piping/flange weld could be strained if the piping took any loading.

In a failure of the nozzle/head weld the failure would tend to be along the cladding/head interface rather than round the nozzle above the weld. This meant that a missile guard would not be required and no allowance have to be made for the rapid de-pressurisation of the vessel due to the orifice provided (about 4 sec to reach sub-sonic flow for the 4" dia. hole if a heater flange blew out). The effect, without nozzle ejection, would be a small leak of lesser importance than other possible failures.

Failure of the piping/flange weld would cause an orifice of $\frac{1}{2}$" diameter which would mean that the

de-pressurisation time to sub-sonic flow would take over six minutes and any blast loadings could be ignored. The pressure build up in the area would be very slow and as the room was air conditioned on a balanced intake/ extract system this could be neglected. Any leaks of 0 rings or seals would give smaller orifices than the piping weld failure even if a vent plug blew out or a length of main 0 ring between two studs collapsed so these were covered by the failure considered. The temperature rise was not of importance as no personnel would be present in the area but indication of the ambient condition was available in the Control Room.

5.3 STUD AND SEAL DESIGN

Since the system was self pressurising any leakage losses had to be very small. Confidence could not be put in asbestos filled metal seals as troubles had occurred with previous vessels at lower conditions and the long term sealing properties of these and similar types of gaskets was not well known at the high condition. To meet the leakage requirement metal 0 rings were used for all the vessel flange seals.

Two types of 0 rings were used depending on the operational requirements and the required bolt loads. The small flanges for the 1" nominal bore nozzles used solid Stainless Steel oval 0 rings. These were re-usable

and required 8 $\frac{3}{4}$" dia. bolts to seal giving an overall flange diameter of $6\frac{1}{8}$". On the $2\frac{3}{4}$" bore nozzles the bolt sizes for a solid 0 ring would have created a serious limit due to high sealing forces required but the economic penalty of using single use 0 rings was out weighed by the practical advantages. The economic penalty was small as these seals would need to be broken very infrequently, the only time being when the very large cylinders were being used. The 0 rings used were hollow Stainless Steel toroids vented to the pressure side and were .010" silver plated to improve the sealing properties. The sealing forces were very low, 600lb/in. seal being required for these as against 26,000 lb/in seal for the solid rings and the forces required during bolting up were neglected as the 0 rings were easily deformable and had very little spring back. The reducedforces meant that flanges for the $2\frac{3}{4}$ bore nozzles had an $8\frac{1}{2}$" overall diameter and used $12\frac{3}{4}$" bolts. This meant that all the flanges on the head could be bolted up using standard torque wrenches and to get the required .005/6" and .007/8" extensions on the small and large flanges respectively a force of about 120 ft. lbs. was required. Care was taken not to load the nozzle/head weld by using two spanners but even this torque, if applied, would cause a stress of under 1000 lb/in^2 in the weld.

The main flange seal used an 0 ring similar in construction to those in heater flanges but was 40 ins

and required 8 $\frac{3}{4}$" dia. bolts to seal giving an overall flange diameter of $6\frac{1}{8}$". On the $2\frac{3}{4}$" bore nozzles the bolt sizes for a solid 0 ring would have created a serious limit due to high sealing forces required but the economic penalty of using single use 0 rings was out weighed by the practical advantages. The economic penalty was small as these seals would need to be broken very infrequently, the only time being when the very large cylinders were being used. The 0 rings used were hollow Stainless Steel toroids vented to the pressure side and were .010" silver plated to improve the sealing properties. The sealing forces were very low, 600lb/in. seal being required for these as against 26,000 lb/in seal for the solid rings and the forces required during bolting up were neglected as the 0 rings were easily deformable and had very little spring back. The reducedforces meant that flanges for the $2\frac{3}{4}$ bore nozzles had an $8\frac{1}{2}$" overall diameter and used $12\frac{3}{4}$" bolts. This meant that all the flanges on the head could be bolted up using standard torque wrenches and to get the required .005/6" and .007/8" extensions on the small and large flanges respectively a force of about 120 ft. lbs. was required. Care was taken not to load the nozzle/head weld by using two spanners but even this torque, if applied, would cause a stress of under 1000 lb/in^2 in the weld.

The main flange seal used an 0 ring similar in construction to those in heater flanges but was 40 ins

diameter. Even with this size of seal the gasket sealing force was only 31 tons compared with a hydrostatic force of 2130 tons at the design conditions. This meant that the stud area was as low as possible but even so torque wrenches could not be used for the stud tensioning. These are limited to bolts under about 2" diameter so 64 bolts would have been required which could not have been accommodated on the flange unless double banking was used complicating the design. Stud tensioning methods used on larger studs had to be considered and a stud arrangement of 20 3½" dia. studs on a 46" P.C.D. with 5" O.D. cylindrical nuts was designed giving an overall flange diameter of 4' 5".

A frequently used method of stud tensioning is the use of belt heaters. These are heaters placed in a hole in the centre of the bolt and the stud heated up while the vessel remains cold. The nut is then tightened down and when the stud cools down the stud is pretensioned. This method is very simple but has a number of drawbacks. The bolt is larger than required to allow for the central hole for the heater which would have been difficult in this design and also the process can be lengthy unless there is experience in its use which was not available in the college.

Hydraulic Tensioners are sometimes used but these tend to be expensive. A variant on this method is to force apart a split nut, one part acting on the stud, the other

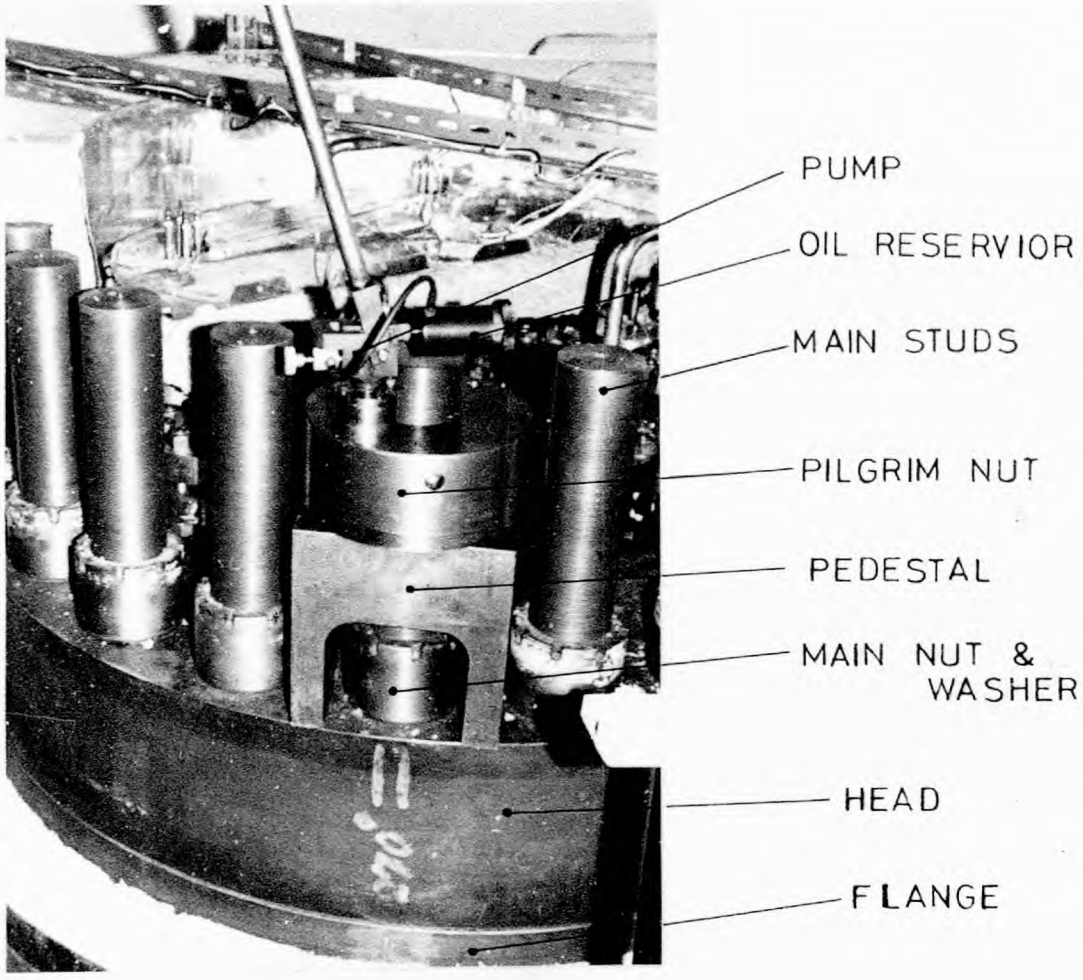

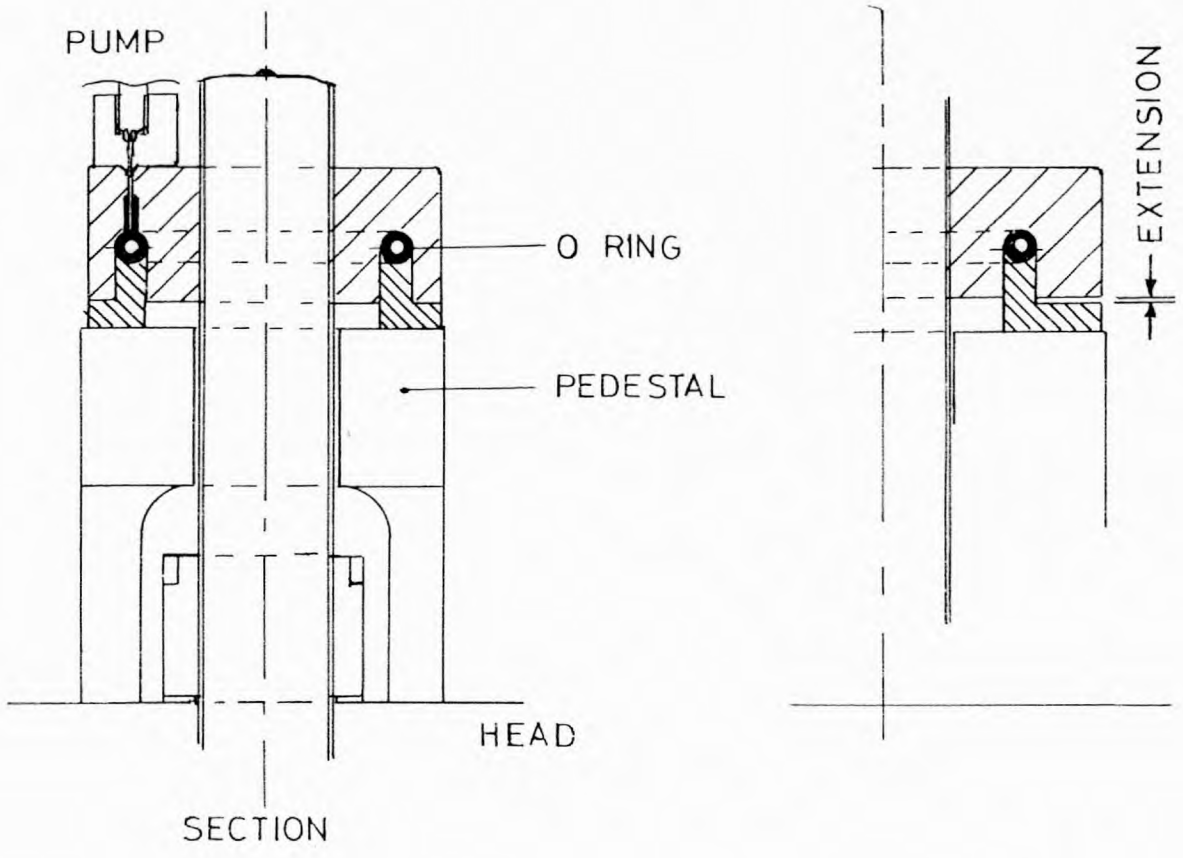

FIG 5.4 STUD TENSIONING ARRANGEMENT

acting on the head stretching the stud allowing the normal nut to be tightened down to give the required pretension after which the split nut can be removed. The form of split nut used on the vessel was called a Pilgrim Nut (Registered Trade Mark).Originally this used Allen Keys acting on a solid PFTE 0 ring to give the seperation force but it was found that this method did not develop sufficient force and an extension of only .017" of the .020" required for the hydraulic pressure test was obtained, which meant that the main seal leaked at a pressure below the test pressure. This nut was redesigned to incorporate a thick walled toroidal rubber 0 ring pressurised by a 40,000 lb/in^2 oil pump which gave the force required. The actual arrangement and the method of operation is shown in Fig. 5.4. To keep a .020" extension the stud had to be extended .042" using the Pilgrim Nut to allow for the extension of the stud between the two nuts and any slackness in flogging up the cylindrical nut. The extension was measured using a distance piece passing through the vessel body flange screwed into the base of the stud. This was done as a true extension measurement was required since the stud could move in the main flange during tightening up. A special micrometer was purpose made out of 1" mild steel bar and some micrometer parts as shown in Fig. 5.5a. As only relative extensions were required this was not calibrated to give an absolute length. Measurements were reproduceable to .001" though on the vessel the measurements depended slightly on the operator as the distance

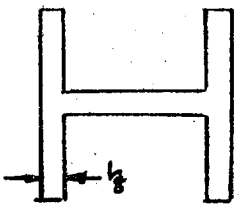

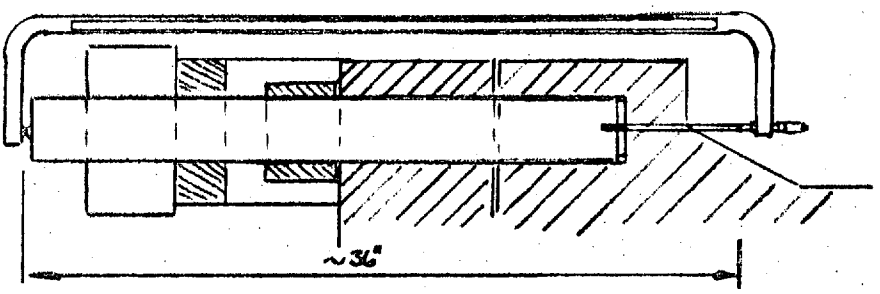

FIG 5.5a MAIN STUD EXTENSION MEASUREMENT.

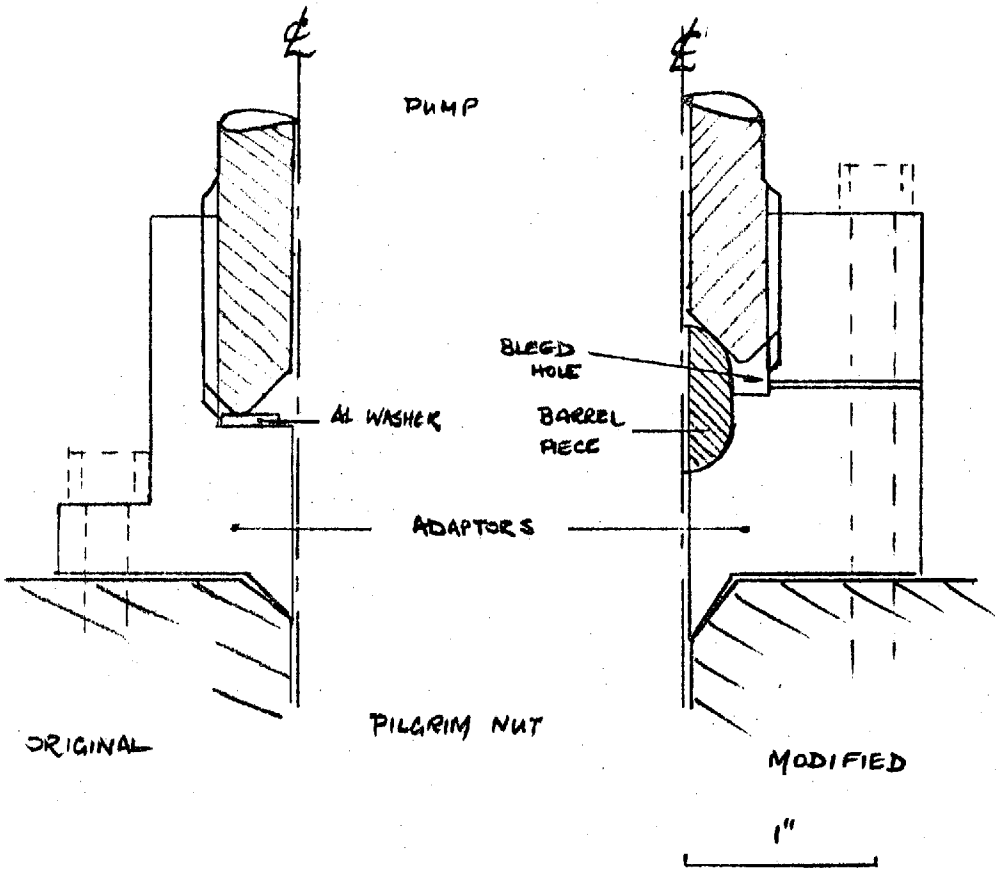

FIG 5.5b ADAPTOR FOR PILGRIM NUT

pieces were not domed which should be carried out. This error was within the required extension measurement accuracy. Any differences in the temperature of the vessel and micrometer would cause a negligible error in the measurements and these temperature differences would be very small as they were both in ths same area.

A design fault was found in the pump/nut adaptor as delivered which resulted in the ejection of the pump from the nut at pressure, luckily with no serious consequence. This was caused by the flat Aluminium washer sealing the pump adapter joint lifting and leaking. No bleed hole was provided and due to the inadequate stiffness of the adaptor it expanded and the pump was forced out. This has been redesigned using a cone seating with a bleed hole and a stiffer adaptor, the two designs being shown in Fig. 5.5b.

The time required for extending a stud was very short and a complete tensioning using three lifts to obtain the required tension was done by two people in two working days. Improvements in the design are possible mainly to reduce the extra length of stud required which would considerably ease the operation as clogging of the threads by dirt occurred as well as time taken to wind the nut onto the pedestal.

The method was accurate as well as easy and the extensions were consistent. The measurement of the extension by using a rod through the centre of the stud would have been easier but the area for this was very limited

due to the bolting up forces and was not incorporated. The slewing ring on the base frame enabled the vessel to be rotated and this greatly eased the stud tensioning as the pedestal which weighed over 95 lbs. and the Pilgrim Nut (75 lbs.) did not have to be carried around the vessel.

To bleed any air trapped in the nozzles when filling the vessel with water $\frac{1}{8}$" diameter vent holes were provided in the nozzle flange, these being sealed with $\frac{1}{8}$" B.S.P. taper plugs as shown in Fig. 5.6a. These were found difficult to seat properly and reliably, the head of the plug sometimes being distorted before sealing was achieved. This was due to galling of the threads even with the use of anti-scuffing paste and also that the sealing threads in the flange were the most likely to be damaged being the outer ones. Since these vents were meant to be used with the vessel slightly warmed just before taking the vessel to pressure it was felt this method did not satisfy its requirements especially with the possibility of distorting the plugs in obtaining a seal. In the short term galvanised steel plugs could be used as required as they did not suffer from galling and sealed better due to the dissimilar hardnesses of the metals. Corrosion was not a great problem as the plugs could be replaced each time but at a high temperature the differences in the coefficients of expansion would act against the seal so they were not considered satisfactory for high temperature work.

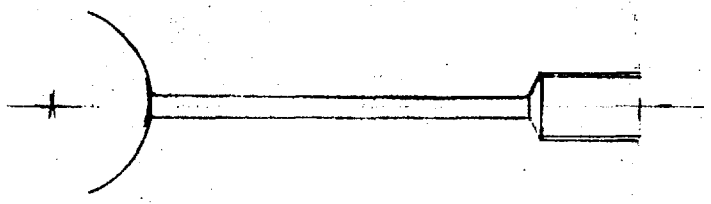

a) ORIGINAL DESIGN USING STAINLESS STEEL 1/8" BSP TAPER PLUGS (SEE DRG. 98/4337/F/R10 R22)

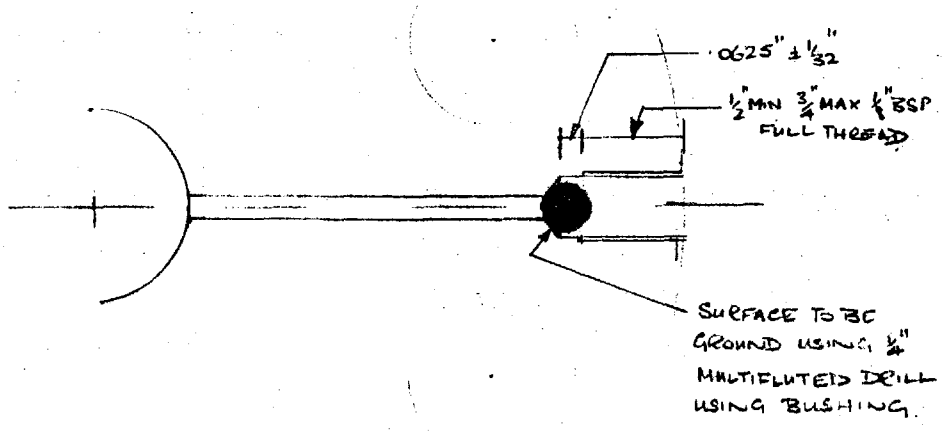

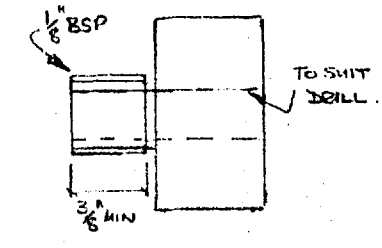

BUSHING HARDENED STEEL.

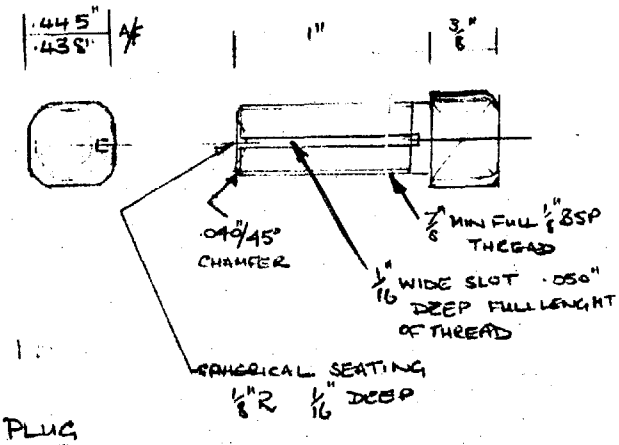

PLUG
STAINLESS STEEL 12off. 1/2" BAR

BALL. 1/4" ϕ HARDENED STAINLESS STEEL.

FIG 5.6 MODIFIED VENT SEAL DESIGN

A new seal design has been proposed using a hardened Stainless Steel ball bedding into a prepared cone being held by a $\frac{1"}{8}$ B.S.P. straight bolt as shown in Fig. 5.6b. The sealing was to be prepared using a modified multi-fluted drill with a bushing guide, as a flexible drive would be necessary for some flanges and to protect the existing threads. The bolts were to be made with a groove along the threads so the bolt would not be pressurised if a leak occurred and the leak could easily be seen. This modification had not been incorporated on the vessel due to lack of time but insurers' approval had been obtained.

5.4 PRESSURE CIRCUIT

Connections to the vessel had to be provided for the necessary control and measurement facilities allowing the safe operation of the system. As previously mentioned the safety valve was connected to the vessel by a length of main piping but connections also had to be provided for the control valves and the pressure measurement. The system was controlled from the Accelerator Control Room for safety reasons and so the valves had either to be remotely actuated with the valves on the Dump Tank or manually operated in the control room. The first method would require a reliable actuator that would operate even in the event of failure of the normal supplies and the reliability requirements would be stringent. Piping to the Control Room was required for pressure indication and

enough difficulty was experienced in obtaining a valve for manual operation that it was decided to use this form of valve operation without the reliability analysis and testing associated with the remote valve method.

The layout of the piping is shown on Fig. 5.7 and can be seen in Fig. 1.3. Two forms of tubing were used, the main piping being .840" O.D. x .187 wall tube to SA 312 TP 321 Stainless Steel and the elbows and used with it being of TP 316 steel and the connecting pieces of EN58B. All these joints were made using argon arc welding by a certified welder and were dye penetrant tested. This was made in two parts, one for the safety valve described in Section 5.2.1 and the other to tubing to the Control Room. This piping was $\frac{1}{4}$" O.D. 18G to the same specification as the main piping and the coupling pieces again to EN58B. These were brased together using a 620/630^{o}C Silver Solder. The necessary washers were made of pure Aluminium but for prolonged operation annealed silver washers should be used. To allow for the thermal expansions in the tubing and moving the vessel without disconnecting the piping it was bent and coiled to give adequate flexibility, a minimum radius of curvature of 3" being used and can be seen in Fig. 1.3.

Two valves in series were used for control and shut off as after operation the seating of the control valve could become scored giving rise to possible leaks. The method of operation was to open the last valve and

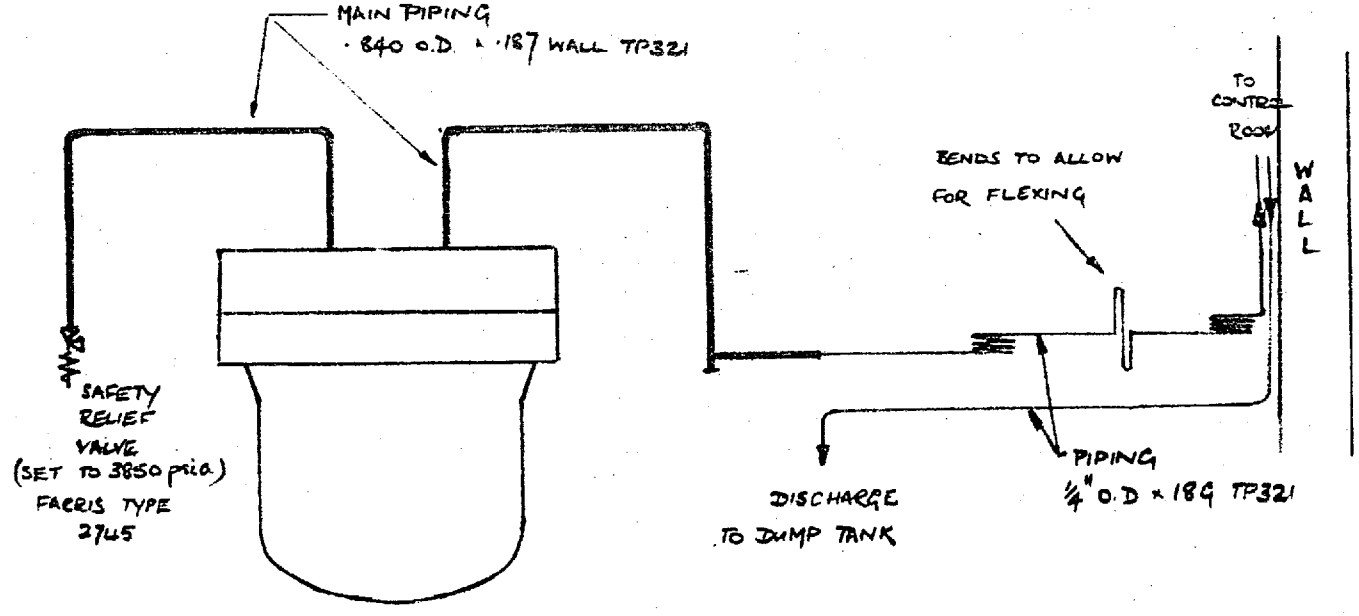

a) PIPING IN EXPERIMENTAL AREA

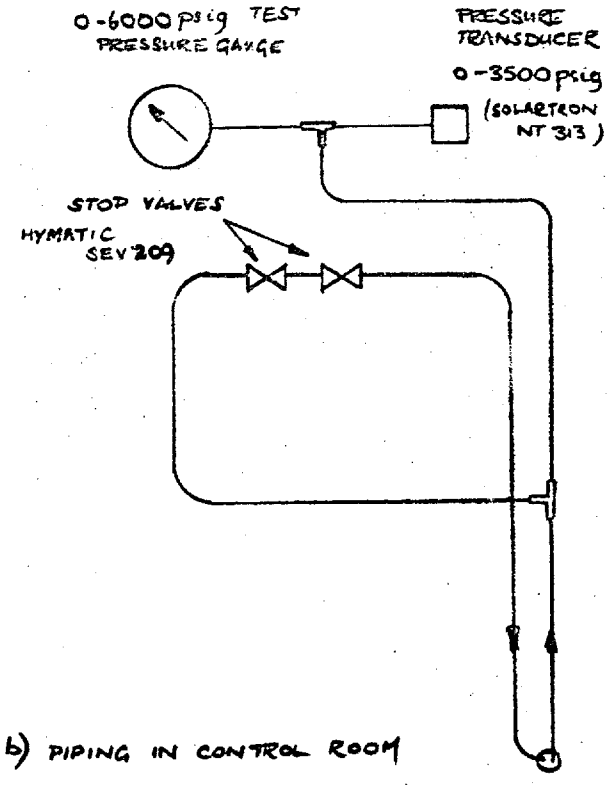

b) PIPING IN CONTROL ROOM

Fig 5.7 PRESSURE PIPING

then use the first as the controller and using the last as a shut off after the first had been closed. The long length of piping between the vessel and the valves allowed some cooling of the water being bled off before it reached the valves. This was helpful as the life of the bellows sealing the valve stem from the downstream flow was very dependent on its temperature and this would prolong its life.

Visual Pressure Indication was done by a 6" $\frac{1}{4}$% test gauge reading to 6000 psi which was used as the indicator in the pressure test carried out on site. For the accurate pressure measurement a test gauge having a quoted accuracy of $\pm$ .05% was to have been used but due to the failure of the maker to supply this item a pressure transducer was obtained with its associated high stability D.C. Supply. This gave full scale output of about 20 mV for a supply voltage of 5 volts which could be adjusted for sensitivity as well, a balanced measurement being based on the Wheatstone bridge method. The output was measured by a digital voltmeter having a sensitivity of 2.5μv equivalent to .3lb/in^2. This was calibrated over a limited range with a dead weight tester though a full scale calibration would have to be carried out for future work.

A pressure switch was also connected to the piping. This was adjustable over the operational range and had a set differential of 500 lb/in^2. This was used in the heating control circuit to prevent pressure increases whilst

heating reaching values at which the safety valve might operate.

The exhaust from the control valves was fed by $\frac{1}{4}$" O.D. 20G tubing similar to that used on the pressure circuit to the Dump Tank where it could be cooled and kept. The lengths of piping were connected using stainless ermeto couplings.

5.5 VESSEL SUPPORT AND MOVEMENT

The Base Frame had to be designed to enable the required movements of the vessel as mentioned at the beginning of the chapter to be carried out. The major movement was from the well to the experimental position as shown in Fig. 5.1. Movement in line with target would enable other experiments to be set up at the target when work was being done on the vessel. The vessel support structure had to allow for the thermal expansion of the vessel on heating up with the minimum straining of the vessel or the support legs.

The Base Frame was designed to carry the Pressure Vessel and the Dump Tank together reducing such problems as the safety valve restraint structure. The well size was 11 ft. x 6 ft. setting an overall limit on the Base Frame size but the actual width limitation was less than this, because other apparatus would have been difficult to move. The Base Frame was made up of 8" x 6" x 35lb.

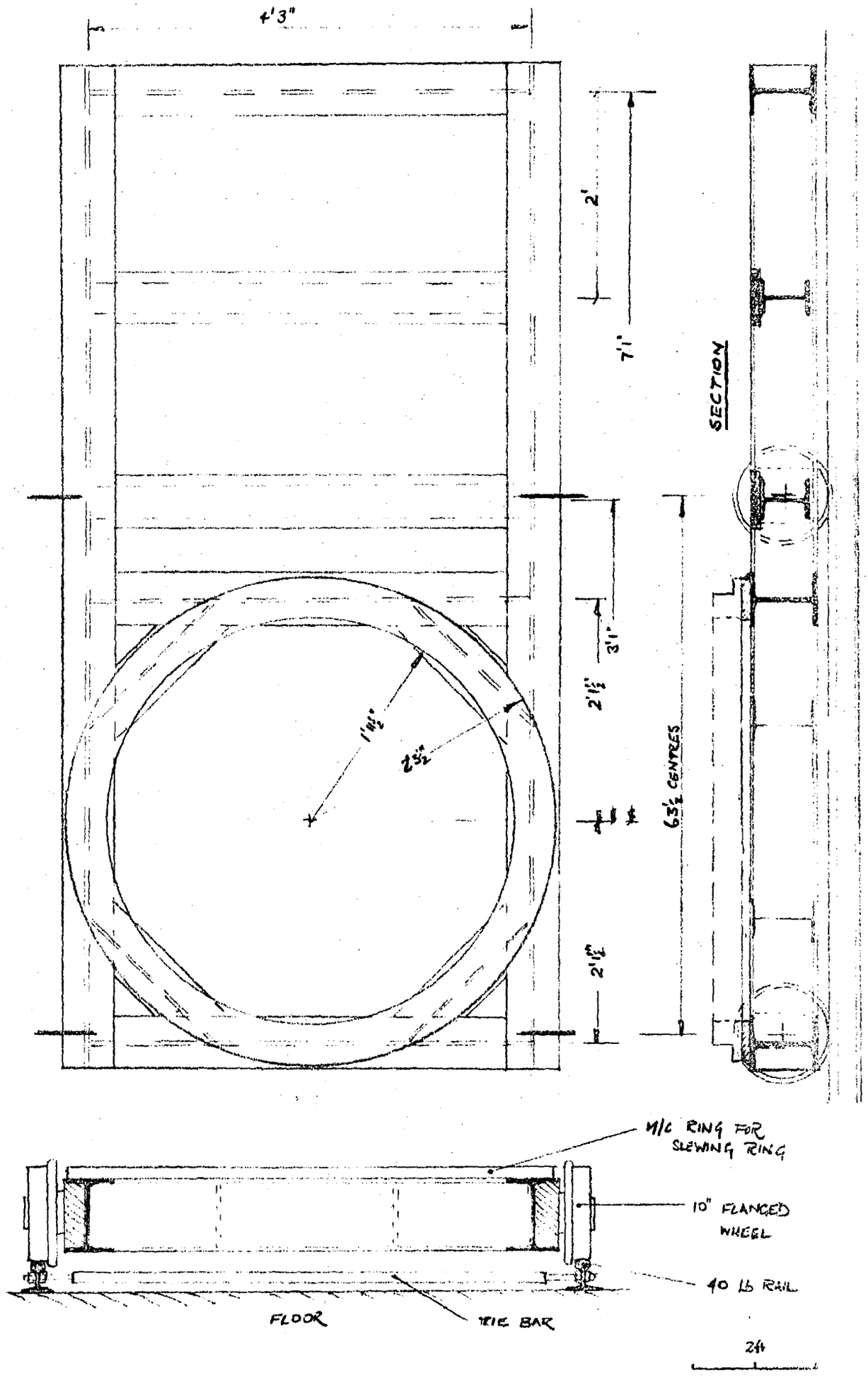

Fig 5.8 BASE FRAME & RAILWAY DESIGN

R.S.J. basically forming a braced structure 116½" x 54" weighing 17 cwt. the design being shown in Fig. 5.8. The three vessel support legs acted on a Slewing Ring of 43½" I.D. using a single ball bearing race running in flame hardened races, this allowing the vessel to be rotated easily by one person. The Slewing Ring was bolted to a 4" x 1" x 23½ O.D. mild steel rolled ring welded to the base frame. This ring was machined to provide a flat surface after the frame had been stress relieved. The notched pieces of R.S.J. were welded into the frame to improve the ring support over the whole area. The area inside the ring was kept clear as the vessel and lagging extended below the top level of the base frame.

The Frame ran on rails laid on the laboratory floor. The wheels, incorporating dry bearings, were made of steel being 10" diameter flanged on the inside edge. They were bolted to the Base Frame as shown in Fig. 5.8 giving a distance of 61¾" between centres. This distance was chosen to allow the vessel to be manoeuvred without any major readjustments to existing equipment and this gave the largest rail radius of curvature (25ft.) for which only minor changes were required. The wheels gave an overall width of 5' 5½" to the frame.

The wheels ran on 40 Lb Bull Head Rail using a track of 4' 11". Tubular tie bars were used for the rail spacing as sleepers were not required because of the flatness and strength of the floor area and would not only

increase the vessel height causing design problems but would also have made the rail sections much heavier. A chain pull acting from bolt positions let into the floors and walls was used to manoeuvre the vessel to the experimental position in line with the accelerator flight tube on the straight rails using the four lengths of track (2 straight, 2 curved) as required.

Thermal expansion of the vessel would cause a radial movement of the support legs of $\frac{1}{8}$" and bearing pads were incorporated to allow for this. Often these take the form of pads of dissimilar metals but they are not only uneven in action but make it difficult to accurately predict the loadings on the vessel and support structure. This would have made the support legs difficult to design but also the slewing ring would have had to be stiffened which would have been difficult within the design limitations. To give a much better and predictable response without such stiffness requirements on the legs and support structure flat needle roller bearings were used. These were limited in their operating temperatures so some thermal insulation was incorporated between the legs and the bearing pads. This also reduced heat losses and would have been difficult to incorporate with the other design due to the higher stresses that would occur.

The actual arrangement is shown in Fig. 5.9. The vessel support leg had a recess cut into it similar to one

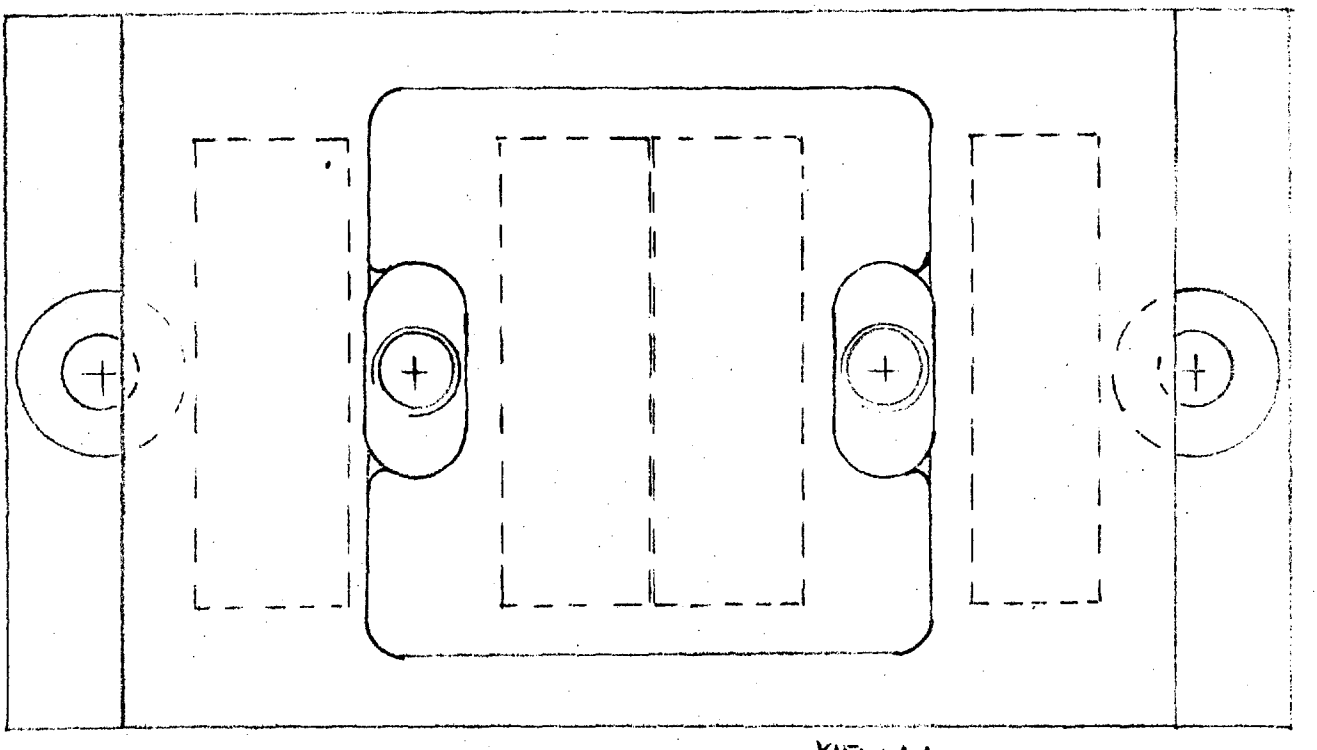

VIEW AA.

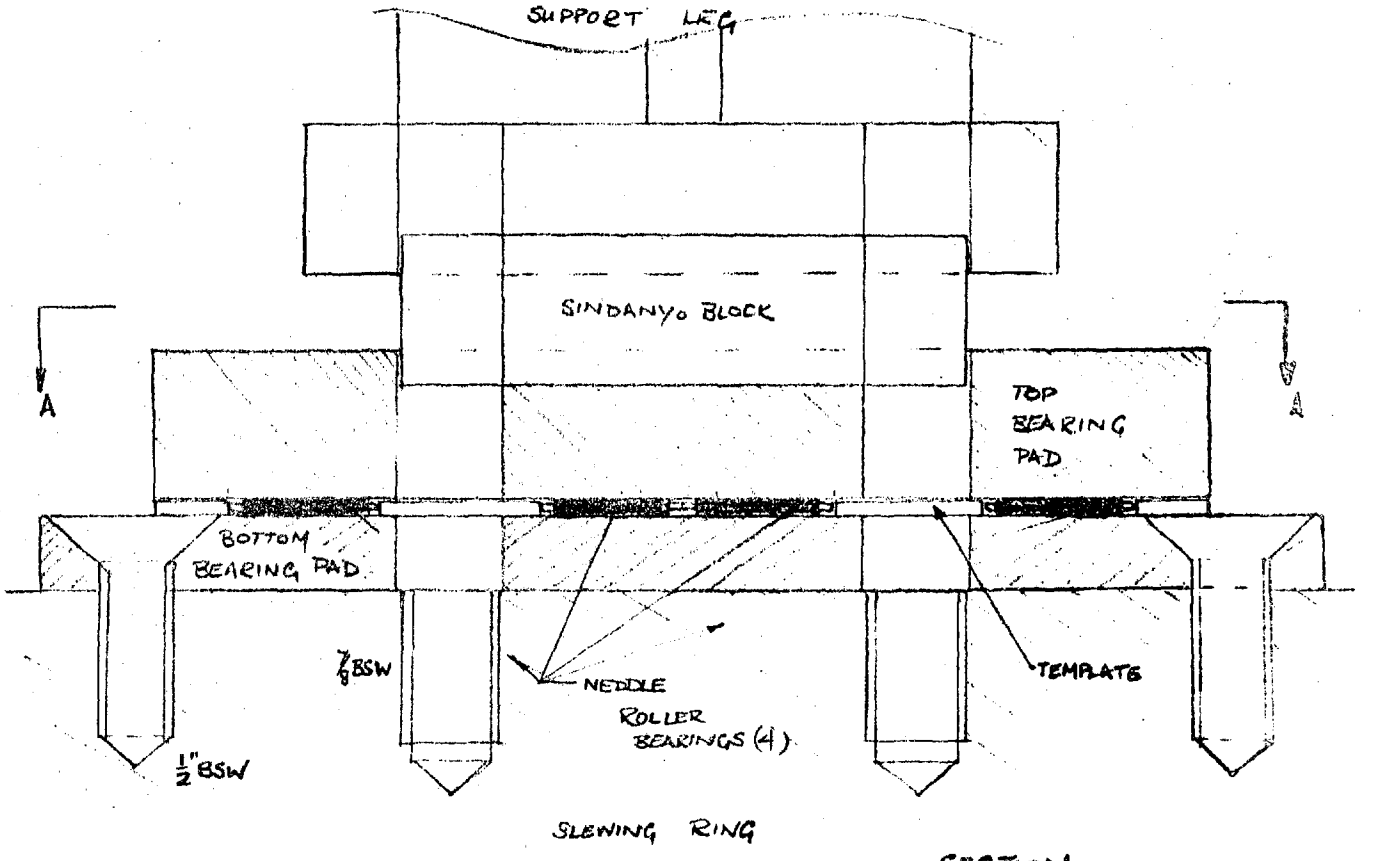

SECTION

1"

FIG 5.9 VESSEL SUPPORT BEARINGS

in the top bearing plate to take a 1" thick block of Sindanyo insulating material. This would reduce the maximum heat loss to under 100 watts neglecting any temperature drops in the support legs. The bearing plates were hardened to Rockwell 60 - 64 and ground. They held four bearings in each leg support guided by a tem-plate. The bearings were derated from the straight load requirements by a factor of four to allow for the small movement of the bearings. The bottom bearing plate was bolted to the slewing ring as shown. For the main movement, as security, the vessel was clamped to the Base Frame using bolts, passing through the legs and bearings, screwed into the ring. This increased the loading on the bearings but the vessel was empty and there was no relative movement easing the limitations. The holes formed were closed with Sindanyo blocks normally to reduce any heat transfer.

The Dump Tank was bolted onto the back of the Base Frame, greatly simplifying the design and allowing for the jacking requirements. The Tank rested on the back cross frame and the two side beams and to give better overall support on two 6" x 1" flats which in turn were welded to 6" x $3\frac{1}{2}$" x 11bl. R.S.J. which fitted neatly into the side beams. The Dump Tank was bolted to the frame by eight $\frac{3}{4}$" bolts passing through the Dump Tank Stiffeners.

The design of the various parts was based on converting the two dimensional structure into equivalent one dimensional structures and taking the worst conditions and arrangements of loads. Any stiffening effects such as the notched R.S.J.'s supporting the ring would provide have been neglected. In all cases the maximum stresses have been well under 5000 lb/in^2 the calculation being based on Macauley's Method.

Since the rail track extends up to the target it is recommended that other experiments using the accelerator are made up of frames that can be placed directly onto the track by a crane which would simplify the change-over of experiments and would allow the setting up of the experiments, which takes most of the time, to be carried out away from the target increasing the accelerator availability.

5.6 DUMP TANK DESIGN

As mentioned in the accident analysis the Safety Valve exhausted into the Dump Tank. This had to have sufficient volume to take up not only water exhausted but also to cool this with the water already in the tank. During a run, up to 200 gallons of demineralised water would be bled out of the vessel and the replacement of this quantity of demineralised water each time would be difficult, so it would be useful to retain as much as

possible. The tank would have to have sufficient cooling to keep the water temperature down in case the safety valve operated. If the water was to be used again then the corrosion rate would have to be low so impurities were not present in the water for the later experiments.

The Dump Tank was chosen to have a capacity of 400 gallons and was made of 14 gauge EN58B Stainless Steel using argon arc welding. The sides of the tank were beaded for stiffness and braced by a structure of $1\frac{1}{2}$" x $1\frac{1}{2}$" x $\frac{1}{4}$" angle, the top ring being made of Stainless Steel but for reasons of cost the side and bottom members were made of mild steel. The Tank can be seen in Fig. 1.3. Stainless Steel was chosen in preference to metal or plastic coated tanks due to the freedom from corrosion caused by scratching or abrasion of the coating and the possible effect of the safety valve exhaust on the coating as the cost differences for the various types were small.

The water in the Dump Tank was cooled by economy water flowing through three $\frac{1}{2}$" OD 18G Stainless Steel tubes 14ft. long. The filtered supply to the tubes was controlled by electrically operated solenoid valves which for safety reasons were on the battery backed supplies. These were connected so that if the water temperature in the tank rose above 50°C the valves were automatically opened whatever the valve positions before. This condition meant that the water in the tank would condense the steam blown off if the safety valve operated. Indication

of the valves position was provided in the experimental area on the heater supply panel to ease checking as well as in the Control Room. The water level could be reduced by pumping out to waste if required but the water level indicator used suffered from corrosion so another probe will be required for future use.

The cooling tubes could remove about 7kW for an overall cooling water/tank water temperature of 30^{o}C but they were not placed in the best positions for various reasons. They were placed to one side in the bottom half so they were not directly under the safety valve exhaust and would be always covered and these factors might reduce the natural convection heat transfer. If required forced circulation could easily be introduced increasing the heat transfer, but was not considered necessary, by placing an impellor under the tubes using the cross beams to support the motor.

If the safety valve blew and was unrestrained the piping connecting the valve and the vessel would fracture because of the high strains that would be caused by the reaction force. To stop this the valve was clamped to the Dump Tank the design of the restraint structure being governed by a number of factors. The main one was that the valve had to be able to be clamped in all the positions that it could occupy. This condition whilst being basic was of importance as the flange could be placed on any of the small flanges the position depending

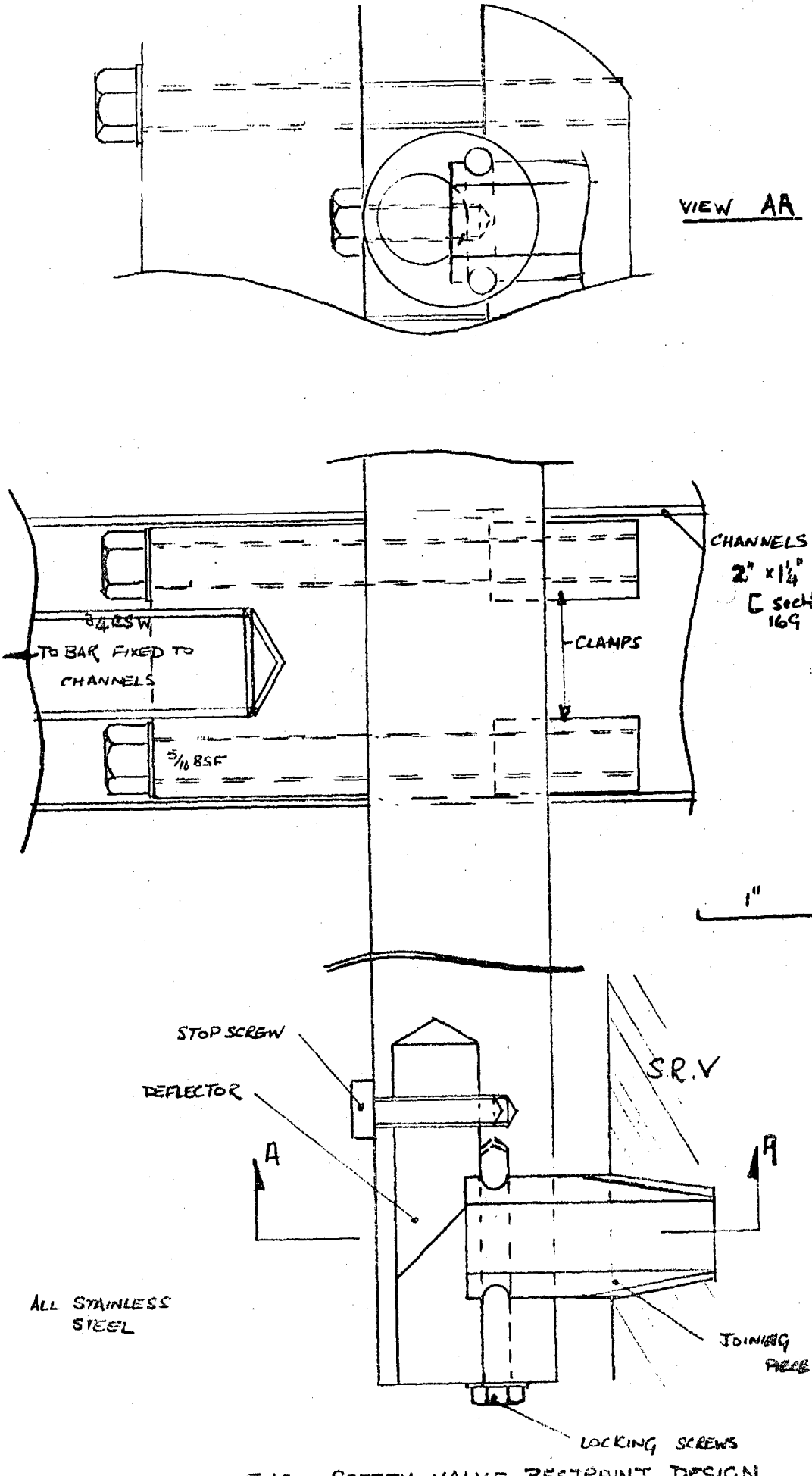

FIG 5.10 SAFETY VALVE RESTRAINT DESIGN

on the experimental arrangement and governed the overall variations that had to be allowed for. At the same time the connection between the valve and piping was a ½" BSP taper thread so its radial orientation was not fixed.

The overall movement was allowed for by adjustable blocks running in channels spanning the Dump Tank. The fine adjustments were made with a ¾" B.S.W. rod. This had the support bar, a 1¼"Ø Stainless Steel bar, clamped to it which gave the vertical and rotational variation required. This carried the exhaust deflector in it and was fixed to the valve exhaust as shown in Fig. 5.10 showing the restraint design.

The stresses involved in clamping the valve and not allowing for the thermal expansions in the piping were very small as the piping was relatively flexible and was not considered a problem calculations verifying this for the worst possible case provided the valve was clamped in the neutral position at room temperature. The structure was designed to take the full reaction force sideways and vertically to provide an extra safety factor and notice taken of the nature of the load and stress were held under a third of the yield stress.

6. HEATING AND COOLING

The heating and cooling capacities had to be such that the experimental cycle time was not too long while remembering the limitations set by the allowable temperature differentials and the available supplies. These consisted of a 75 kw three phase supply and two 30 Amp single phase supplies near the experimental position.

As the water temperature was of concern we would like to have as much heating in the water to reduce the control time lags and possible hunting in the control circuit. This would also help as at the low temperature conditions, when most of the heat would be required by the water, the heat transfer coefficient from the metal to the water is lowest so the maximum temperature differentials would be reduced as the capacity of the external heaters could be reduced. The installed power of 44kw would give an initial heating rate of $40^{\circ}F/hr$.

In this chapter the design of the heaters and insulation are discussed with the factors governing their design and then the control and safety circuits will be described. The proposed cooling arrangement will be outlined at the end of the chapter.

6.1 INTERNAL HEATERS

These were designed to incorporate as much heating capacity under the design limitations. The major one was that the elements and heater flanges were to be removable from the head which meant the elements had to pass through a nozzle 2¾" bore 14" long. They would also have not to foul the cylinders in the vessel but this was only of importance when the largest cylinder was used. The heaters were placed on four flanges, their positioning on the head having been already mentioned in considering the counter flange positions and are shown in Fig. 2.3. These were roughly roughly 45° to the small flange positions, the actual layout being governed by the three lifting lugs. The actual flange and element design is shown in Fig. 6.1 which gives the cranking and form of the heaters.

The heaters were made of a resistance element packed in insulation contained in a ½" O.D. Inconel sheath. The heaters after forming into shape were silver soldered into the flanges using Stainless Steel Sleeves. These were used to compensate for the differing thermal capacities of the heaters and the flanges and were argon arc welded into the flange. The heating section was started 2" below the level of the bottom of the head, an unheated section was used above this so no hot areas were formed in the nozzles giving rise to thermal stress problems. The heaters were controlled individually by seperate relays

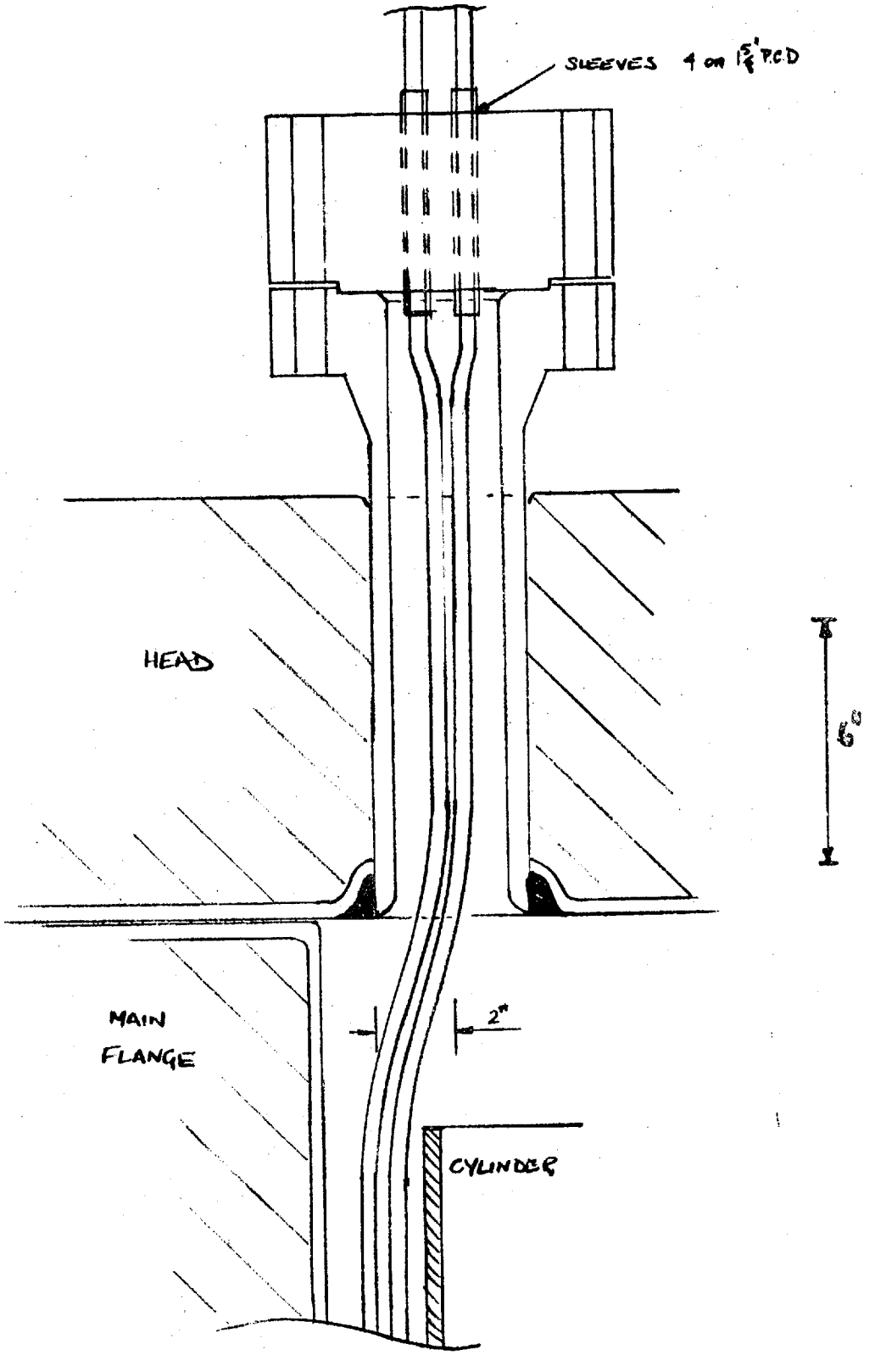

FIG 6.1 INTERNAL HEATER DESIGN

controlled from the control room and supplied from two single phase outlets one element on each flange being connected to each supply. If one supply was lost then the heating could still be evened out over the vessel within the heating requirements.

6.2 EXTERNAL HEATERS

The External heaters could have been of rod or tape form, the advantages of the latter being the ease of installation and the evenness of heating that can be achieved and the reduction of the temperature differential problem. They are however far more expensive the relevant costs being £650 and £125 for the two systems. At the time of ordering due to the lack of funds it was decided to try and overcome the disadvantages of using the rod type of heaters. These were similar in construction to the internal heaters and would be clamped onto the outside of the vessel using straps and the studs welded to the vessel body.

The main disadvantage of the rod heater was the presence of hotspots of unknown intensity where the elements were in contact with the vessel. It was decided that these would have to be removed or reduced to a known value. This implied that the heat transfer had to be evened out over a much larger area by the use of a good conductor between the heater and the vessel.

As a check on the calculations and for proving the actual arrangement to be used an experiment was set up to simulate the conditions that would occur on the vessel.

This was a slab mock-up of vessel arrangement and consisted of a 3" slab of steel 1' 3" square onto which two small heaters similar in construction to those to be used on the vessel could be clamped. The heaters were supplied from the mains using a Variac to control the power input. The fluctuations in the mains supplies were noticeable but only caused a small change in the overall temperatures and had little effect on the temperature differences measured. The temperatures were measured by a 0 - 450°C or a 0 - 150°C indicator controller with a range suppressor wiich enabled a back emf to be applied to the thermocouples in steps of 100°C and this will be discussed later. To cover the number of thermocouples put on the rig two single pole eleven way switches in series gave twenty possible thermocouple connections. The slab and heater arrangement was covered with brick type insulation the gaps being cemented over except at the back of the iron block where there was no insulation so the heat could be removed by the natural convection of the surrounding air. The arrangement is shown diagrammatically in Fig. 6.2.

Initially the experiment used only a layer of good conductivity material between the heater and the steel. Copper which would have been best on a conductivity

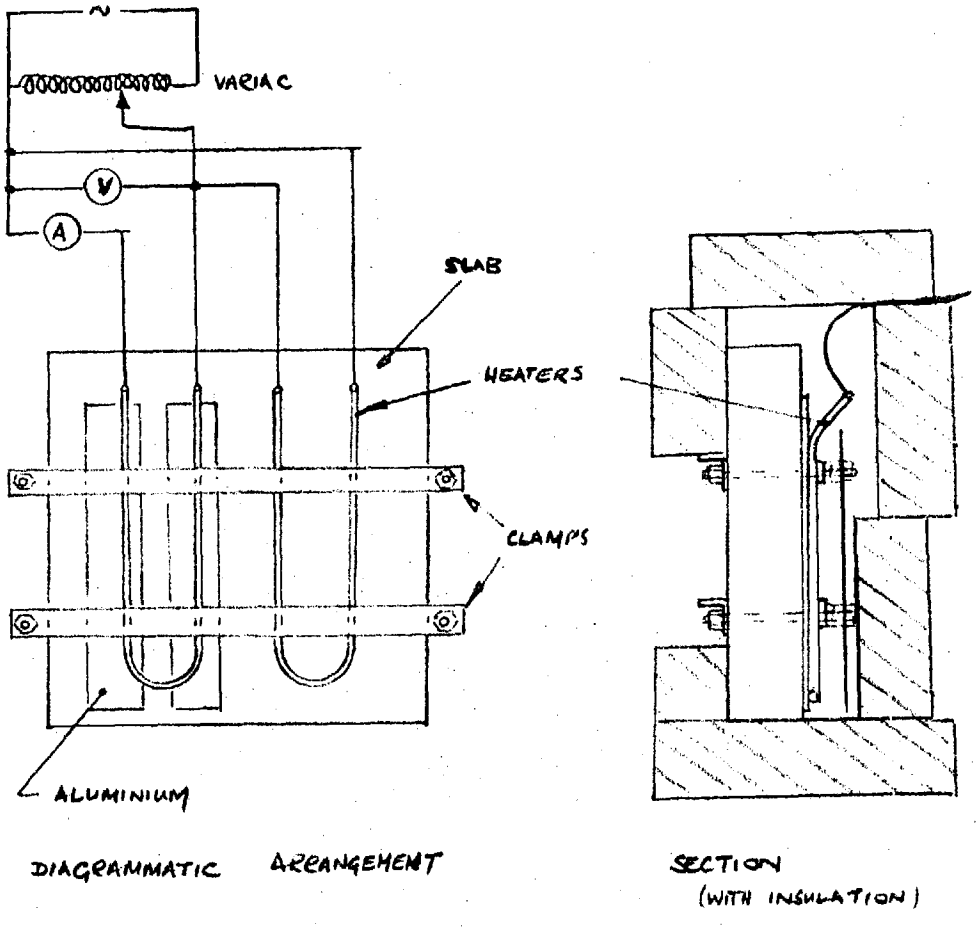

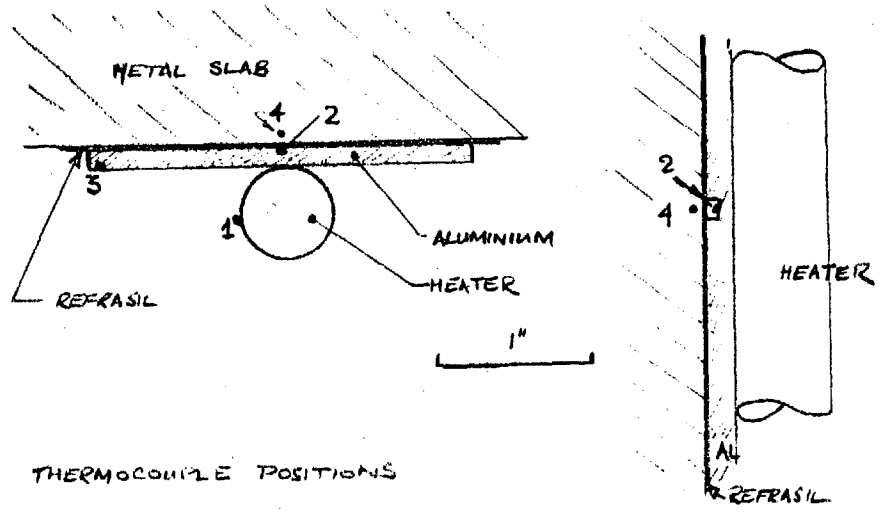

FIG 6.2 HEATING MOCK UP EXPERIMENT

basis oxidised too quickly but Aluminium performed satisfactorily. It was found that the contact between the heaters, Aluminium, and the steel varied and sharp changes in the temperature distribution occured because of thermally induced movement. This meant that there was a large scatter on the results and to cover the worst results the worst total temperature differences possible were near the limit for uniform vessel sections. For this reason it was decided to even out the temperature distribution and remove the metal to metal contact causing the problems. This could be done by placing a thin layer of insulation between the Aluminium and the Steel the maximum heater temperature limiting the allowable thickness of the insulation. Cf the possible insulator materials having controlled thickness and available in the sizes required only a cloth type was suitable and a .020" thick Refrasil Cloth was used in the experiments.

The arrangement with the Refrasil under 10 gauge pure Aluminium gave the observed temperature differences in Table 6.1 between the points shown in Fig. 6.2 with the heater power at 600 watts, this being equivalent to the vessel heaters at full power.

Table 6.1 Temperature Differences

Positions (see Fig 6.2)	Temperature Measurement positions	Temperature Differences °C
1 - 2	Heater - Al in groove	150
2 - 3	Al. in groove - Al. at edge	<10
2 - 4	Al. in groove - Metal Adjacent	45
4 - 5	Max. Metal temp. diff.	<20

The groove temperatures and the adjacent metal were measured by using thermocouples at the positions shown in Fig. 6.2 by leading them through a slot 3/32" wide x .060" deep machined in the Aluminium. The thermocouples were positioned using a high temperature cement and were Chromel-Alumel types. Aluminium spacers 2" wide were used in the test but on the vessel larger continuous sheets were used which would reduce the Al/Steel temperature differences due to the increased evening out that would occur. The high temperature condition was not reached because of the heat losses but the maximum heater temperatures would not be excessive.

The arrangement removed the need to consider the possibility of hotspots and the temperature differences that have to be considered are those in the metal caused by transferring the heat from the outside surface to the water. This has been considered earlier but the possible angular variations have also to be considered.

If one part of the vessel was unheated then this could have the heat transferred to it by two possible methods, the direct conduction of the heat from the heated zone through the metal or from the heated water.

The heat transfer through the water would mean a maximum temperature drop from the heated zone to the water of $55^{\circ}F$ as previously calculated. The temperature variation in the vessel would be low ($<5^{\circ}F$) and the temperature drop from the water to the cold metal on the outside would be under $5^{\circ}F$ so the total temperature drop would be under $70^{\circ}F$ well inside the limits laid down by the design codes. This is pessimistic because the code applies the criteria only to adjacent parts and the required heat transfer would be by conduction along the shell and the maximum temperature drop would be the $25^{\circ}F$ temperature drop in the metal to the water surface.

The arrangement on the vessel used the same basic layout of Aluminium and Refrasil and is shown in Fig. 6.3. This can be simply considered in sections the simplest being the cylindrical body above the main weld. Two pieces of Aluminium rolled to the correct curvature were used with the insulating cloth underneath. The heaters were clamped by a 2" wide strap and some Stainless Steel tapes which were used during the clamping up and were left on. The bottom parts were seperated from this by the main weld over which nothing was placed and the heater temperature rise caused by having the gap would be less than $50^{\circ}C$ not causing a limitation.

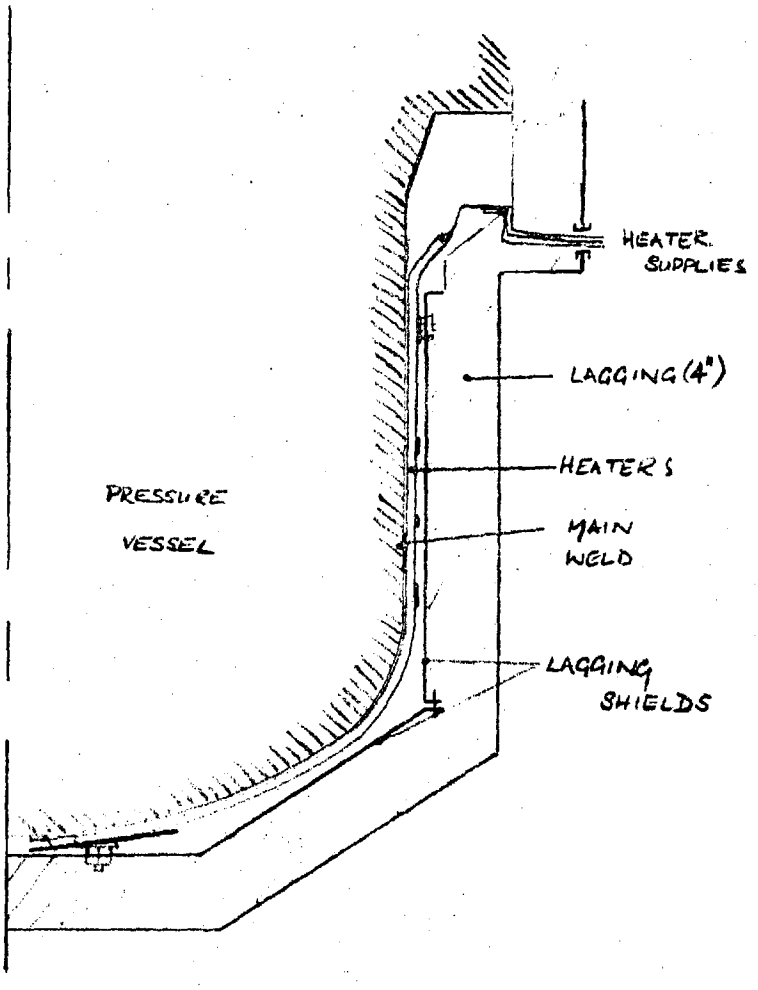

a) SECTION OF ARRANGEMENT

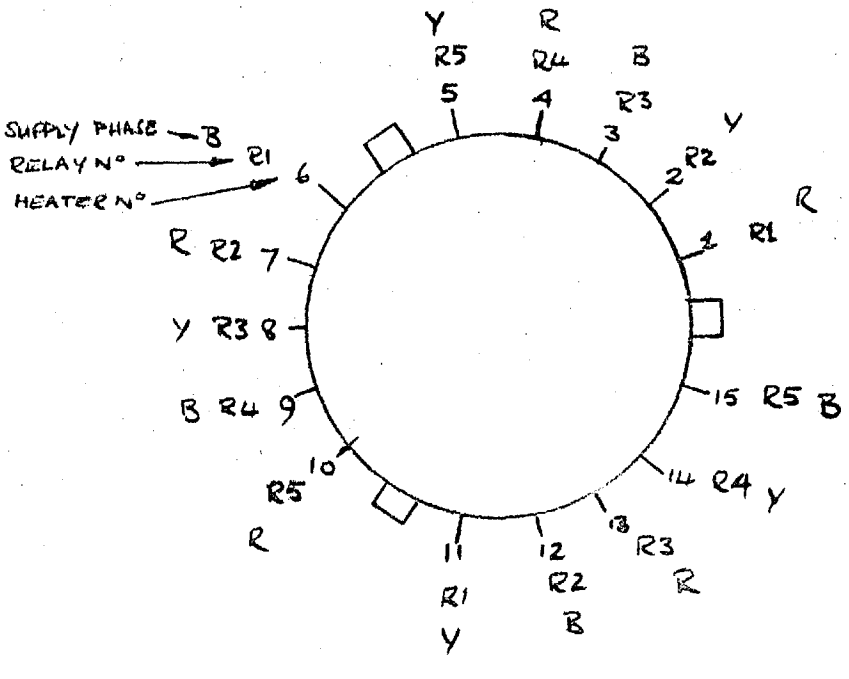

b) PLAN VIEW OF HEATER CONNECTIONS

FIG 6.3 EXTERNAL HEATERS

The bottom part was made in two sections. The underneath part used three pieces one each for each part of the vessel between the support legs. The spaces up to the weld area used segments, one for each heater, as it was difficult to form a larger shape. Both used a nibbling machine to form the curves and were annealed to retain their softness. Two clamps were used, one between the support legs similar to the one used on the cylindrical part the other was a disc 15" diameter with a central hole 6" diameter cut in it. This clamped against the heater as shown in Fig. 6.3 using the four ½ Whit studs welded to the base of the vessel.

The heaters were connected by single strand copper wires covered with Refrasil sleeving and led to three lead-outs in the insulation where soldered connections were made to ordinary P.V.C. covered multistrand cables, heat shrinking sleeving being used as insulation over the joins and to anchor the sleeving on the copper wire.

The heaters were connected in threes to form balanced star loads for the three phase supplies taken from the 75 kw 4 wire mains through an isolator, the three heaters being controlled by one relay. The connections were arranged around the vessel to minimise any temperature variations and were also arranged on the phases so if one phase was lost then the unsupplied elements would be spaced round the vessel and not concentrated at one point which could make the control more difficult. This is shown in figure 6.3b

where the numbers refer to the controlling relay and the letters to the phase the heater was supplied from.

The external heaters were not used in the work carried out on the vessel because of the problems with the vent plugs. It was felt that the vessel ought to be heated up to as high a temperature as possible using the internal heaters only to let the external heaters bed down on the Aluminium this being softer at these temperatures and let any relaxation take place before using the external heaters. Because of the problem with the vent seals the vessel condition was limited to under 100°C until the modification had been carried out as work was being done on the Accelerator at the same time and so temperature runs were not carried out above 95°C and the external heaters not used.

6.3 INSULATION

The rod heaters had to be used with a lagging shield providing an air gap over the back of the heaters the shield being made of 14 gauge mild steel sheet. The two half cylindrical panels rested on the support legs and were fixed to the studs welded onto the side of the vessel for this purpose. A split shell was used underneath and was fixed to the side panels and the studs on the bottom of the vessel. The arrangement is shown in Fig. 6.3

The lagging was basically a 4" layer of rockwool clad on the outside with 20 gauge Aluminium for protection. The bottom half of the vessel was finished in a permanent manner and only had the three heater lead outs and the support legs complicating the arrangement. The top part of the design was governed by the need to be able to quickly and easily remove the small flange over the piston movement so the piston height could be changed for another run. To give enough room to bolt this up again the insulation over the main studs had to be removed. This was arranged by making the insulation over the main studs in segments fixed together with quick release fasteners, and the central part of four sections, allowing the heater and counters to pass through, which could easily be removed. The layout can be seen in Fig. 1.3 and 5.2 which show the vessel with some of the top lagging removed.

6.4 HEATER CONTROL

The safety limits on the temperature control of the vessel have already been given in Chapter 5 and they will not be repeated here but the methods of incorporating them into the heater control circuits will be outlined. The basic control of the supplies to the heaters was by relays in the experimental area operated by switches in the control room. All the heaters were individually fused as well as the supplies having their normal fuses

so if a heater failed it would not cut off the supplies to the other heaters on that supply,

The relays could either be on or off but could be controlled manually or automatically and an indication of the state of operation was given on the control panel. This enabled some of the heaters to be switched on and used to balance the heat losses to the surroundings with only one or two heaters on automatic control reducing the variations and oscillations that would occur if they were all on automatic control. The supplies for the relays and controllers could be chosen from two seperate fused supplies incorporating low pass filters but so the vessel could be shut down safely even in the event of a complete loss of electrical supplies the Indicators and Dump Tank cooling controls were backed by a battery operated DC/AC converter.

Fig. 6.4 is the block diagram of the heater control and supply circuits. The connections between the relay panel and the heaters were by single 10A cables running in Kopex Reinforced Tubing which protected them from normal damage but also from water as the area was liable to flood if the main sump pumps failed. The cables for the internal and external heaters were lead seperately to the panel and used 50 and 18 multiway connectors at both the panel and the vessel allowing their easy disconnection if required when moving or rotating

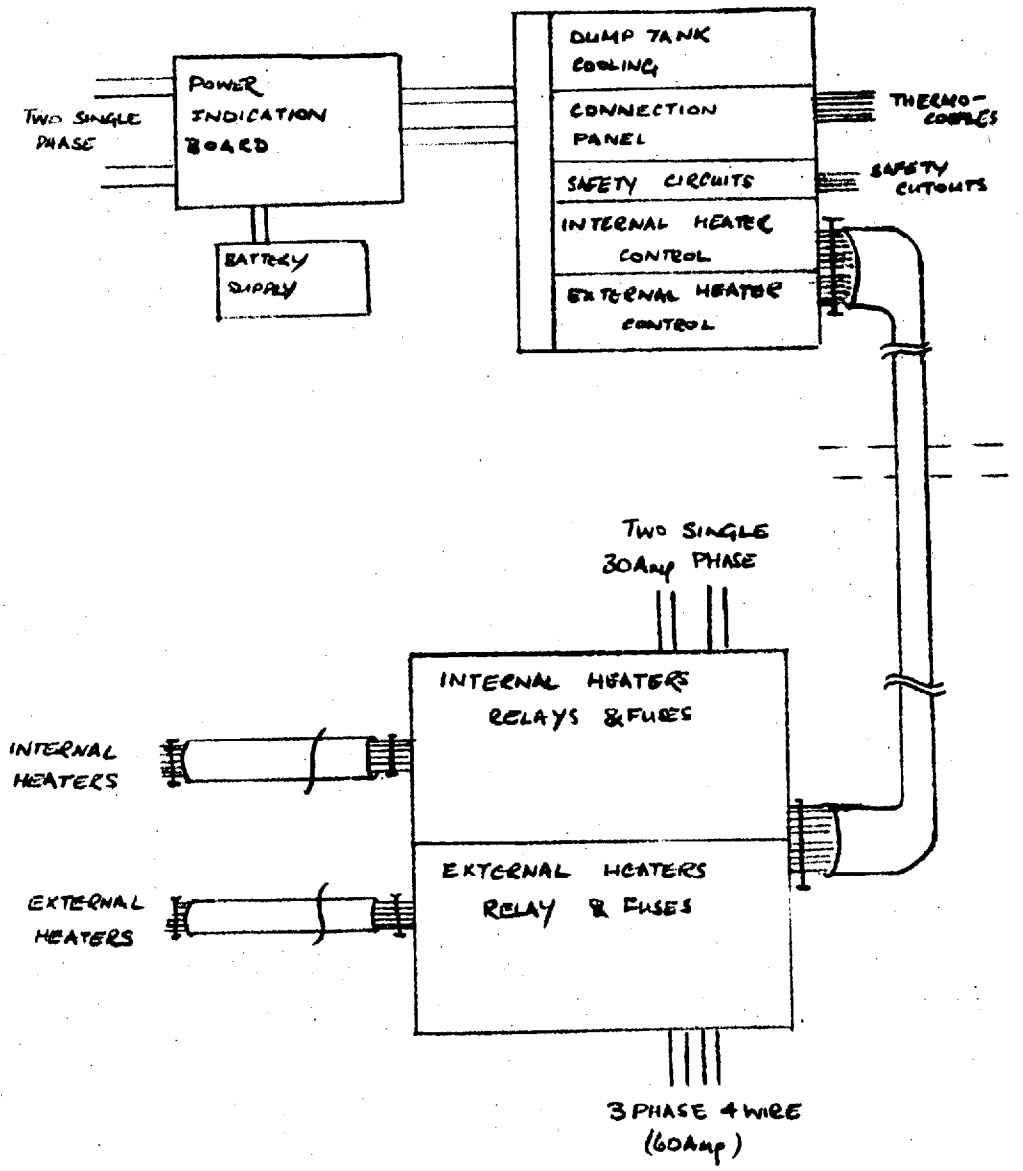

FIG 6.4 HEATER CONTROL BLOCK DIAGRAM

the vessel. The supplies were taken from nearby isolators and the relay panel was enclosed with expanded Aluminium mesh for safety as were all panels which had live circuits on them. The relays for the internal heaters were single contact types controlling the supply to one heater but the relays for the external heaters had four contacts for the three phase supplies.

The relays were controlled from the control room using a 34 way cable 56 ft. long made up of three 12 way cables. This cable also provided indication by neons on the control panels of the state of the actual supplies as although visual indication of the operating condition was given this did not indicate whether the heater supplies were in fact on. Seperate indication for each heater was not wired up because of the extra cable requirements as other cables had to be used for such things as the Dump Tank cooling and the ducting space was limited.

Different operating limits would be relevant during an experiment and it was decided to allow the controlling thermocouples to be changed during an experiment and this was arranged by the use of a common connecting block. This used three pin DIN plugs and sockets and enabled the controllers to be connected to various thermocouples as well as providing for an indicator to read the other thermocouples. The system can be modified and expanded in the light of further operating experience and extra positions were provided for this. Because the

control requirements would be different for the internal and external heaters they were arranged seperately after the incorporation of the safety circuits into the relay supplies.

Indicating controllers generally available have a calibration accuracy of 1% and a repeatability of $\frac{1}{4}$% of the full scale reading which for a 450°C instrument would give possible errors of 4.5°C and $1\frac{1}{4}$°C respectively which would not be accurate enough especially when operating near the critical point. To obtain the required accuracy without the use of expensive or complicated equipment a smaller range instrument with the same percentage errors was used with a zero suppression unit to keep the readings on scale. 0 - 150°C instruments were used which gave instrument errors of 1.5°C and under $\frac{1}{2}$°C to which must be added the errors due to the zero suppression unit. The use of a similar but more accurate instrument in which the control circuit was independent of the indication circuit enabled the set point to be held to under $\frac{1}{2}$°C with a resolution of under $\frac{1}{4}$°C with the same indication accuracy. This was used in the internal heater circuit and a similar instrument should be used for the external heaters. Temperature indication of the other thermocouples was done on another similar indicating controller but for accurate work this could be replaced by a higher accuracy direct reading instrument when funds become available preferably with a data logging unit.

The backing off zero suppression unit was a potential dividing resistance network fed by a mercury cell, the circuit shown in Fig. 6.5. This enabled voltages equivalent to up to 400°C to be switched into the thermocouple circuit in steps of 100°C. These voltages were set up and could be checked by a digital voltmeter and the errors in the unit were considered negligible as the voltmeter had a sensitivity of 2.5μV (.06°C). Facility for checking the units was built into the thermocouple connection panel and they could be checked during experiments. The resistance network values were a compromise between the life of the cell and the increased effective resistance of the thermocouple which could be a source of noise and error if the input impedance of the controller was not high enough. The errors due to the unit on the measured values were considered negligible and the cell life was over a year for the network shown and had a constant voltage output over its life. There is an error in the indicated value when using the unit however because the temperature/emf relationship is not linear and the errors in the 100°C indicated values when using accurate suppression are given in Table 6.2

Table 6.2 Span Errors

Suppression °C	Error in + 100°C reading
100	- 1.3°C
200	- .5°C
300	+ 2°C

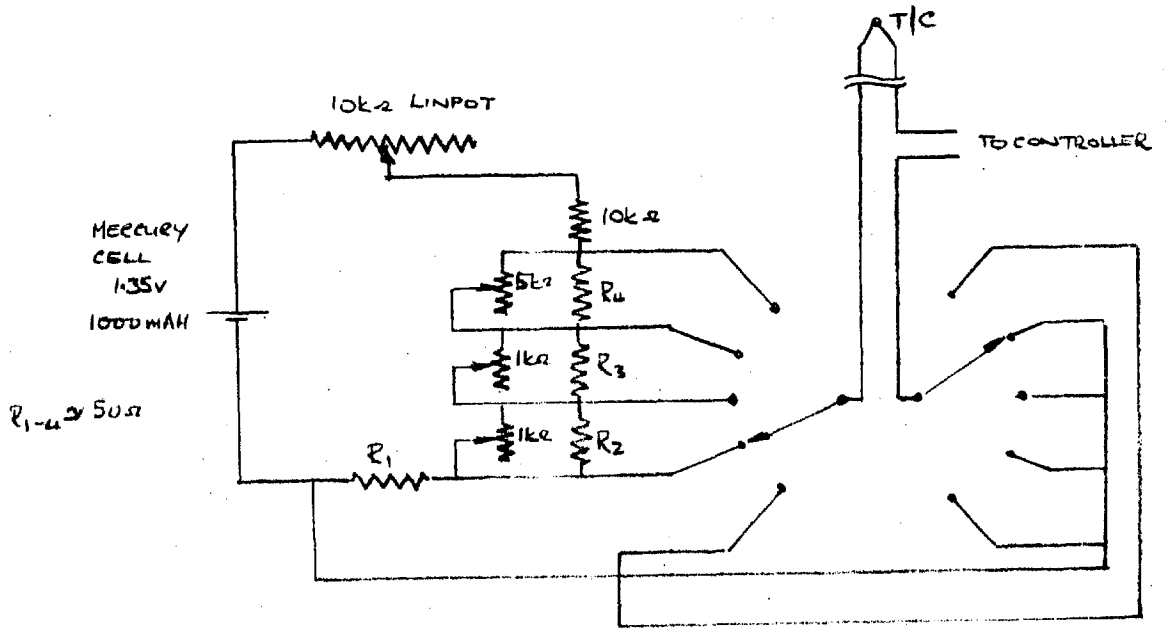

FIG 6.5 TEMPERATURE INDICATOR ZERO SUPPRESSION UNIT

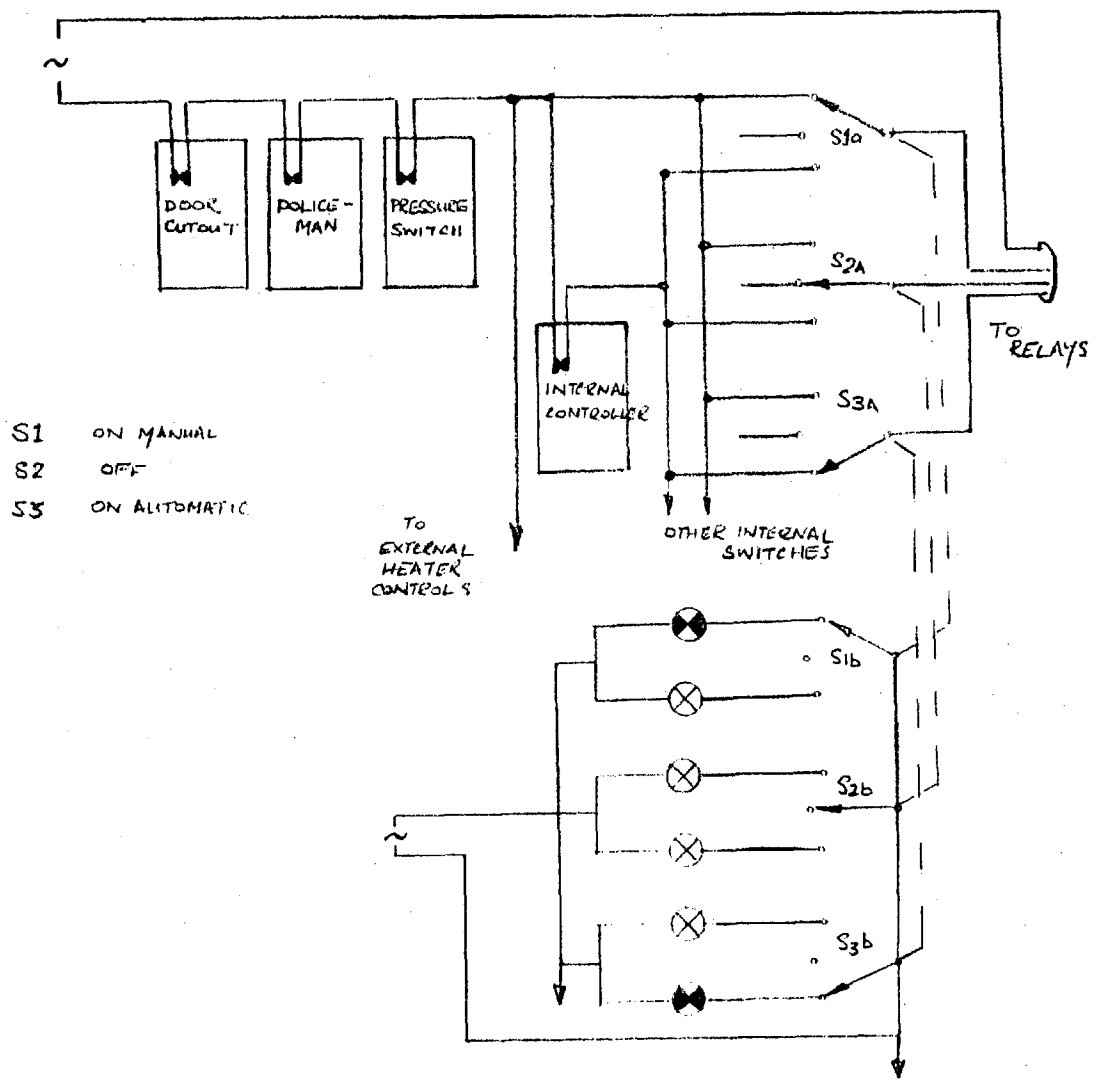

FIG 6.6 HEATER CONTROL CIRCUIT DIAGRAM

By tabulating the observed values they can be accurately corrected and the errors can be neglected. The errors in using the more accurate form of controller were taken to be

Set point $< \frac{1}{2}^{o}C$

Resolution $< \frac{1}{4}^{o}C$

These were considered of a high enough accuracy for the present project if the setting up procedures were carried out properly.

The control and safety cutouts worked as a series of switches in series in the supply to the heater relays. The circuits for the internal and external controls were identical inform but used different controllers and the circuit for three relays is given in Fig. 6.6. The first control has not been wired in yet as it is linked to the Accelerator's safety circuits which are still being incorporated, but it will cut the supply if the special castle key is removed from the belt start circuit. This will prevent the vessel being heated when personnel are present in the experimental area. The high temperature limit was controlled by a non-indicating controller which could be set to the required value (normally $450^{o}C$). This could be set up using the digital voltmeter and a low voltage supply removing the calibration error but the repeatability error would be $1.5^{o}C$ which was allowed for by setting the controller to $447^{o}C$. The limiting thermocouple would change during an experiment and by

using the connection block the correct one could be used. All the controllers drove up scale if a thermocouple went open circuit which was a fail safe condition. It was found, in the operations carried out, that a large pressure increase was caused by a small temperature increase (150 psi/^{o}C at 90^{o}C) and to guard against inadvertant safety valve operation a pressure switch was obtained and is to be incorporated into the pressure circuit. This had a set pressure that could be varied over the pressure range with a set differential pressure of 500 psi and it would greatly ease the long term operation of the vessel.

6.5 COOLING

The cooling was designed to be safe and simple to operate and control. A heat removal of 8 kw was specified so the time required to cool the vessel would not be excessive and cause delays in the experimental programme. The only cheap materials suitable for cooling over the temperature range were air and steam as otherwise only expensive oils and organic compounds would be suitable at the high temperature and would involve a complicated layout and control system. The use of steam could suffer from corrosion problems and the possible formation of cold areas at the inlet where the steam was formed unless a preheater was incorporated and would not be a fail safe system. From the problems involved with

the use of other coolants it was decided to look at a system using air as the coolant.

Air has a low heat capacity and density and heat transfer coefficient but fans are readily available for the capacities and pressures that would be required and the associated equipment would be simple and easy to install.

The heat would be removed from the rim of the flat head and the flange on the body of the vessel these being the only available areas, the external heaters taking up most of the other available space. The temperature gradients in the metal were within the code limits for the heat removal rates being considered and cold spots were eliminated by the use of the Refrasil/Aluminium construction as used under the external heaters.

The basic calculations were carried out on the assumption of a required heat removal rate of 8kw equally split between the flanges using the Refrasil arrangement with air as the coolant in tubes 6 ft. long, 1" internal diameter of Aluminium welded to the Aluminium plate. The flow of air, with an inlet temperature of $100^{o}F$, was to be such as to remove the required heat with a pressure head of 10" water gauge available from the fan. The monogram given in McAdams (1954) as Fig. 9.15 was used which is based on the relationship

$$N_u = .023\ R_e^{.8} P_r^{.4} \qquad 6.1$$

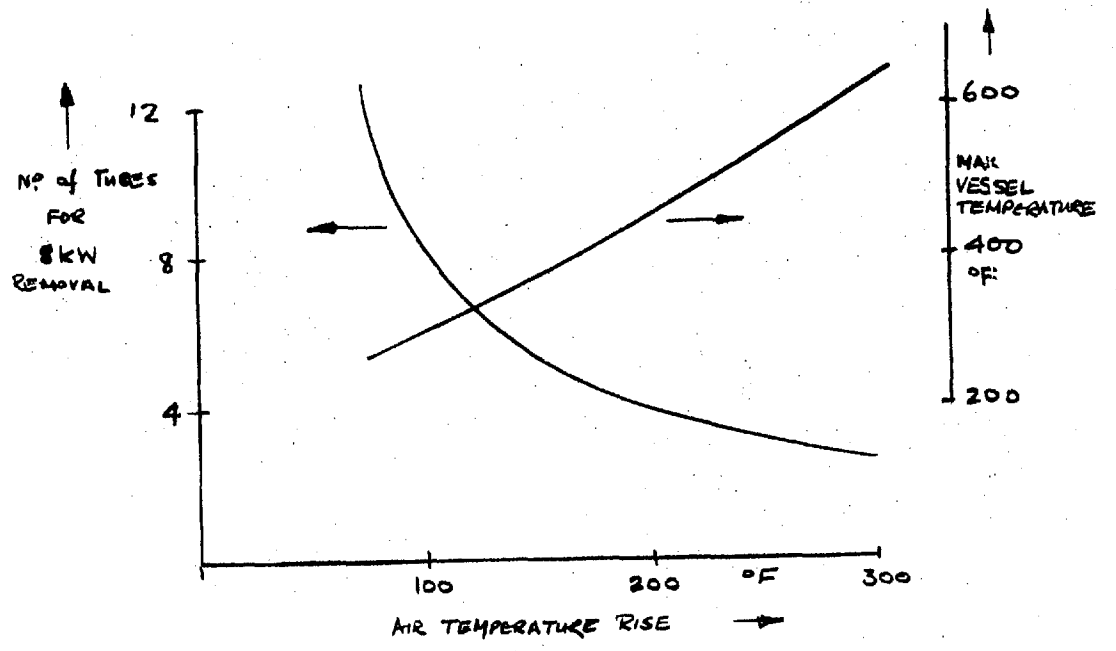

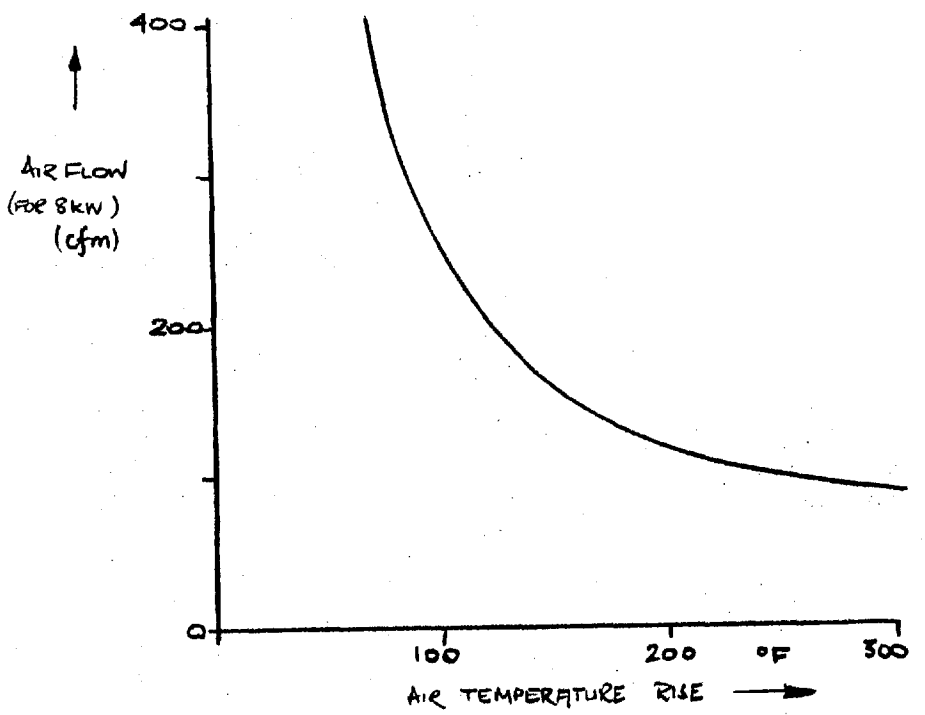

Fig 6.7 Air Cooling Requirements

The constant is pessemistic by 10% over that obtained using the correct values for the physical properties of air in the equation but the results have not been corrected and give conservative results.

The results for various air temperature rises are shown in Fig. 6.7 using the given assumptions. A A maximum vessel of temperature of under 200°F must be obtained before the vessel can be refilled with water at 60°F for the next run and over twelve tubes would be required to keep the cooling rate up but the available space limited the number of tubes that could be incorporated.

The flange arrangement was split into two halves and each part could have three tubes on it giving a total of twelve tubes using the two flange areas. To provide as much of the area at the high Aluminium plate temperature and to reduce the profile height an arrangement as shown in Fig. 6.8 was designed. This consists of 2" angle welded to the plate and had an equivalent diameter of just over 1". The number of tubes used at a certain vessel temperature could be adjusted to give the required heat removal rates at the designed flow rates.

The heat would have to be removed from the air before discharging to the atmosphere as otherwise the room would soon warm up and either a water spray or large radiator could be used though the latter might introduce

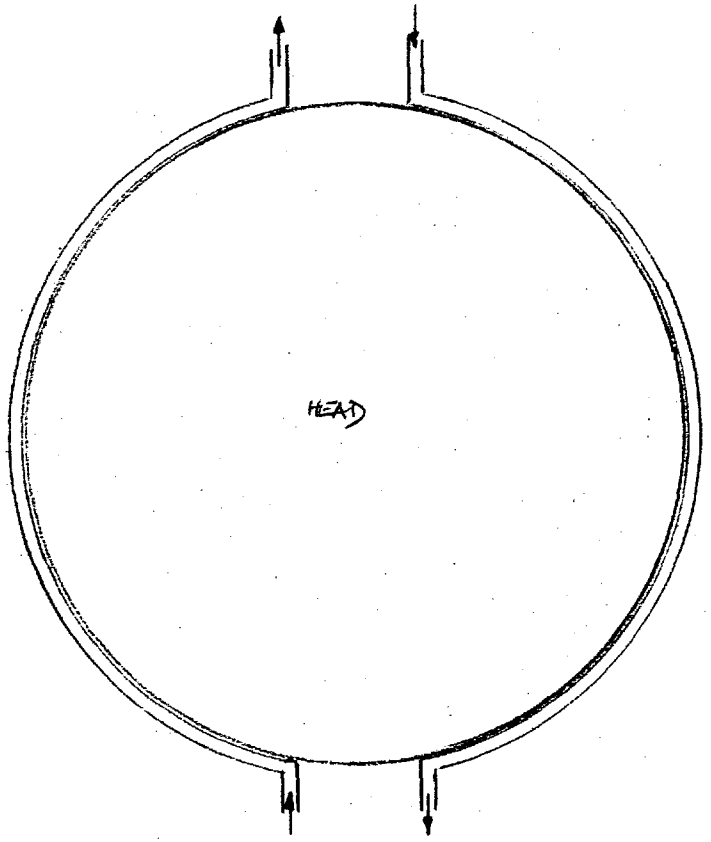

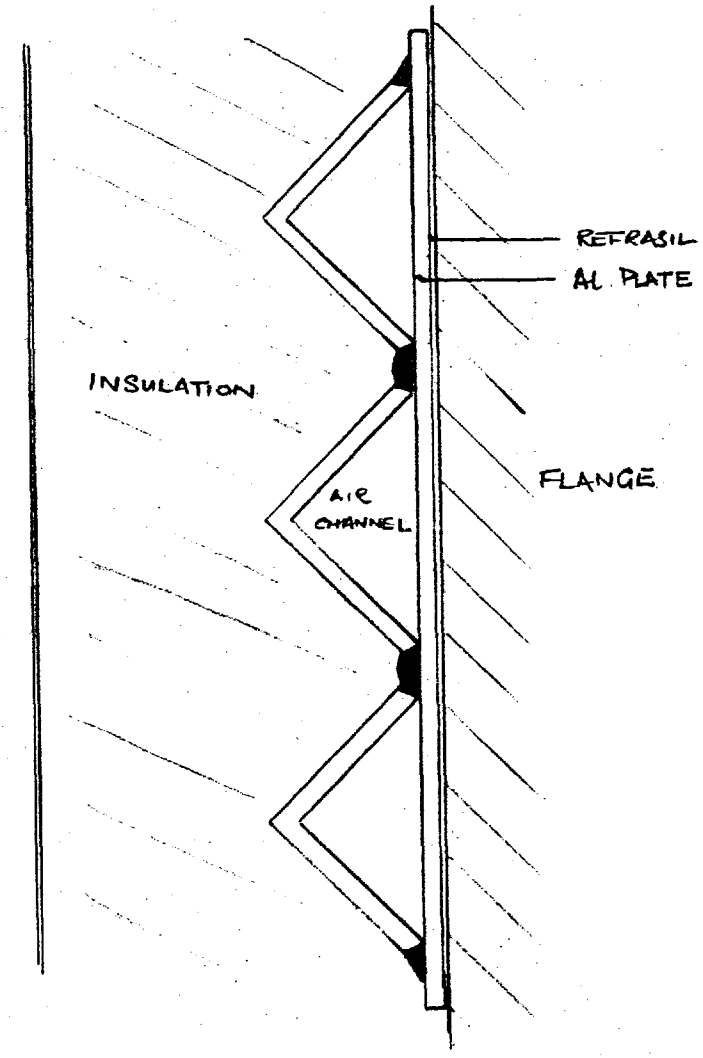

FIG 6.8 AIR COOLING ARRANGEMENT

too high a flow resistance into the circuit. The control of the system would be easy to operate and control using heat balances and using dampers to regulate the flow. The use of a number of fans in parallel would simplify the control and would allow the fans to operate at their most efficient condition at the varying flow requirements.

This system has not been installed on the vessel but no snags can be seen in the incorporation and use of the proposed layout.

7. NUCLEAR EQUIPMENT AND DESIGN

The nuclear equipment had to satisfy the two conflicting basic requirements of reliability and sensitivity. Due to the arduous operating conditions and the length of the experimental cycle time the failure of any part of the equipment would cause a long delay. This reliability criteria not only applied to the operating characteristics of the equipment but also to its general robustness and ease of handling. The simplicity of operation would also be a consideration as the vessel and the accelerator would both have to be operated and controlled while counting which could cause difficulties.

The Van de Graaff accelerator which was used as the pulsed neutron source will be first outlined followed by the discussion of the design and manufacture of the thermal neutron cylinders to go in the vessel. These posed some problems unfound in previous experiments due to the higher temperature limit in this project. The counters and counting equipment will be described last the unusual feature being the simultaneous seperate counting of the two counters in multiscale mode.

7.1 NEUTRON SOURCE

To carry out the experiments a pulsed neutron source was required having a repetition rate of about 500 $H_{\frac{Z}{4}}$ and a pulse length of about 10 μs.

The neutron source used in this project was an $\frac{1"}{8}$ thick Beryllium disc 1" diameter which was bombarded with high energy deuterons the reaction being

$$Be^{9}\ (d,\ n)\ B^{10} + 4.36\ Mev$$

The emitted neutrons were not monoenergetic but had a spectrum of energies as the Boron nucleus could be left in an excited state. The neutron distribution was peaked in the forward direction being essentially flat over an angle of 30° from the forward direction but then dropping off sharply. There was also a possible source of neutrons due to the (d, n) reaction with deuterons previously absorbed in the target, also giving rise to 4Mev neutrons.

The deuterons were produced by a Van de Graaff Accelerator rated at a continuous beam current of 50 μ Amps at the target with an accelerating voltage of 2Mev. The physical layout is shown in Fig. 5.1 and a more detailed diagram of the accelerator in Fig. 7.1. It can be seen that the accelerator was vertical which reduced space requirements with a horizontal flight

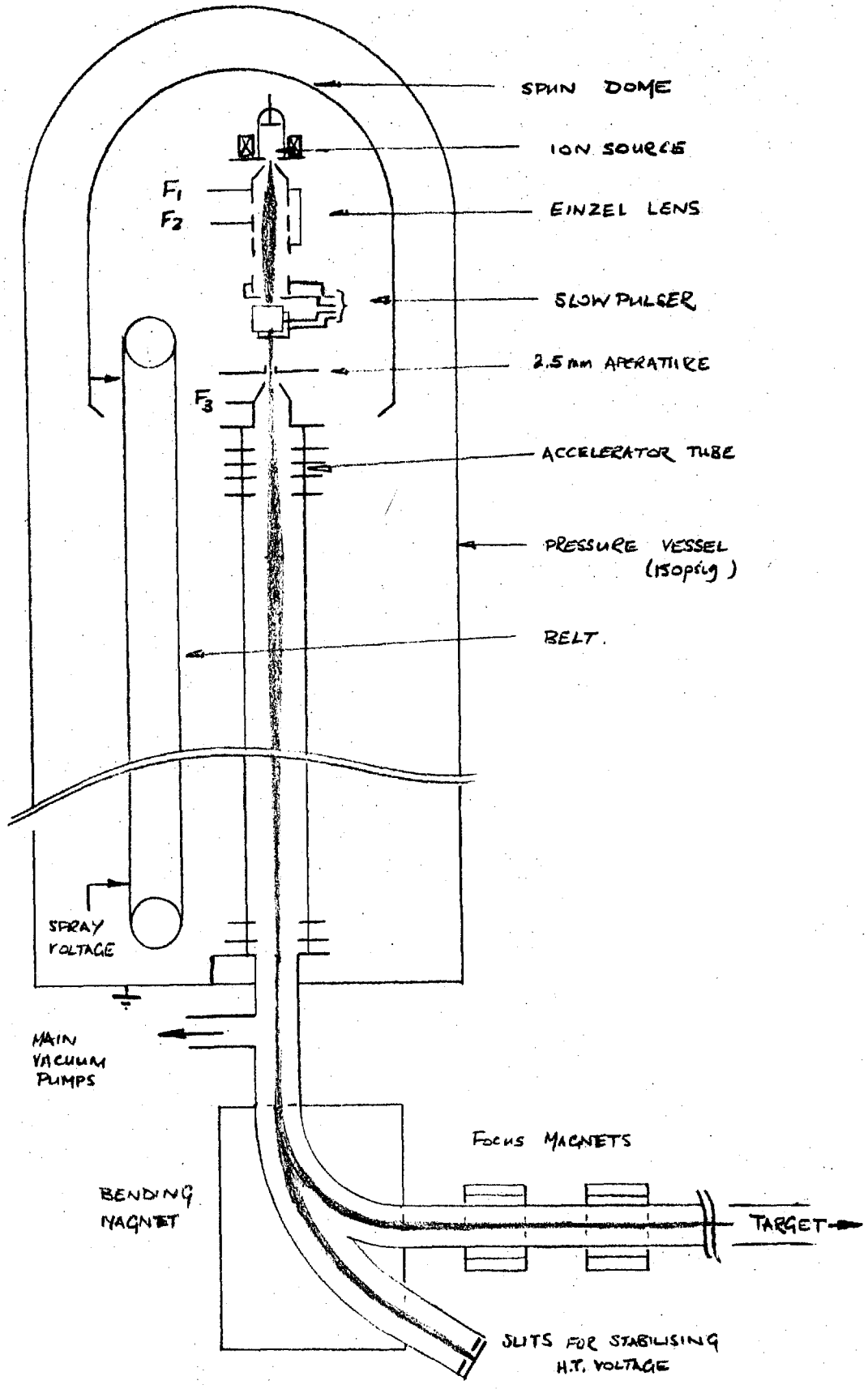

FIG 7.1 SCHEMATIC DIAGRAM OF ACCELERATOR

tube, an electro-magnet being used to bend the beam.

The high voltage was achieved by removing, at the top terminal, the charge sprayed onto the moving belt, made of rubber and nylon, at a potential of up to 60 kv at the bottom. The pulley at the top contained a 1 kw 240 v alternator which using an autotransformer provided the electrical supplies for the units in the top terminal enclosed in a spun Stainless Steel Shell carrying the charge. The whole of the top terminal, accelerating the tube and belt arrangement was enclosed in the pressure vessel which after evacuation was filled to atmospheric pressure with Freon and then with Oxygen free Nitrogen to the working pressure of 150 lb/in^2. To improve the insulation resistance of the system the gas could be dried by passing it over Alumina pellets or could be cooled to reduce the temperature rise of the gas that occured when operating.

The deuterium gas was stored in a small gas bottle in the top terminal and was fed to the ion source through a regulator and needle valve. All the controls in the top terminal were operated by servo motors at the earth base of the pressure dome moving nylon strings acting on the required control at the top terminal. The ions were extracted from the source bottle and focussed in the usual manner using an Einzel lens. The pulser used electrostatic deflection of the beam to cut the beam

off for the required period and has a variable repetition rate of $1kH_2$ to $100H_{\frac{z}{2}}$ with a mark/space ratio of about 1:100 giving a pulse length of about 10μs for the $1kH_2$ repetition rate. The deflection occured before the beam was accelerated so there was no possible neutron background from the (d, n) reaction with the deuterium previously deflected and absorbed in the plate.

After passing through the deflection plate the beam was accelerated down the tube through 50 stages each having an equal potential across it and an interstage resistance of 300 MΩ. The vacuum in the tube was kept to about $.2 \times 10^{-5}$ mmHg at the bottom of the tube by a 6" diffusion pumping system.

After acceleration the beam was bent through 90° to a horizontal flight path by an electromagnet which was set manually to give the required field for the deuteron energy required. The control of the beam and accelerating voltage was done by the unwanted beam having a charge/mass ratio of half that of required ions acting on slits set about 30° below the horizontal. The difference current from these slits was amplified and acted on the corona probe used to keep the accelerating voltage constant. The probe acted as a discharge path and by altering its position could alter the leakage path and hence the top terminal voltage. This meant that only the required beam reached the target and the unwanted

partially ionised beam was used to stabilise the system. This operated satisfactorily in the pulsed condition but difficulty was experienced with the stability of the magnet supplies causing troubles in the operation and limited the high voltage that could be used.

The bending of the beam caused the spot to become ellipsoidal in cross sections so a quadrapole magnet was used to focus it tending to give a line at 90° and this was focussed to a spot by another quadrapole magnet. The two magnets were adjusted together to obtain the required focus at the target seperated from the magnets by about 10 ft. of evacuated flight tube. Two 3" pumping systems were used to keep the vacuum in the flight tube and removed any gases thrown off by the beam hitting the flight tube or the target and one system was positioned near the target.

Immediately before the target was reached the beam passed through a 2" long insulated brass tube ¾" bore. This was connected directly, using a modified car spark plug acting as a lead through, to an amplifier and emitter follower. The pulse caused by the passage of the beam was amplified and used as the start pulse for the counting system. This system removes the need for synchronised counter starting and pulsing which either requires transmission over a high potential difference or using post acceleration deflection which can give rise to background

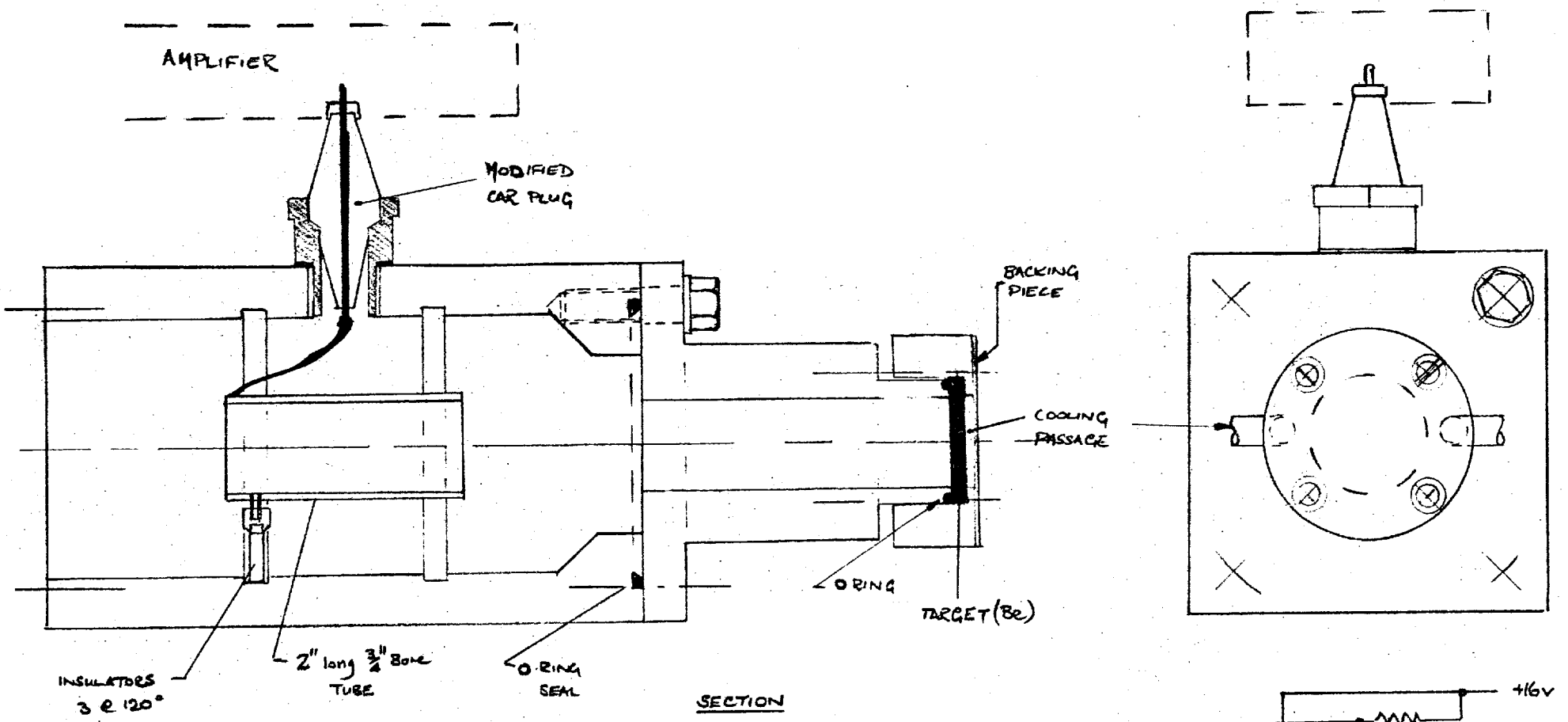

FIG 7.2 PULSE PICKUP & TARGET DESIGN

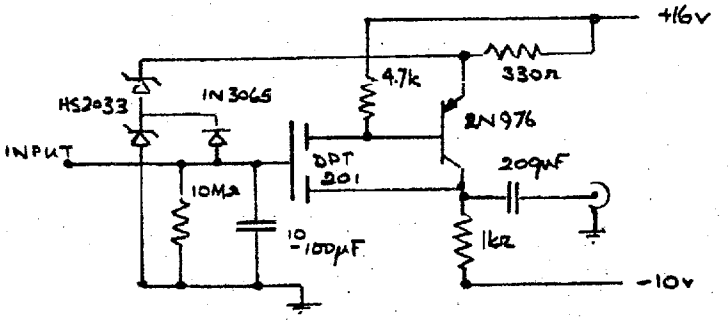

AMPLIFIER CIRCUIT DIAGRAM

problems. The design of the pickup was based on an A.W.R.E. Aldermaston design modified to suit the Imperial College flight tube arrangement and the amplifier emitter follower was loaned by Aldermaston whose help is gratefully acknowledged. The supplies for the amplifier were provided by a low voltage supply having two independent outputs.

The target and pickup designs are shown in Fig. 7.2 and can be seen in Fig. 8.2. The target assembly was designed to enable the target to be cooled either by air or water passing through a thin space .030" thick across the back of it. This cooling would not only remove the heat generated in the target but also any heat radiated from the vessel when the high temperature experiments are carried out. This cooling path was made very thin to reduce any degradation of neutron energy.

The use of a thick Beryllium metal target meant that it was very robust and would have a very long life, unlike tritium targets often used which not only suffer from a rapidly decreasing yield with use but also since they consist of tritium absorbed in a metal backing are susceptible to evaporation of the tritium if overheating occurs. These are normally used with lower energy accelerators for the best yields but even so give lower yields than a thick Beryllium target for the same beam current. Also the high energy γ background produced by the decay

of N^{16} formed by the $O^{16}(n\ p)\ N^{16}$ reaction is avoided as a threshold energy of 10.24 Mev is required this being possible with neutrons from a tritium target which have a mean neutron energy of about 14 Mev. This reaction has a $7\frac{1}{2}$ sec half life and with the large water volume and the resultant gamma energies of 6 and 7 Mev it could be a problem especially if the counter's discrimination against gammas was not very good.

The method of operation of the accelerator was limited by the normal neutron safety requirements. This meant the control of the accelerator and any equipment in the experimental area had to be carried out from a seperate shielded area. During the experiments carried out the safety control was based on the special door key to the area being held by the operator and quick radiation check was carried out and the observed levels were very low. The system is to be made more secure by incorporating the castle key into an interlock fitted to the accelerator belt start circuit and visual indication and warning lights are to be provided. These are being fitted. A full radiation survey will have to be carried out when using a steady beam under the maximum yield conditions.

Some of the neutrons produced were thermalised and diffused in the thermal neutron cylinder where their rate of decay was measured. The cylinders used to

define the volume under investigation will now be described.

7.2 THERMAL NEUTRON CYLINDERS

The main design features and requirements of the thermal neutron cylinders have already been mentioned and only a brief review of those decisions will be given. The cylinders were chosen to be non-pressure vessels incorporating a moveable piston which could be moved after undoing one of the small flanges. The design was basically governed by the position of the counters which were placed in re-entrant tubes in the pockets let into the sides of the cylinders because of perturbation and movement considerations as mentioned in Chapter 2. The characteristic distance of the cylinders is the distance between the counter centre lines and was also the nozzle distances and the actual diameter was less than this. The cylinder layout being shown in Fig. 7.3 showing the various sizes.

One major problem was that the volume under investigation had to be shielded from the neutrons in the outer water volume in the vessel as these would decay at a slower rate and could act as a time dependent source of neutrons if the boundary was not black enough invalidating any measurements. This was linked with the

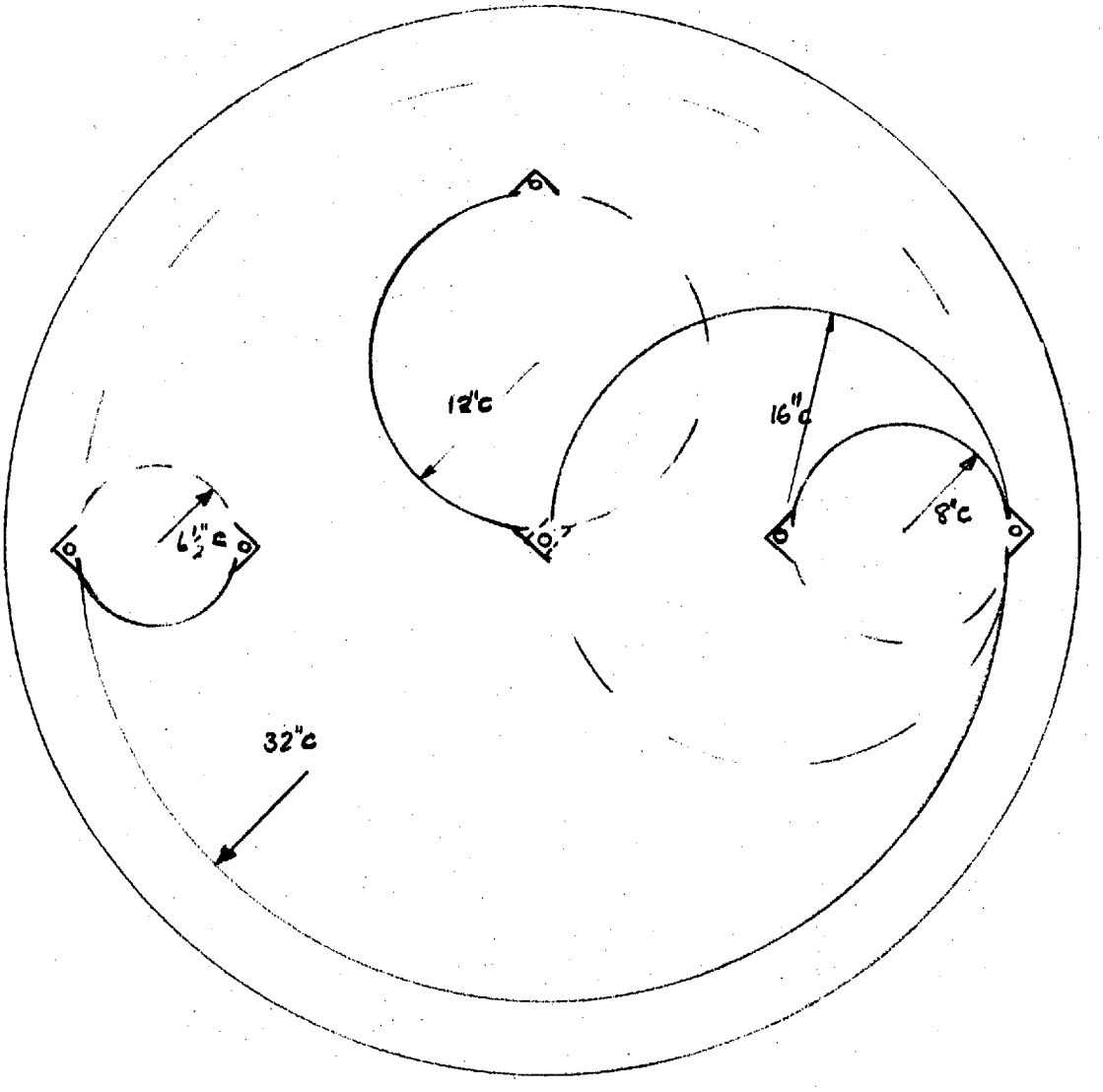

Fig 7.3 CYLINDER POSITIONS UNDER HEAD.

problem that the cylinders could not be closed as adequate passages had to be allowed for quick pressure equalisation without stressing the cylinders.

Another major problem involved in the design was a material one. The cylinders had to be made of a material having a high thermal neutron absorption cross section and able to withstand the conditions in the pressure vessel. Usually a .030" thick Cadmium sheet or cladding has been used but this melts at 321^{o}C and could not be used in the project. Most other high cross section materials are costly even if their corrosion properties are good such as hafnium which has been used as control rod material in water reactors.

Boron is a commonly available material with a high thermal neutron absorption cross section normally in the form of Boron Carbide. This is a ceramic and as such could be formed and sintered into the cylinder directly but this would be a very costly process and virtually impossible to machine once made. Boron can be incorporated in Steel but only up to 3% as Boron or 8% as B_4C which would make the cylinder very heavy if adequate blackness was to be achieved. Boron Carbide can be incorporated in an Aluminium matrix and is normally clad on the outside with a pure Aluminium layer which not only protects the core but also greatly increases the material's strength and ductility. The material

in this form being often called Boral. This material would however corrode at the high temperature conditions but due to the lack of any other suitable material it was decided to use it but to clad it with Stainless Steel to protect it from the steam.

The actual material was a $\frac{1"}{8}$ thick plate made of a core of Aluminium containing 30% B_4C clad on the outside with a .010" layer of pure Aluminium. This plate was called Hindu m inium 430 and was obtained from High Duty Alloys Ltd., Slough. The Stainless Steel cladding used was 22 gauge EN58B sheet. The Hindu m inium had a definite brittle form of failure when rolled but was ductile up to this point. This was because the cladding ensured ductile behaviour even in the presence of fractures in the core material but at a certain point this cladding failed and the subsequent brittle failure was characteristic of the core material. The minimum cold bending radius was about 2" which severely restricted the design of the cylinders especially the pockets for the cylinders.

The method of frabrication was to make and clad each part seperately and then weld the parts into the cylinders. The Hindu minium 430 and the Stainless Steel were cut and rolled seperately as required and then clamped together so the sealing edge weld between the two stainless sheets could be carried out using an argon

arc process with a parent metal filler rod. A suitable technique was developed to carry out this weld satisfactorily but it was not easy, requiring a good welder and welding machine the major difficulty being the thinness of the Stainless Steel sheets and the gap to be sealed. The welding of the parts together to form the cylinders was also done using the argon arc process.

To reduce any possibility of neutron leakage into the cylinders it was decided to use a double wall form of construction with the smaller cylinders so the volume under study was surrounded by volumes decaying at a faster rate and hence reducing any leakage problems into the centre volume. The water in these would also help to moderate any room return fast neutrons before they reached the volume under study. The passages left for pressure equalisation were governed mainly by the design of the pockets for the counters but neutron leakage was reduced by making these gaps long and narrow and preferably with no direct path from the outside to the centre volume. Passages would also have to be allowed in the surrounding volumes to allow pressure equalisation complicating their design. The 8" cylinder was arranged to sit round the 6½" cylinder acting as a double barricade for it and greatly simplified the smallest cylinder's design at a small increase in the complexity of the support arrangement.

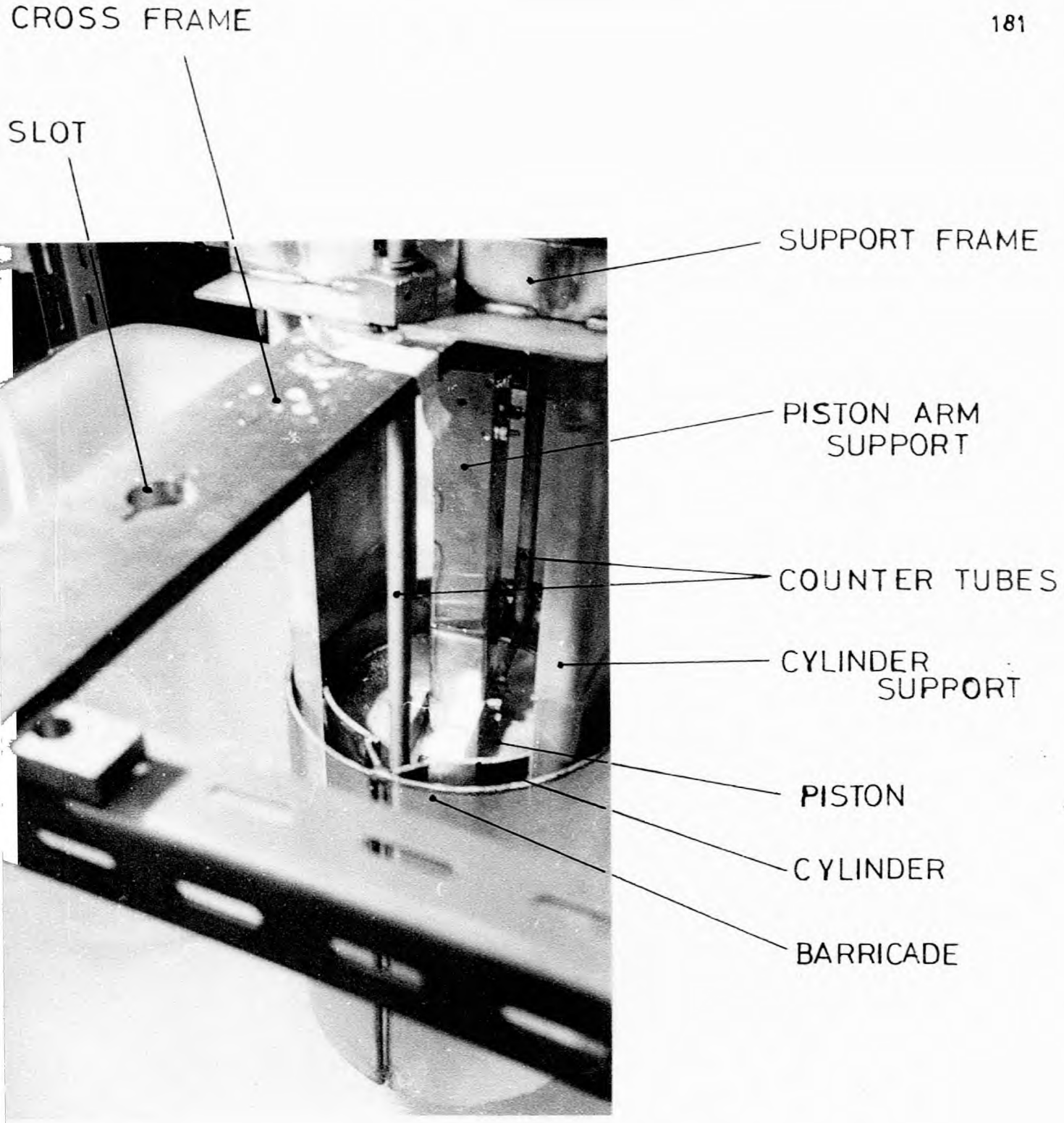

FIG 7.4 8" NOM. DIA CYLINDER

(AS SET UP FOR EXPERIMENT)

The design of the cylinders can be split into two types, one covering the small cylinders where only indirect access to the piston was possible and the other for the direct access cylinders, the difference being mainly in the movement design, the cylinder designs being similar. The larger, direct access, cylinders design was however simpler due to the ease of fixing them to the cross frame and the straightforward piston movement. The design of these will not be discussed except to note how they differ from the design of smaller cylinders. The 8" cylinder as used in the experiments carried out is as shown in Fig. 7.4 and Fig. 7.5 is a diagram of the piston movement as set up for the experiments in the pressure vessel. This can be compared with Fig. 7.6 which shows the corresponding drawing for the 16" direct access cylinder.

The description of the cylinders will be general but the 8" and 6½" will be specifically mentioned. The cylinders were made up of two curved plates joined by two V's to house the counter tubes. A larger V than required by the tube diameter was necessary because of the welds on the end of the counter tubes. The base was welded into the central part 1¼" above the bottom of the side pieces and a double base welded in using spacers. This was necessary as the counter tubes extended below this level but the distance for the double bottom was limited by the vessel. The volumes at the sides of the

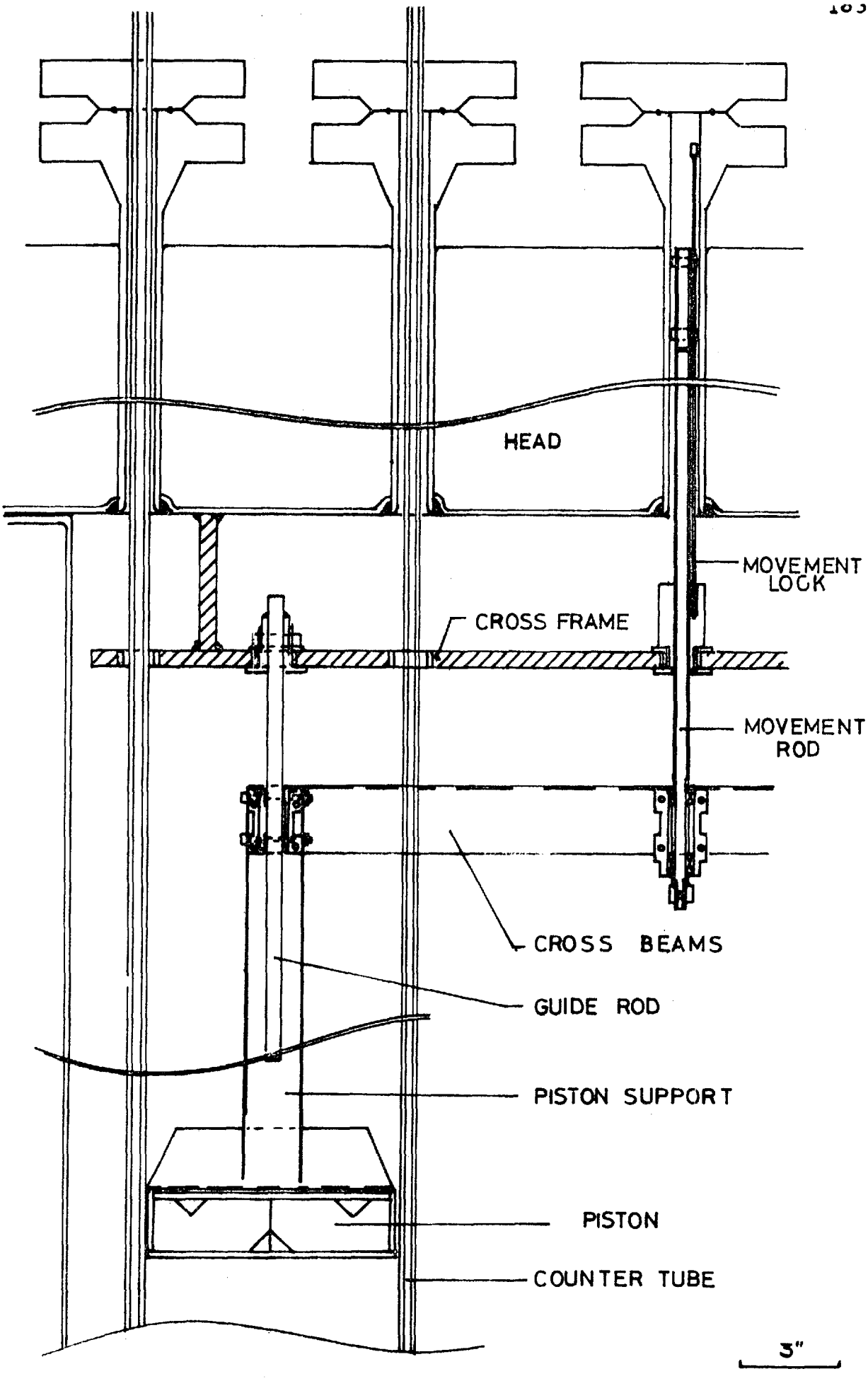

FIG 7.5 INDIRECT PISTON MOVEMENT
(8" CYLINDER)

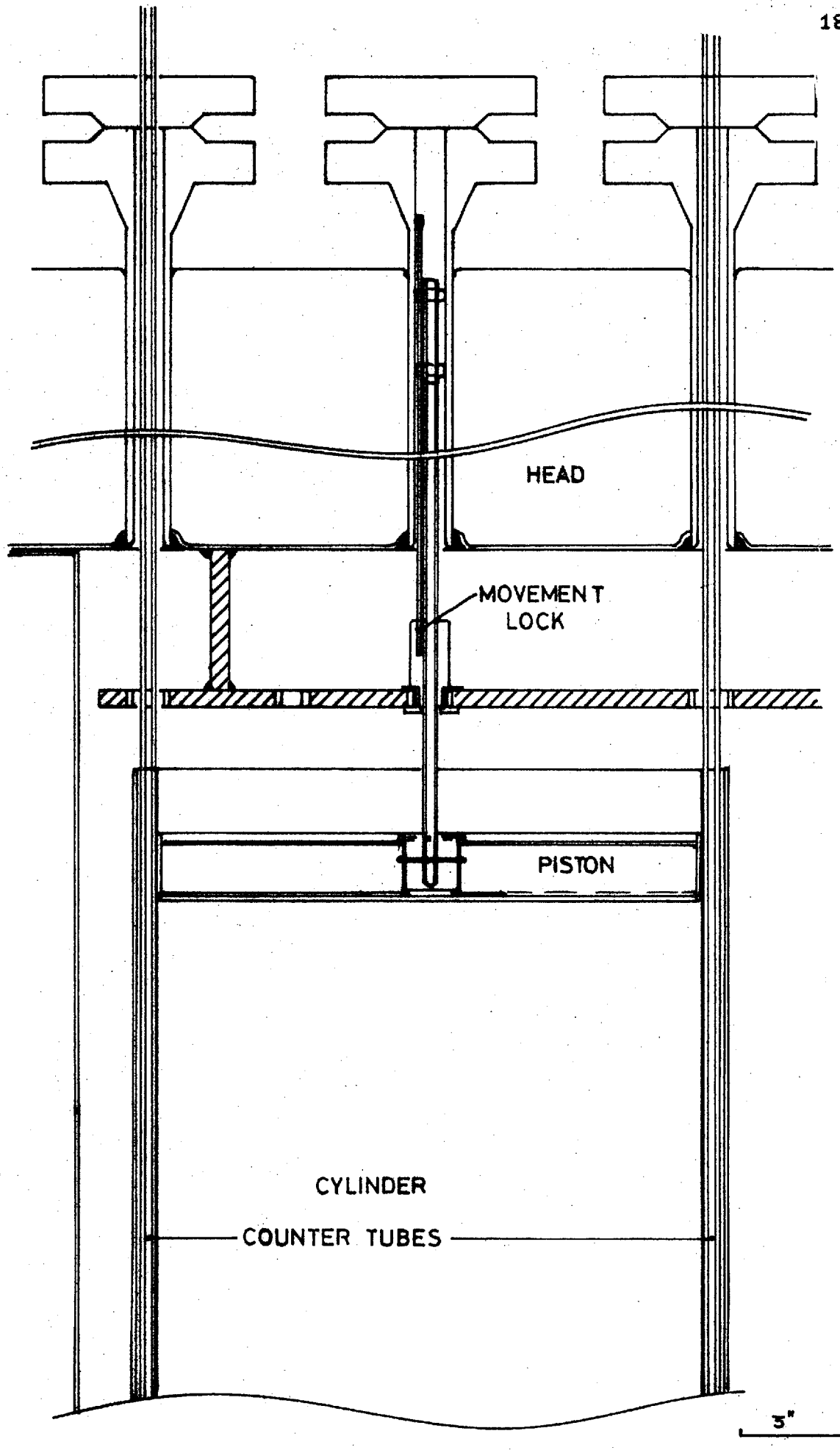

FIG 7.6 DIRECT PISTON MOVEMENT
(16" CYLINDER)

8" cylinder were made by welding two barricade pieces round the cylinder welded to the apexes of the V's. To reduce leakage up the space left for the counter tubes a plate with a 5¼" dia. central hole was welded in giving a gap of about 3/16" between it and the double bottom. A cutaway of the cylinder arrangement for the 6½" cylinder is shown in Fig. 7.7 with the support structure used to fix it to the cross frames.

The cylinders were supported by two wide C sections welded to the cylinder. These were bolted, using angles welded to the top, to a special support frame which enabled most of the assembly to be done away from the vessel head where access was much easier. This form of support was arranged on the 8" and 6½" cylinders so they could be fixed together and depended mainly on the design of the support channels which had also to allow the free movement of the piston arrangement.

The piston was made on the same principle as the double base having a top and a bottom plate seperated by a split rim and spacers as shown in Fig. 7.7. Two angles pieces were welded across the rim to which the piston support arms were bolted.

In the direct access design the piston was moved by the threaded rod attached to it moving through a special nut fixed to the cross frame the arrangement being similar to the indirect access movement design in

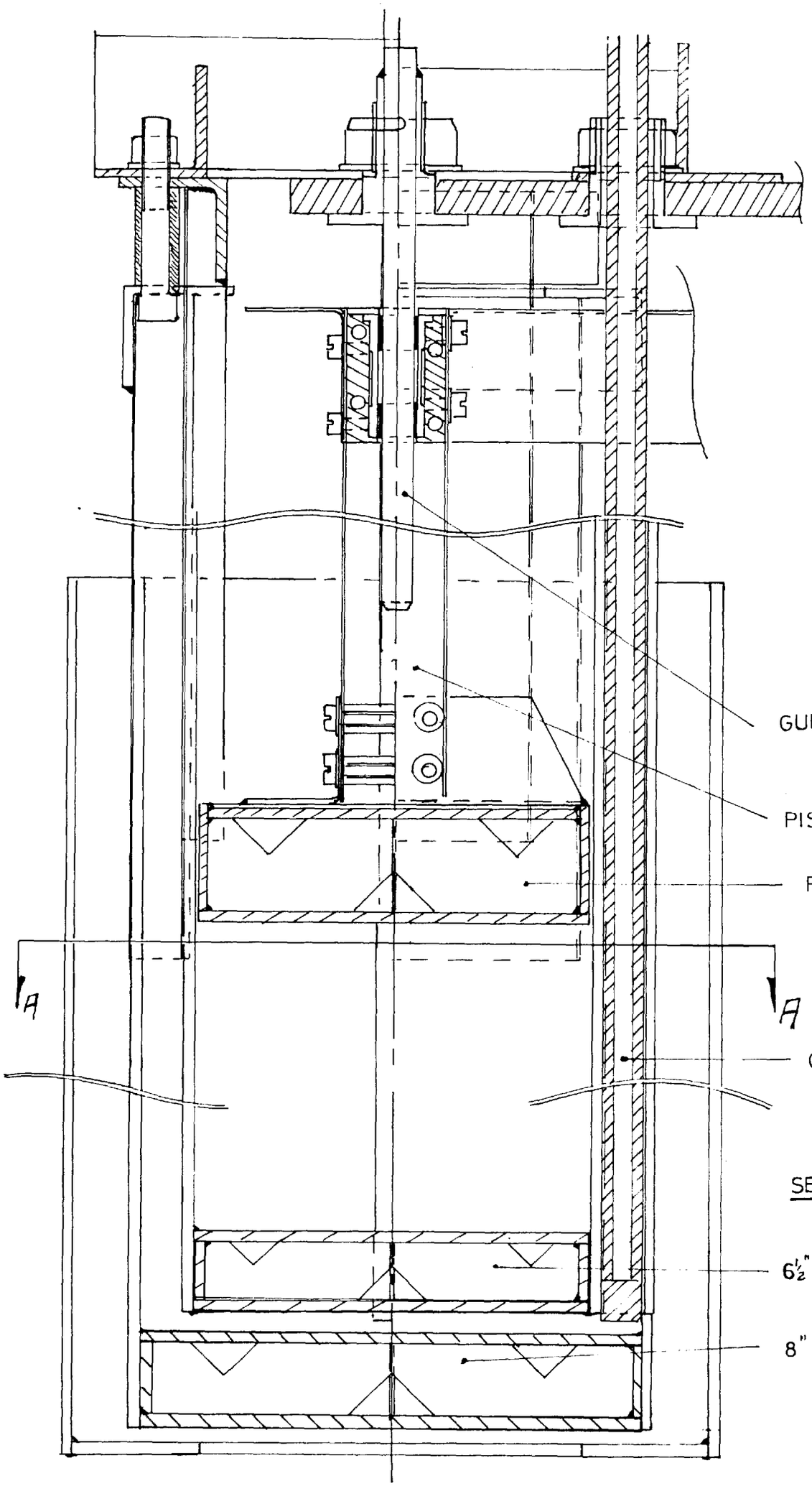

SECTION BB

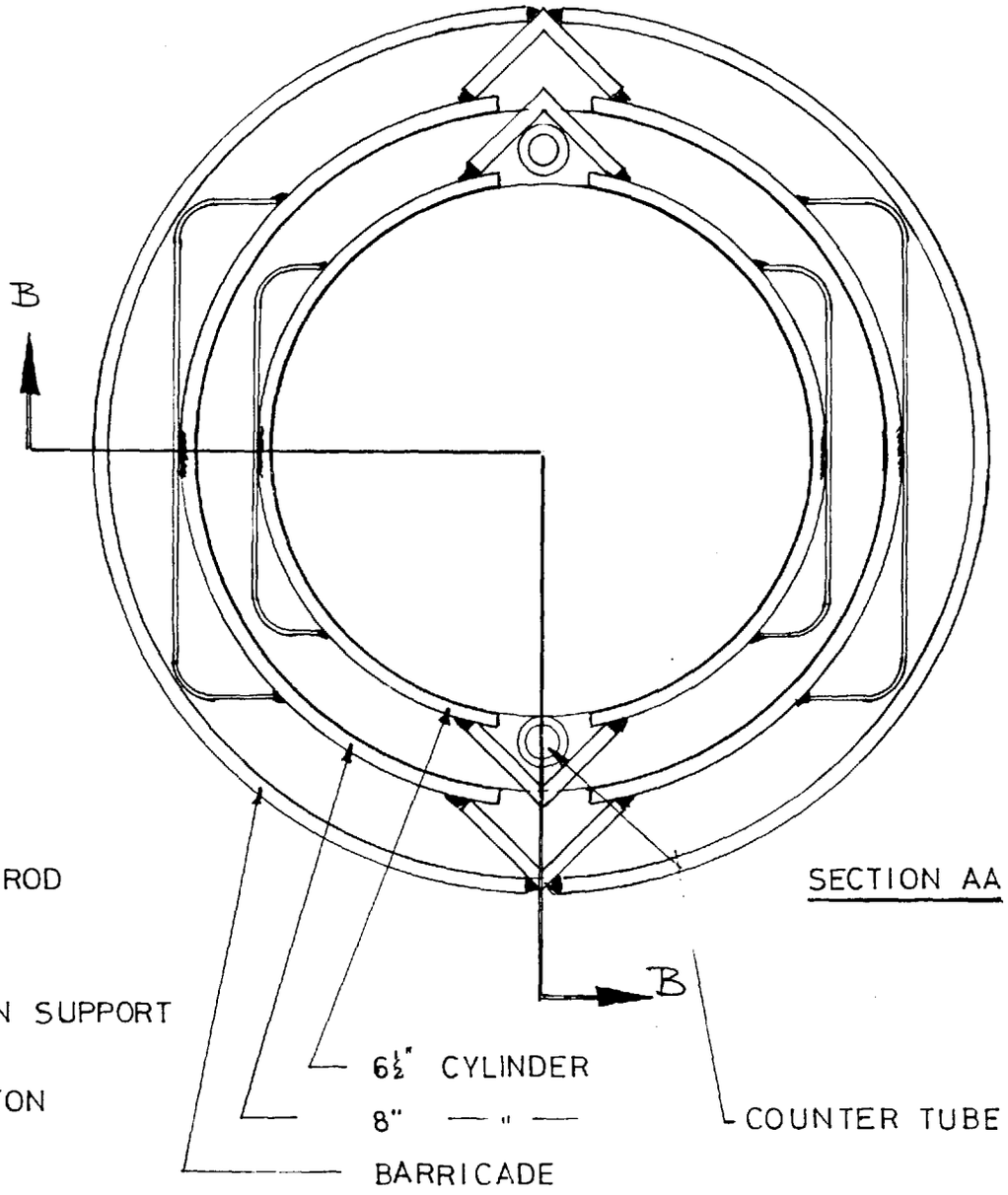

SECTION AA

FIG 7.7 6½" CYLINDER CUTAWAY

this respect. In the indirect access the vertical movement had to be done away from the cylinder cross arms being used to move the piston as shown in Fig. 7.5. The pistons position was controlled by a guide rod fixed to the cross frame on which a bearing in the piston support arms moved. The threaded rod could be locked relative to the nut on the cross frame by a 3/16" dia. rod passing through a top piece on the threaded rod and fitting into holes drilled in the nut piece. These positions were arranged so a locking position was available every 15^{o} giving a height spacing of .005". The size of the nut and top piece were arranged so nothing bigger than 3/16" diameter could drop into the vessel and the locking rod was made with a head welded into it to stop it falling through. The bearings were initially designed to be based on P.T.F.E. linings but as it was felt that these might not be suitable for prolonged operation at the high conditions these might have to be replaced by other materials but this would become apparent with use. The other materials would have greater friction and would be made of hard metals or hard faced stainless steel.

If it was felt necessary the friction could be reduced by using a precision recirculating nut and rod arrangement which has recently become available in Stainless Steel and has very low coefficients of friction and small backlash. These could easily be incorporated

into the design without major modification.

To reduce any failures the structure was welded up as much as possible but all bolts were either locked by tab washers or split pins for security. The holes in the cross frame had slots to lock the position of the parts fixed to it and one can be seen in Fig. 7.4. The cross frame shown is similar in arrangement to the one welded onto the vessel head but a direct form of movement was used. All the parts going into the vessel were made of Stainless Steel for corrosion reasons.

This section has described the thermal neutron cylinder's design and the problems involved in their manufacture which was not only difficult in itself but also had to satisfy some stringent requirements. These cylinders defined the volume of water for which the decay rate was to be measured using the equipment that will now be described.

7.3 COUNTING EQUIPMENT

The counting techniques used in this project were basically standard though incorporating a few unusual features to improve and ease the counting. The basic arrangement consisted of two fission counters with this associated equipment feeding a time of flight Unit linked to a 400 channel Analyser in which the counts from

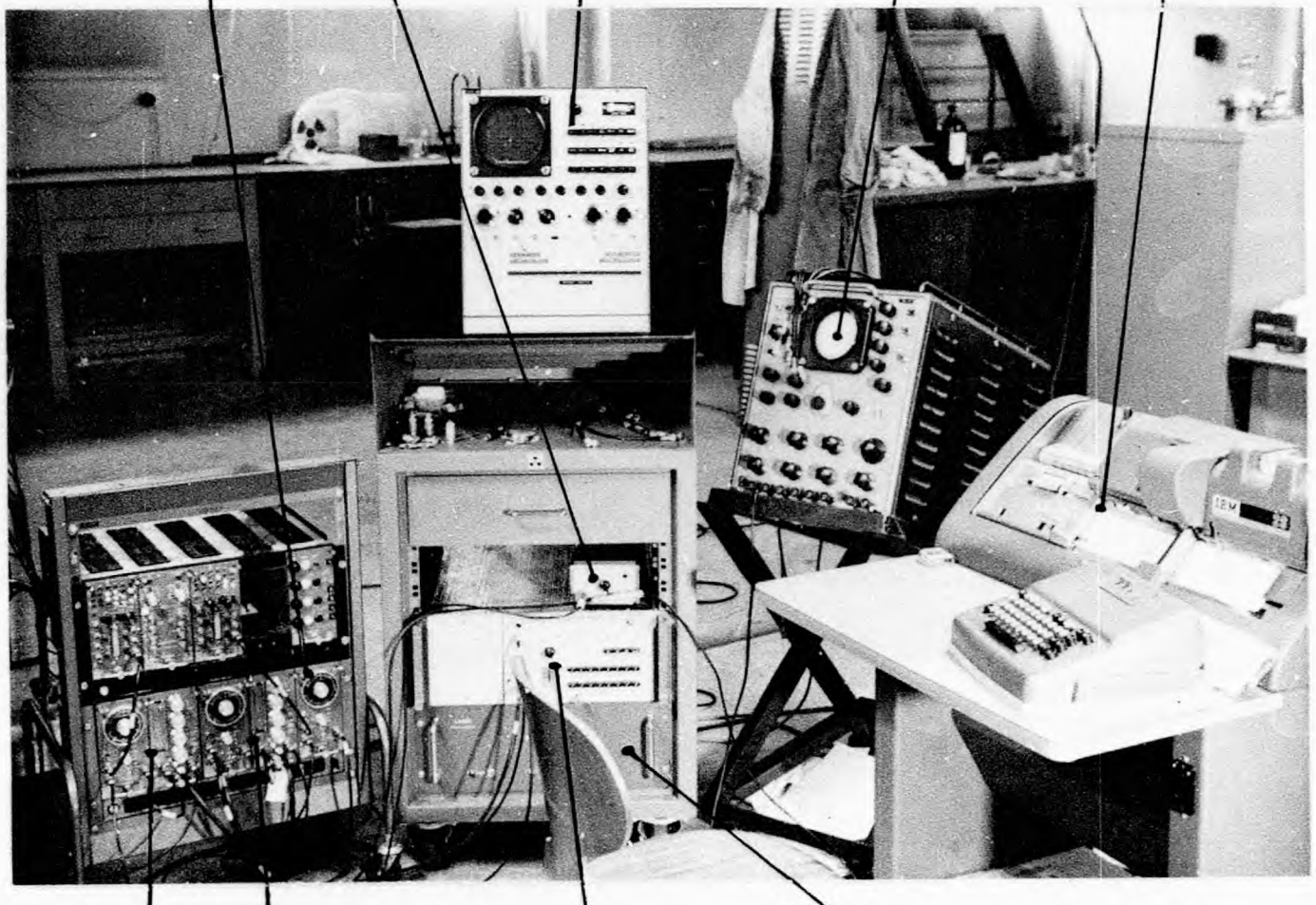

FIG 7.8 COUNTING EQUIPMENT

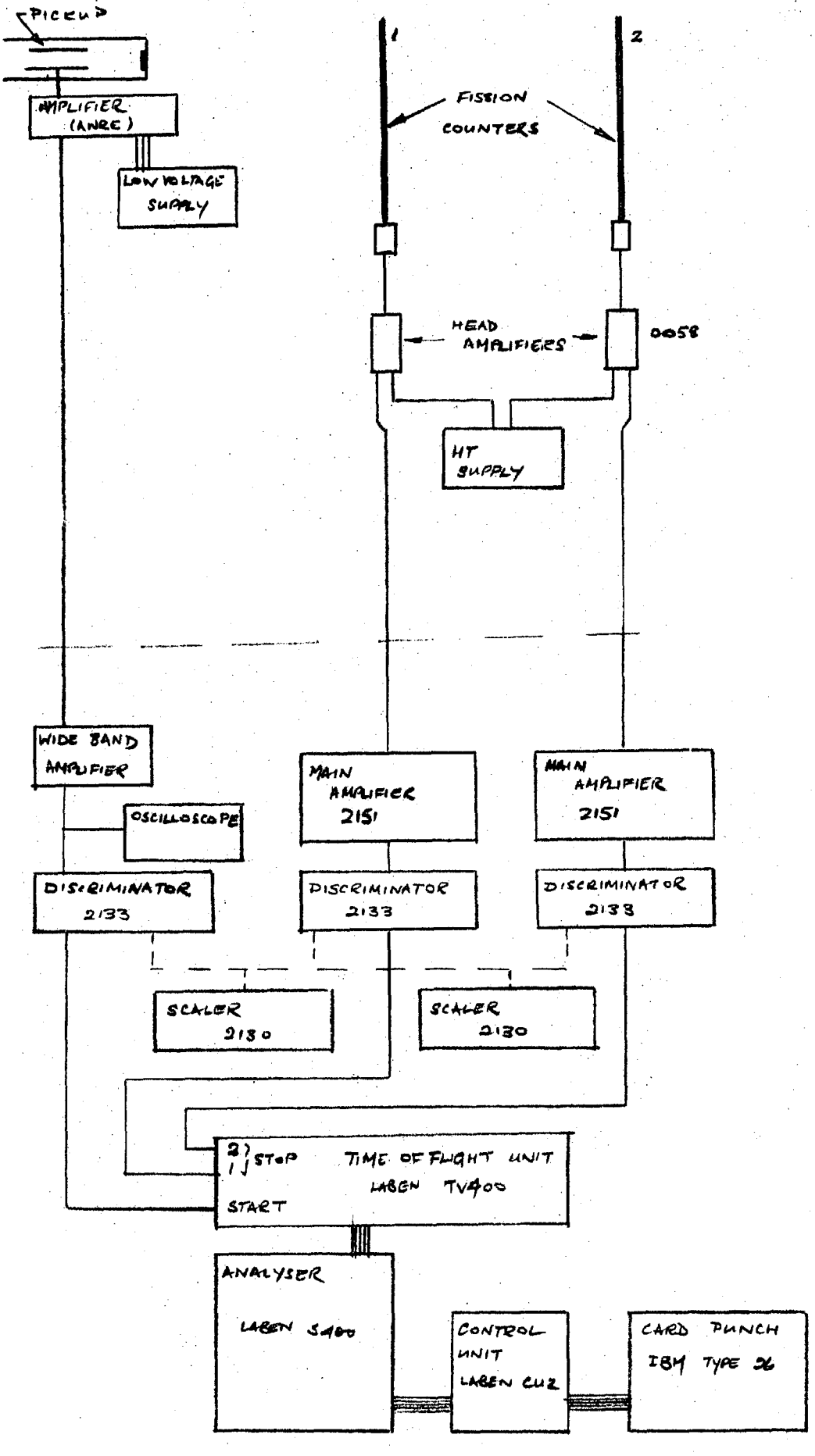

Fig 7.9 BLOCK DIAGRAM OF COUNTING EQUIPMENT

the counters were seperately stored in the multiscale mode. The start pulse was obtained from the pickup in the accelerator flight path mentioned in section 7.1. The results could be output on to cards for input to the computer for analysis of the results. The equipment is shown in Fig. 7.8 and a block diagram is given in Fig. 7.9.

7.3.1 Counters

So that the experiments could be carried out quickly, easing the problem of vessel control and enabling adequate statistics to be achieved, the counters should have good neutron sensitivity but a poor response to gamma rays because of the presence of 2Mev gamma rays from the $H^1(N,\gamma)H^2$ reaction which can cause trouble. The counters would have to operate at temperatures up to 450°C but would not have a pressure loading on them as they would sit in re-entrant tubes in the pressure vessel. The ruggedness and reliability of the counters would also have to be considered as the $\frac{1}{4}$" external diameter of the counters would have to extend for over a 5 ft. extension before it could be increased and a low temperature environment reached. If the counters were fragile and susceptible to damage this would make the handling very difficult.

The choice of the counter was limited because the development of a new counter would be a project in

itself and liable to be expensive. A Boron loaded counter whilst having good neutron sensitivity, reliability and gamma discrimination requires a high voltage supply. At the high temperature conditions this would give insulation breakdown problems and the counters would have to be specially developed and this open ended form of expenditure with a probable cost of about £2000 made this impracticable.

Glass Scintillators give very good neutron sensitivity but they suffer from gamma sensitivity but this could possibly be overcome if a thickness of under 1 mm was used. The pulse height response data was only available up to 250^{o}C but this could have been extended if required. The major problems were the transfer of the light pulses from the scintillator plate 1 x 50 x 5 mm to the photomultiplier and the ruggedness of the counter. The only possible light pipe materials on attenuation grounds were quartz or air. It was considered impossible to obtain an adequate coupling between the 5 mm dia. quartz rod and the top edge of the vertical scintillator plate mainly due to the differing coefficients of thermal expansion. The problems in handling would also be great as the quartz would be liable to crack under its own weight if held horizontal due to the length of the light pipe. The thickness of the sheath was limited and would not stiffen the structure very much. An air light pipe would have relied on the reflection from the walls of

the sheath which would have had too high losses and this together with the difficulty of supporting the scintillator meant the system was not developed further. Other scintillators were unsuitable at the high temperatures so the use of a scintillation counter was ruled out.

Fission counters while satisfying all the other requirements have a low neutron sensitivity. They are readily available for operation at the required temperatures being rugged and have a very low gamma response. It was decided to use these counters and to try and increase the neutron sensitivity as much as possible. The active cathode coating was increased the limit being set by the adherance of the active coating to cathode and the degradation of the pulse height spectrum due to the thickness of the coating. The cathodes are made in cylinders 1" long and slipped into the counter tube.and as the smallest cylinder height envisaged was over 4" it was decided to put four cathodes in parallel increasing the overall sensitivity by a factor of four. By these means the neutron sensitivity of a counter was raised to 1.2×10^{-2} ops/nv.

The electronics were arranged so both counters could be counted at the same time which not only helped the sensitivity but would help the analysis of any harmonics present in the data.

Two counters were obtained from 20th Century Electronics based on their type FC4C $\frac{1}{4}$" nominal diameter high temperature fission counter. The ones obtained however used 4 x 1" cathodes coated with 1000 μ grm/cm^2 U^{235} and had a rigid extension extending 5'2" from the bottom of the active length to the bottom of the connection piece which used a P.T.F.E. insulated socket. The dead length was limited to 3/8" at the bottom of the counter by the physical layout.

7.3.2 Electronic Equipment

Since the counters were positioned a long distance (55 ft.) from the main amplifiers in the Control Room head amplifiers had to be used which were positioned near the counters. The E.H.T. was provided for both counters from a common supply to reduce any variations due to H.T. drift. The cables for the signal and head amplifier supplies from the main amplifiers were laid in ducting and were seperated from the heater controls cables by sheet metal. The signals were fed into two similar sets of Harwell 2000 equipment. The amplifiers were set up to give a maximum pulse height of .8 volts and the differences between the systems was under $\frac{1}{2}$ dB so identical settings were used for each counter. The noise level was low but a discrimator setting of .15 volts was used. The loss in neutron counts at this

condition was small as most pulses were larger but it gave a good safeguard against noise or gamma background pulses. The counters were originally set up using a 1 mcurie Am/Be neutron source and the settings were checked when using the accelerator, no differences being found. The counters were also checked using a Co^{60} gamma source and no increase in the background was observed using a discriminator setting of .15 volts. The output from the discriminators could be fed to a scaler as well as the Time of Flight Unit enabling a check on the count rates to be carried out during an experiment.

The Time of Flight Unit required a start pulse to initiate a counting cycle and the pulses from the counting equipment acted as the stop pulses. The unit had a delay circuit built in which could be varied from 0 μs to 9 x 2^{19}μs and a range of channel widths from $\frac{1}{4}$ μs to 128 μs. It could be arranged to count one or two counters at the same time. The start pulse was obtained from the pickup in the Accelerator flight tube and fed to the Control Room by the amplifier emitter follower as described in the first section of the chapter. This was amplified by a wide band amplifier to give a pulse of about .4 volts which was fed into a discriminatorr. This was done because the maximum output of this amplifier was below that required by the time of flight

unit. Also this enabled any noise to be cut out and the back edge of the pulse to be discriminated against as the wide band pulse differentiated the pulse giving a bipolar pube from a basically square wave this being outlined more fully later when the setting up experiments are described.

The pulses output from the wide band amplifier could be monitored by an oscilloscope giving a visual check on the accelerator operation and gave a good indication of the pulse stability and the accelerator running.

The start pulse started the Time of Flight sequence and when a pulse from the counters was received the time interval was measured and the count stored in the relevant channel in the analyser. The analyser could be controlled by the Time of Flight Unit so it split its memory store into two and enabled the counts from the two counters to be stored seperately. This not only gave an increase in the overall sensitivity of the counting equipment by the use of two counters but enabled any differences in the decay curves to be analysed. This would greatly ease the analysis because of the harmonics present due to the counter positions that had to be used in the experiment. The results could be output to a typewriter or normally punched onto cards directly using

a control unit linked to an IBM card punch. The format used was suitable so the cards could be fed as data for the programme used in the analysis.

Modifications were required to the analyser as it was found initially that the Time of Flight Unit and the Card Punch Control could not be connected up at the same time and the normal operation of the analyser was stopped. An extra socket and the suitable modifications were carried out and the system checked out.

8. EXPERIMENTS

As a check on the counting equipment and as an independent measurement a series of experiments using the 8" cylinder were carried out. These were not done in the pressure vessel but used a similar but simpler set up. A check was first made on the probable effect of the vessel wall on the neutron flux in the water and this was done at an early stage in the project as a check on the project's feasability.

8.1 VESSEL WALL EFFECT

As a check on the probable effect of the 3" thick vessel wall on the neutron flux a steady source experiment was carried out to check the theoretical calculations predicting an attenuation in the flux by a factor of over two. The experimental set up is shown diagrammatically in Fig. 8.1 and used a 1mCurie Am/Be neutron source in a slab representation of the actual situation. The source gave a similar neutron spectrum as the target used in pulsed experiments.

The fluxes were measured for various distances from the water boundary with a 1" BF_3 counter using standard equipment. The counts were corrected for background, dead time and Cadmium counts and had at least 1% statistical accuracy. The ratio of the fluxes with and without the slab is shown in Fig. 8.1 in which it can be

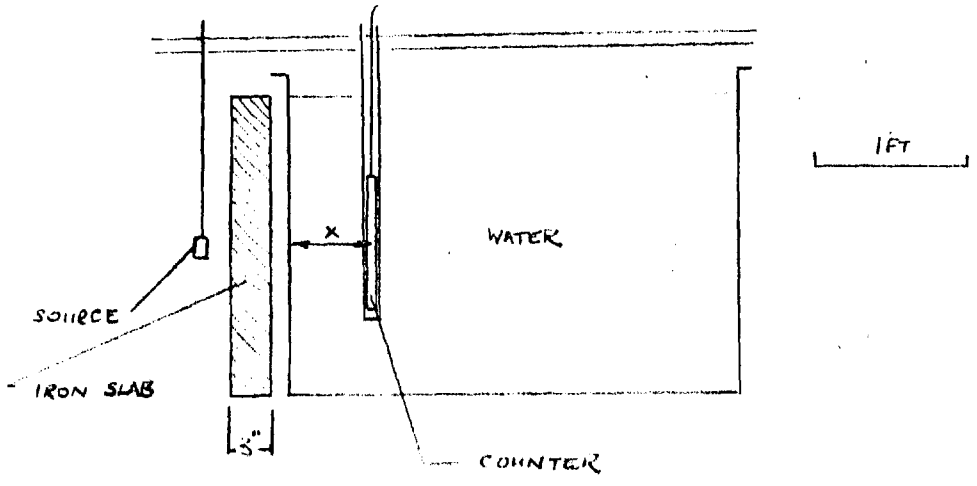

EXPERIMENTAL SETUP

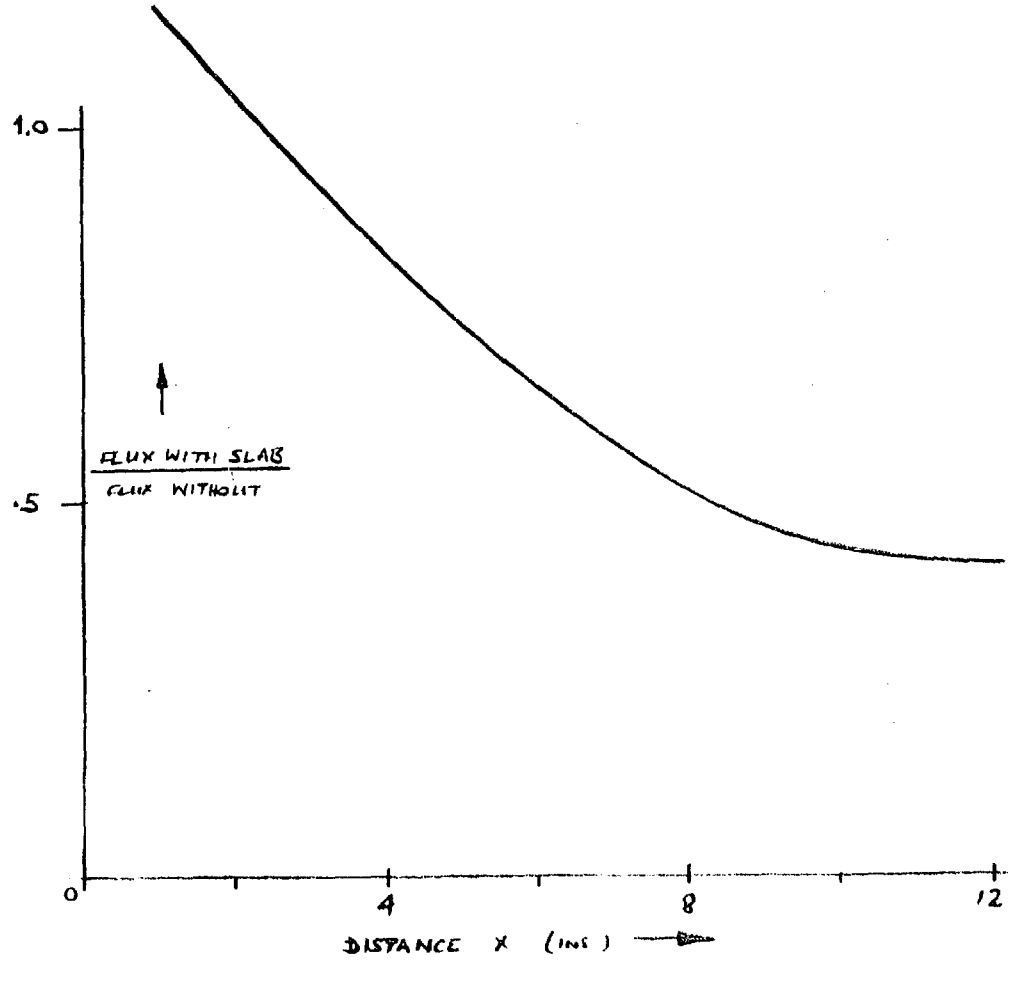

FIG 8.1 VESSEL WALL EFFECT EXPERIMENT

seen that the ratio tends to be about 40% away from the boundary but near it the ratio exceeds 1. This was due to the reduction of the energy of the neutrons undergoing only scattering collisions in the steel and gave the neutrons reaching the water a lower average energy than is the case without the presence of the slab. This experiment confirmed the predicted attenuation effect of the vessel wall but the near wall effect would help when using the smaller cylinders to reduce the required experimental time.

8.2 PULSE PICKUP TESTING

The start pulse was obtained from the pickup unit in the flight tube of the accelerator and was the only part of the counting equipment that could not be set up without the use of the accelerator. The preliminary tests were carried out using a proton beam and the checking was carried out in the experimental area as there was no radiation hazard. A bipolar pulse was obtained from the wide band amplifier as it differentiated the pulse output from the pickup unit as it had a very short time constant and the relationship between the output pulse and the neutron pulse is shown in Fig. 8.3.

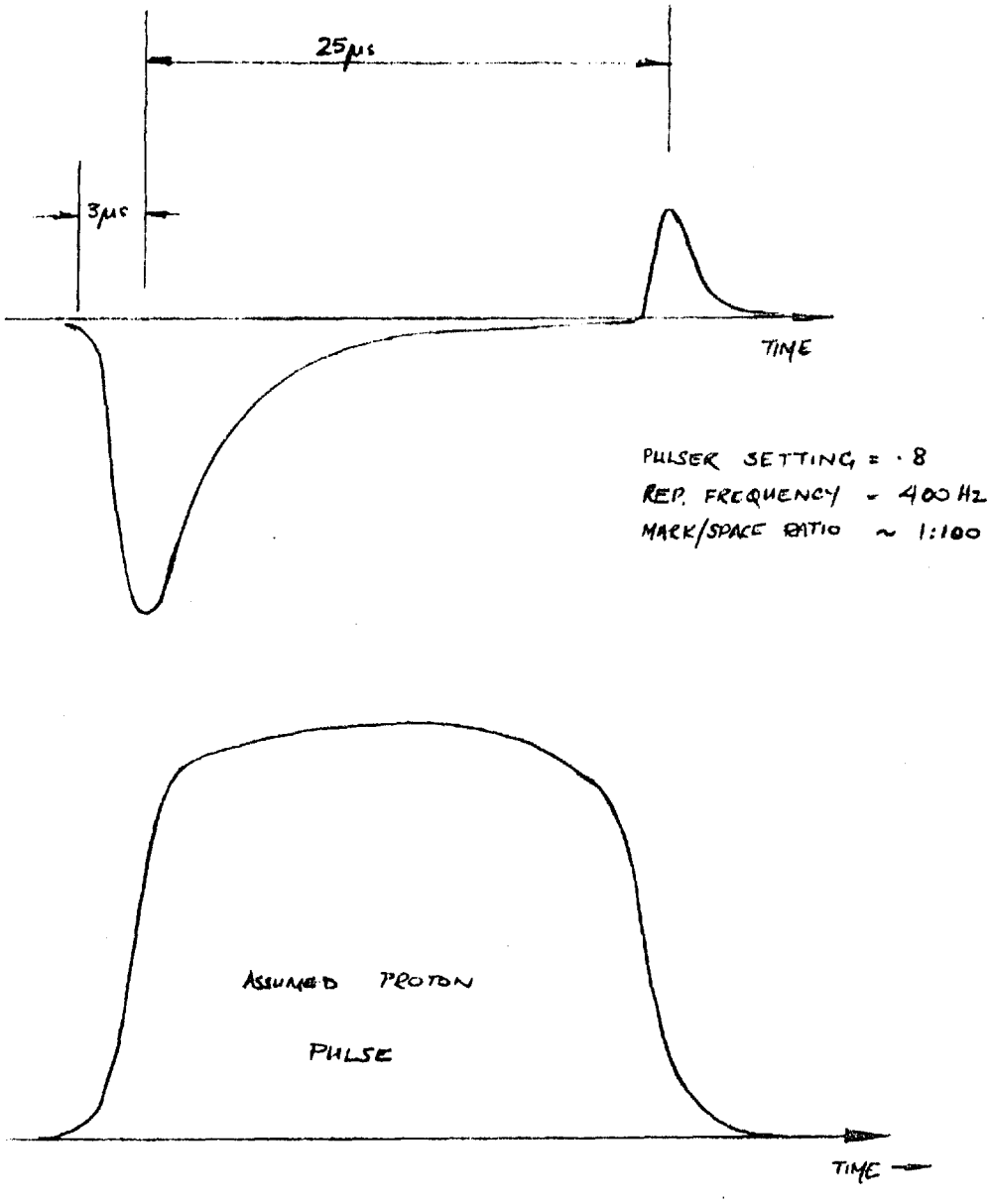

FIG 8.3 OUTPUT FROM PULSE PICKUP

The rise time of the output pulse was due to the rise time of the ion pulse in the flight tube. The jitter on this and the second part of the pulse was very small and not observable. This meant that the jitter on the start pulse would have a negligible effect on the measured decay curves. The repetition rate could be varied from a control on the Accelerator control panel and the variation of this with the pulser setting is given in Table 8.1.

Table 8.1 Pulser Setting v. Repetition Rate

Pulser Setting	Repetition Rate
.4	220 pulses/sec
.6	300 "
.8	440 "

These values are not accurately reproduceable because the length of the controlling string depended on its temperature and there was backlash and dead spots in the indication unit. The mark/space ratio was roughly 1/100.

Similar results were obtained using deuteron ions and a 55 ft. cable between the amplifiers which was run in the same ducting as the counter cables. The low gain setting of 20 dB was used on the wide band amplifier with a X5 attenuation in the input for most experiments but the settings were checked before each run as the

pulse height depended on the ion beam strength.

8.3 DECAY EXPERIMENTS

The arrangement for the decay experiments carried out is shown in Fig. 8.2 in which the 8" cylinder was placed in a tank 35" x 25½" x 30". The cylinder arrangement in the tank is shown in Fig. 7.4 in which the Cadmium sheets have been removed and the piston is set for a 12" high cylinder and the tubes represent the re-entrant tubes to be used in the pressure vessel experiments in which the counters will be placed. The tank was made of polythene supported in a special frame and was covered with Cadmium sheets to reduce the room return background. The water was de-mineralised and the tank was filled till the target was at the mid height of the water.

The cylinder was supported from a cross frame similar in design to the one welded to the underside of the head but the movement was modified so a direct access type movement was used without the locking device. Chocks were used were used between the cross frame and the general support structure so the cylinder was at the correct height relative to the flight tube and target. The counters were

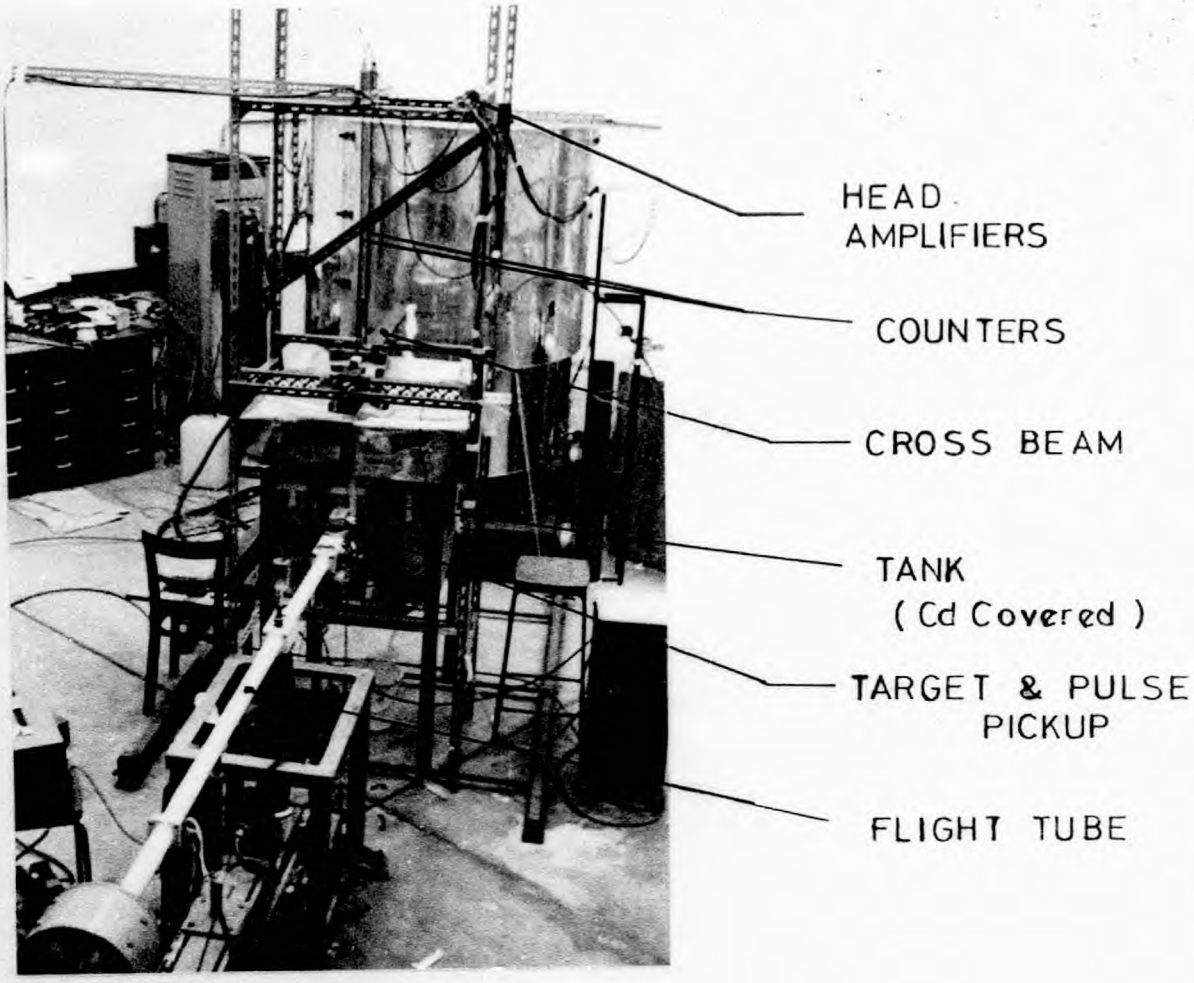

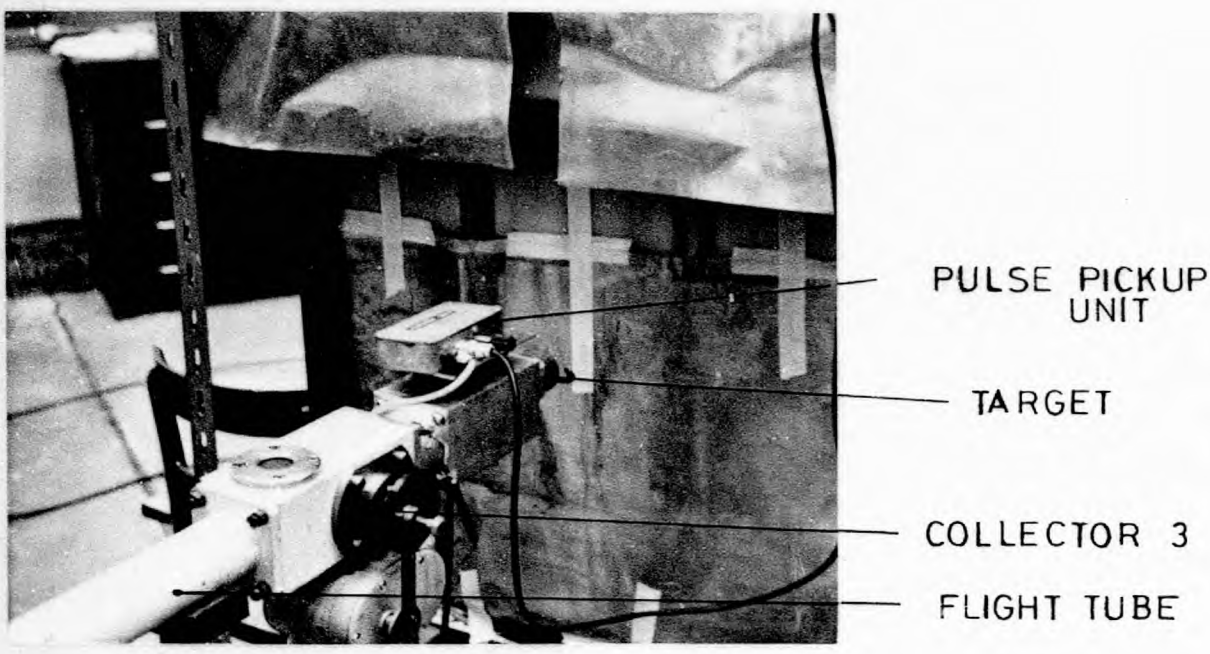

FIG 8.2 EXPERIMENTAL ARRANGEMENT

supported from the dexion structure which carried the head amplifiers close to them as can be seen in Fig. 8.2 and the signal cables were led to the control room in the ducting provided. The counter height was adjusted until the active region was symmetrically placed about the target. The in-line alignment of the equipment was done by eye using the cross frame and the flight tube.

A series of runs were carried out for various cylinder heights and also checks done on the effects of the pockets on the measured decays. The experiments were all performed in a similar fashion and the counting equipment settings were kept constant. The setting up of this equipment was described in Chapter 7 and the various settings are given in Table 8.2.

Table 8.2 Counter Settings

Counter HT		275v
Head Amplifiers	time constant	300ns
Main Amplifiers	Gain	52dB
	time constants	.5μs
Discriminators	Threshold	.15v
	Upper Limit	0.9v
Time of Flight Unit	Delay	0
	Channel Width	4μs

The same settings were used for both counters and were fed from a common H.T. supply. As these experiments were the first runs to use the accelerator the whole decay curve was counted but for subsequent work only the relevant part should be measured which would allow an improvement in the statistical accuracy on the required part of the decay curve. The counting of the whole curve did enable a check on the peak and the harmonic decay as well as the background level and was used to check if there was any apparent time variation of the background.

Runs varied from about five hours initially to under two hours depending on the accelerator behaviour. These took longer than will be required by latter experiments when the system has been optimised mainly by the points noted in Chapter 7. These effects caused a reduction in the operating voltage to $1\frac{3}{4}$ Mev and was mainly attributed to the instability in the bending magnet current. The leakage current down the belt in the later experiments was very high and the belt will require replacing. It is an old belt and has been often run in the open during setting up. This reduction in operating voltage had a very important effect on the neutron yield obtainable as a 10% increase in the deuteron energy, at this voltage range, increases the neutron yield by 50% (Olive et al 1962) and allows a significant reduction in the running time. It should also be noted that the surface condition of the target is of paramount importance for this reason.

The flight tube and the focussing magnets were not properly aligned and prevented all the beam reaching the target and this caused further degradation of the beam focus as the misaligned beam reduced the vacuum in the flight tube by the outgassing caused where it hit the tube. It is felt that the correction of these factors and the general improvement in the accelerator running with use will allow the yield to be increased by at least a factor of four reducing the counting times required.

8.3.1 Backgrounds

The sources of background have been mentioned previously (Chapter 2) and only the precautions taken to avoid them will be outlined. The tank as has been mentioned was covered with .030" thick Cadmium Sheet. The isolation of the cylinder from the rest of the tank can only be shown in an analysis of the decay curve. The backgrounds normally inherent in a counting experiment were reduced in the setting up procedure but a reduction in the time for a run due to an increased neutron yield would help especially with the interference type backgrounds.

One form of this was found during the experiments and was characterised by a sudden burst of counts which lasted for a few seconds. This was not thought to

be due to the malfunction of the accelerator but due to the use of some equipment in the nearby workshops as it only occured during normal College working hours. The prime suspects are the cranes and the arc welding equipment but the actual source has not been identified and the method of pickup and its removal will have to be investigated further. In these experiments this was not a problem as the run could be repeated but could be annoying for the high temperature experiments.

To check the backgrounds the decay curves were mensured over a longer time interval than is usually required and was found to be reasonably constant but its reduction to lower levels would greatly assist in the analysis as the fitting is very dependent on the background not blanketing the fundamental mode part of the decay after the harmonics had decayed to a sufficiently small level and was very important in these experiments with the in-line counter positions.

8.3.2 Buckling Errors

The errors in the bucklings were mainly due to innaccuracies and irregularities in the piston and base plate surfaces. Due to the use of a spigot fitting into the slots in the cross frame the errors in the relative piston heights were very small and estimated to be less than .002". To this had to be added the uncertainty in

the absolute height of the piston from the datum level. A major effect was that the base plate was not perpendicular in the cylinder and from the out of verticality and height of the piston when resting on the base plate the errors and datum distances were chosen as shown in Fig. 8.4. To this source of error was added the relative height error and the height of the cylinder was given by

$$h_{actual} = h_{nom} + .029" \pm .022" \qquad 8.1$$

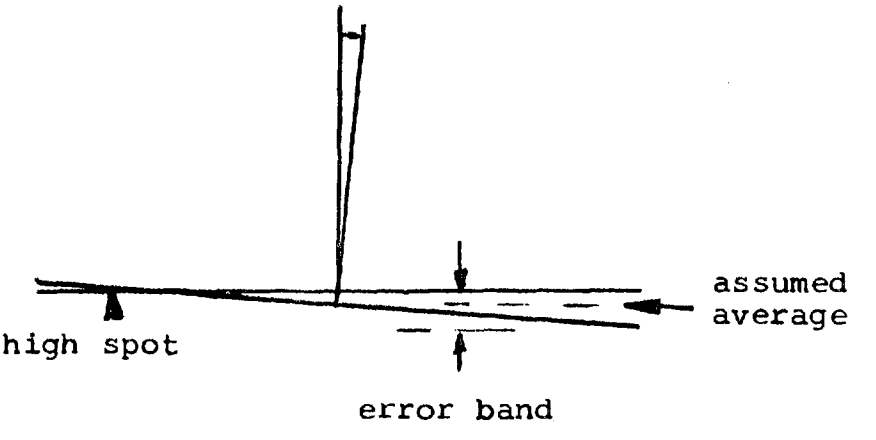

8.4 PISTON HEIGHT ERRORS
(exaggerated)

The diameter of the cylinder was measured with an internal micrometer and the errors taken as the range of values about the mean diameter of 7.190" which gave $\pm$ .015". A complete dimensional survey using jigs to measure the dimensions would enable the average values to be obtained more accurately and the errors to be

reduced due to greater confidence that could be placed in the results. The sizes used gave bucklings and errors in the range .1310 $\pm$ .009 cm^{-2} for the 4½" high cylinder to .07460 $\pm$ .0003 cm^{-2} for the 12" high cylinders using an extrapolation distance of .34 cms.

8.3.3 Results

The experiments were carried out and the complete decay curves obtained for various piston heights of the 8" diameter cylinder. To check the repeatability of the apparatus two identical experiments were carried out, seven days apart, using a cylinder height of 12". Also the effect of the water in the pockets on the decay was checked by blanking off with Cadmium Sheet the counter position furthest from the target. The water temperature for the runs was 23°C and the variations were under 1°C and neglected.

In these experiments the counters were housed in perspex tubes $\frac{3}{8}$" dia. blanked off at the bottom. Only one counter was used in these experiments but the working of the system with two counters was checked. The use of only one counter greatly increased the difficulty in analysing the results as well as the low statistical accuracy of the results obtained.

The first part of the analysis was carried out to calculate the backgrounds. These were easily found because the whole decay curve had been counted and no time dependence of the background could be seen. The background was subtracted from the counts before any analysis of the decay curves was carried out.

To ease the calculations the counts in each group of four channels were summed together giving an increase in the statistical accuracy of each point but fewer points.

To calculate the harmonic effects the fundamental decay constant was predicted for each cylinder size and this used to calculate the harmonic. In the first place this harmonic was taken to contribute 5% of the total counts at a certain point on the curve, normally about 500 μsec after the start pulse. Analysis showed that 10% was a better figure and this value was used. The predicted fundamental decay was subtracted from the total counts and the resulting harmonic decays plotted out. The constants of the decay curve were calculated directly from the graphs and used in the calculation of the fundamental. If the fundamental calculated was in agreement with that used in the prediction of the harmonic then the method of analysis was consistent. Fig. 8.5 shows the points used to calculate the harmonics for two of the runs.

Using the values obtained representing the harmonic content the fundamental decay constant was calculated A single exponential was fitted to the resulting points. This was carried out by the least square programme DECAN and the results obtained are shown in Table 8.3 in which the bucklings are those obtained using an extrapolation distance of .34 cms. Two of the decay curves are shown in Fig. 8.6 and 8.7 with the harmonic and background levels shown.

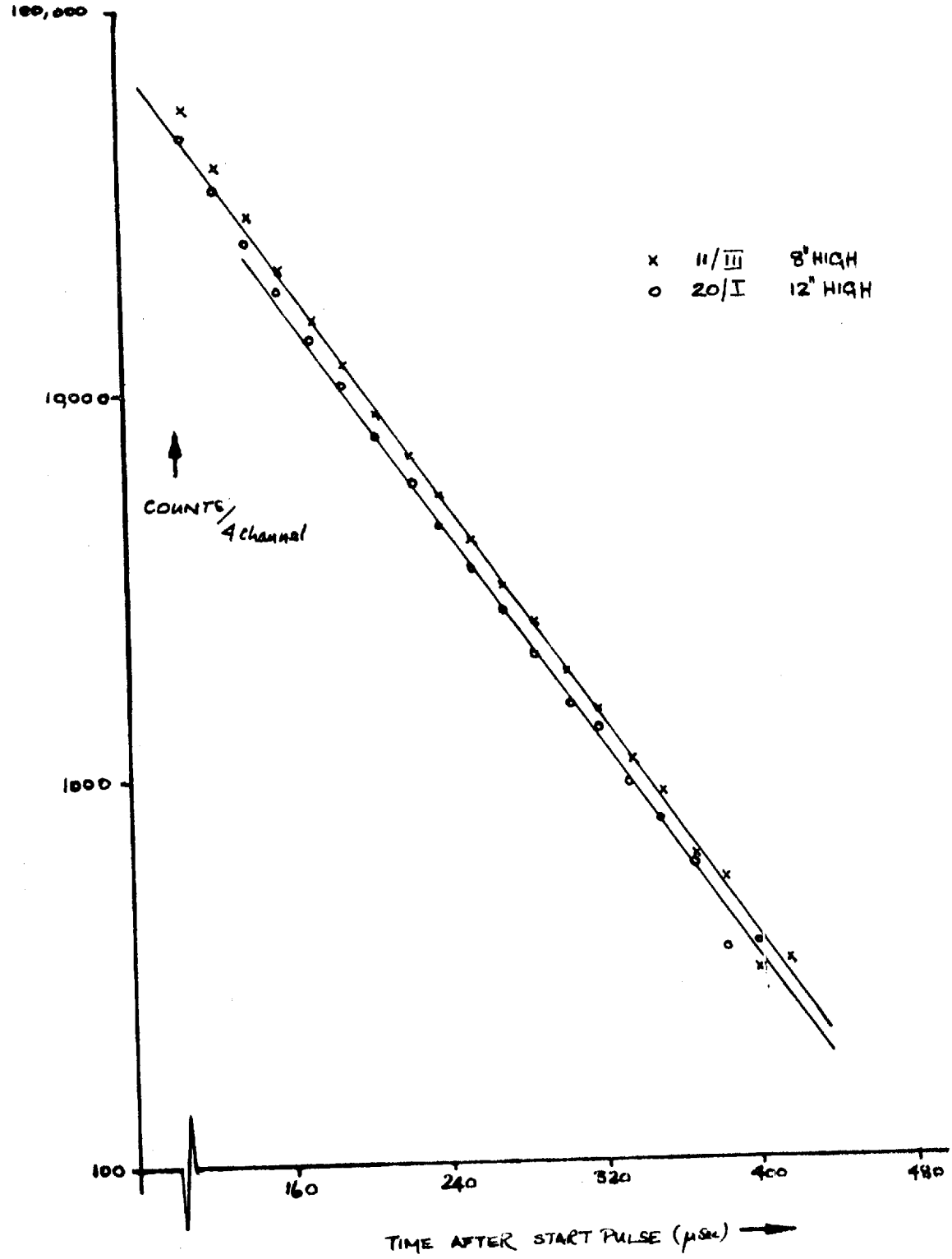

Fig 8.5 HARMONIC ANALYSIS

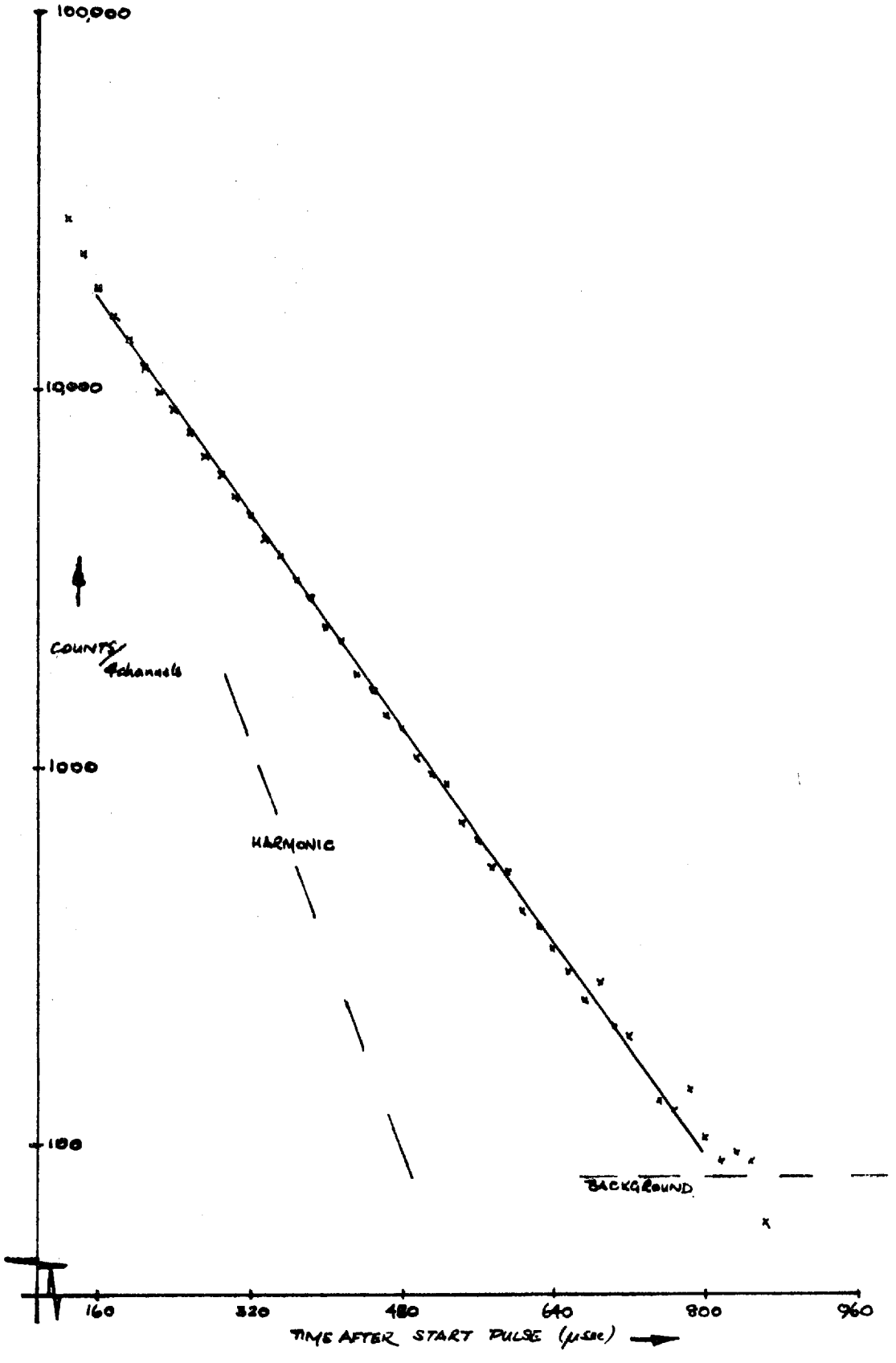

FIG 8.6 FUNDEMENTAL DECAY ANALYSIS FOR EXPERIMENT II/III (8° HIGH)

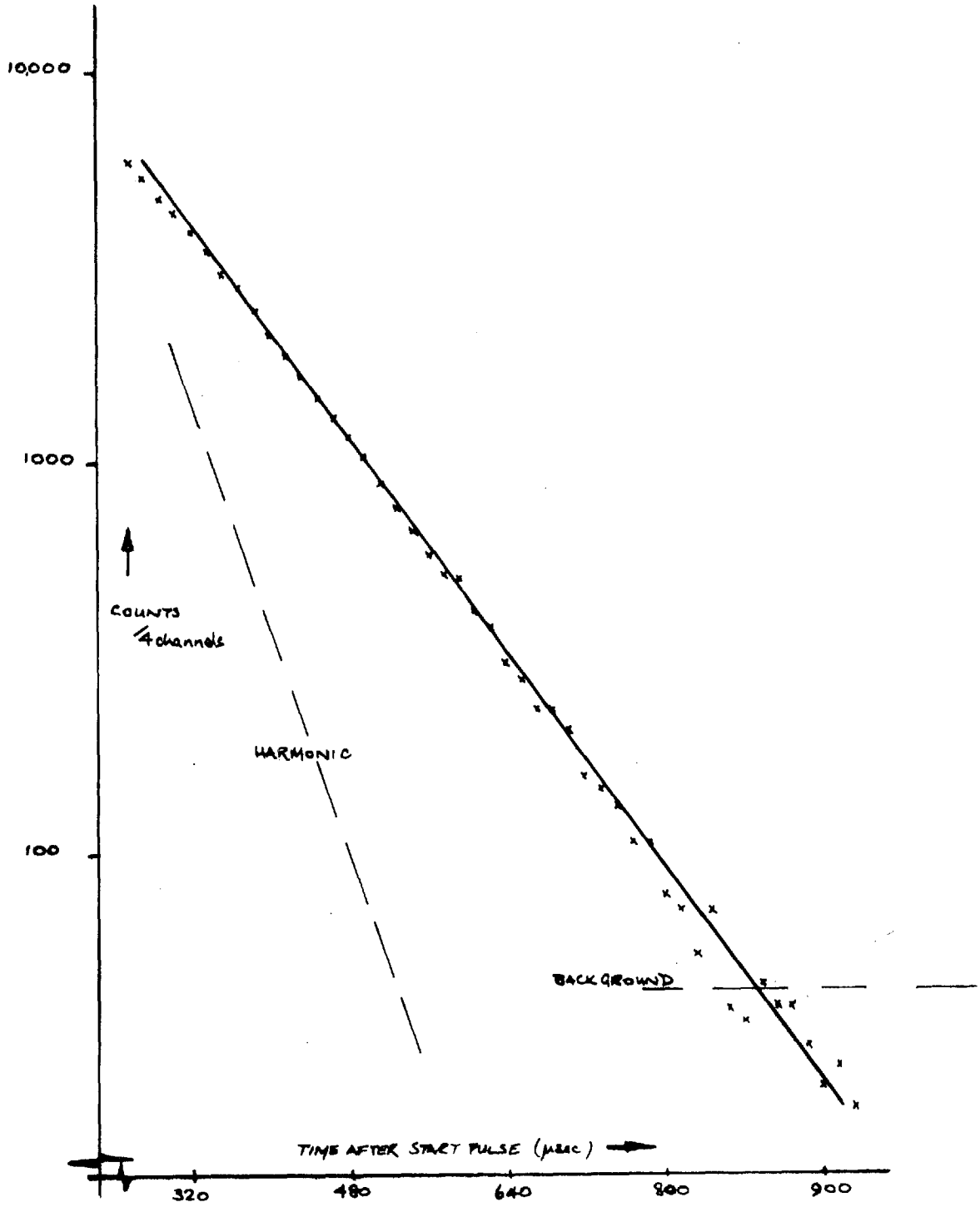

FIG 8.7 FUNDAMENTAL DECAY ANALYSIS FOR EXPERIMENT 20/I (12" HIGH)

Table 8.3 Decay Constants

Run N	Cylinder Height(ins)	Buckling cm^{-2}	Decay constant sec^{-1}
10/III	12"	.07460	7694 ± 63
11/I	6"	.1031	8746 ± 70
11/II	4.5"	.1310	9905 ± 128
11/III	8"	.08671	8033 ± 66
11/IV	5"	.1190	9437 ± 100
19/I	12"	.07460	7635 ± 70
20/I*	12"	.07460	7826 ± 60
26/I	12"	.07460	7712 ± 95

*Run with Cd in other counter position

The errors on the decays are the standard deviations of the fitting but the results were dependent on the region over which the fitting was done. The fittings were carried out over the reasonably constant middle region where any errors in the predicted harmonic or the background would have less effect.

The results were fitted to a linear equation as the predicted effect of the quadratic term was less than the errors on the points but the points were corrected for an assumed value of C in eqn. 1.1 of -4000 cm^4/sec. The points and the fitted curves are shown in Fig. 8.8. The fitted value of 4893 ± 170 sec^{-1} is in good agreement with the predicted value of 4849 using a hydrogen absorption of .330 barns. The calculated Diffusion Constant is given in Table 8.4 with some other experimental values.

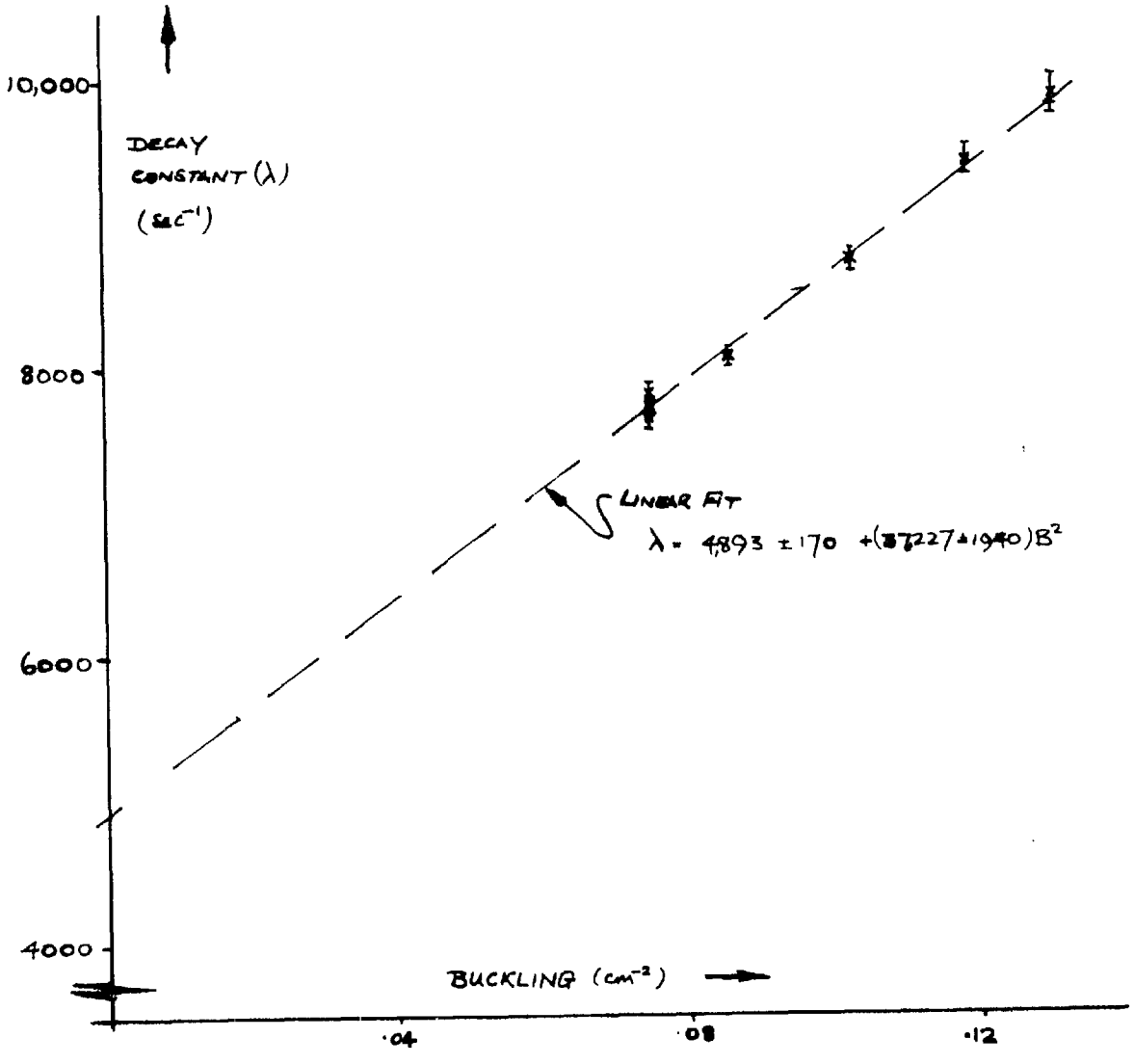

FIG 8.8 EXPERIMENTAL DECAY CONSTANTS v BUCKLING

(corrected for diffusion cooling)

Table 8.4 Experimental Values 23°C

Ref		Do cm^2/sec	C cm^4/sec
Lopez and Beyster	(1962)	36950 ± 400	4950 ± 805
Kulche	(1960)	35530 ± 700	4200 ± 800
Gon	(1965)	36306 ± 650	3700 ± 620
Elkert	(1968)	36870 ± 390	4530 ± 400
This work		37227 ± 1940	4000 (assumed)

(if necessary corrected using $\frac{dDo}{dT} = 130\ cm^2/sec^{\circ}C$)

These results show that the method used gives reasonable agreement with previous results considering the limited buckling range used and the problems of analysis. The differences between the runs without and with the Cadmium in the counter slot (20 I) is just within the error bands but this 2% difference could be significant in a more accurate analysis. Analysis without this point increases D_o by 3½% mainly due to the low decay for the 8" high cylinder.

The experiment has shown that the experimental setup is suitable for the proposed investigation and has proved the method of analysis for the counters in-line positions though this should be considerably eased when the modifications outlined previously are incorporated.

9. RECOMMENDATIONS AND CONCLUSIONS

A method has been developed for analysing the pulsed neutron method using the Discrete Ordinate Method and this has been compared with the results obtained by other workers in Chapter 4. The first topic to be covered in a future study should be the analysis for any geometric effects on the calculated decay constants. The work should then be extended to including anisotropy explicitly in the calculation.

The pressure vessel and its associated equipment was designed and installed as far as was possible. Most of the modifications are minor and have already been mentioned in the thesis. The experimental setup has also been checked and the results obtained are given in the previous chapter. The first experimental requirement after testing the plant over its full temperature and pressure range would be the clarification of the data at $300^{o}C$. This should be followed by an extension of the experiments to the supercritical region.

REFERENCES

ARDENTE AND GALLUS (1968) Nukleonik, 11, 251

ASKEW AND BRISSENDON (1963) AEEW-R-161

BACH (1961) Neutron Physics ed. Yeater p. 195 Academic Press

BECKHURTS (1962) BNL 719, III, RE 1

(1965) Pulsed Neutron Research Karlsruhe IAEA (SM-62/1) p.3

BESANT AND GRANT (1966) Proc. Roy. Soc, 289, 342

BEYSTER (1968) Nucl. Sci. Engng, 31, 254

BOWEN (1967) Ph.D., University of Birmingham

CARLSON (1958) ICPUAE Geneva, 1958, 16, 535

(1963) Methods in Computational Physics, 1, 1 Academic Press

CARLSON AND LATHROP (1965) L.A. 3186

CLENDENIN (1964) Nucl. Sci. Engng, 18, 351

COKINOS (1966) Advances in Nucl. Sci. and Tech, 3, 1 Academic Press

EGLESTAFF (1965) Thermal Neutron Scattering, Academic Press

EGLESTAFF AND SCHOFIELD (1962) Nucl. Sci. Engng, 12, 260

ELKERT (1968) Nukleonik, 11, 159

FEDERIGHI AND GOLDMAN (1962) KAPL 2225

GELBARD AND DAVIS (1962) Nucl. Sci. Engng, 13, 237

GODDARD (1969) Ph.D., University of London

GODDARD AND BESANT (1965) Unpublished

GRANT (1966) Elementary Reactor Physics, Pergamon Press

GON (1965) Trans. Am. Nucl. Soc, 8, 274

HALL AND SCOTT (1962) Proc. Phys. Soc, 79, 257

HAYWOOD (1964) AERE R-4484

(1967) J. Nucl. Energy, 21, 249

HONECK (1962) BNL 719, IV, 1186

JOHNSON (1966) Ph.D., University of London

KOPPEL AND YOUNG (1964) Nucl. Sci. Engng, 19, 412

MCADAMS (1954) Heat Transmission, 3rd Ed, Mcgraw Hill

MACDOUGALL (1963) AEEW - M - 318

NELKIN (1960a) Nucl. Sci. Engng, 7, 210
(1960b) Phys. Rev, 119, 741

LOPEZ AND BEYSTER (1962) Nucl. Sci. Engng, 12, 190

OLIVE ET AL (1962) AERE R - 3920

RAINEY (1969a) DIST)
(1969b) TRIXSE(4)) Unpublished
(1969c) TRAND)

REITER AND JUREN (1961) J. Nucl. Energy, 14, 18

ROCKEY AND SKOLNIK (1960) Nucl. Sci. Engng, 8, 62

RUSSELL, NEILL AND BROWN (1966) GA 7581

VAN HOVE (1954) Phys. Rev, 95, 249

WIGNER AND WILKINS (1944) AECD 2275

WRIGHT AND FROST (1956) KAPL - M - WBW - 2

APPENDIX 1

MAIN EQUIPMENT PARAMETERS

PRESSURE VESSEL

Working Temperature		450°C (842°F)
Working Pressure		3500 psia
Design Pressure		3850 psia
Test Pressure	60°F min.	5500 psia
Internal Diameter		36 ins.
Internal Height		$43\frac{1}{4}$ ins.
Overall Diameter		53 ins.
Basic Shell Thickness	Low Alloy Steel	3 ins.
Head Thickness	Low Alloy Steel	$10\frac{3}{8}$ ins.
Bottom Thickness	Semi ellipsoidal	3 ins.
Internal Cladding	Type 304 Stainless Steel	$\frac{1}{8}$ in.(min)
Nozzles and Internals	Stainless Steel	

Main Closure

Seal	Hollow Silver Plated Stainless Steel 'O' ring	$\frac{1}{4}$" dia x .0258" wall x $39\frac{3}{4}$" dia.
Main Studs	20 on 46" P.C.D.	$3\frac{1}{2}$ in dia. 8 tpi
Extensions	Test	.020" / .021"
	Working	.018" / .019"
Tensioning	Pilgrim Nut with Oil Pump	

$2\frac{3}{4}$" bore Nozzles	4 off	$8\frac{1}{2}$" O.D.
Seal	As main seal	1/8"dia x .010"wall x $3\frac{7}{8}$" dia
Studs	12 on $6\frac{3}{4}$" P.C.D.	$\frac{3}{4}$" dia 10 tpi
Extension	Torque Wrench	.007"/.008"

1" bore Nozzles	7 off	$6\frac{1}{8}$" O.D.
Seal	Solid Stainless Steel	R18 to BS 1560
Stud	8 on $4\frac{1}{2}$" P.C.D.	3" dia 10tpi
Extension	Torque Wrench	.005"/.006"
Pressure Connection Flanges	.840"O.D. x.187" Wall	2 off
Thermocouple Flange	6T/C on $\frac{7}{8}$" P.C.D.	1 off
Thermocouples	Chromel/alumel Stainless Steel	1 mm O.D.
	Sheathed with bushing	5 mm O.D.
Counter Tubes Flanges	.540"O.D. x .119"wall	2 off

Lifting Lugs (for head only)

	Carbon Steel	3 off

Vessel Support

Legs	Carbon Steel	3 at 120°
Thermal Barrier	Sindanyo	1" thick
Bearing	INA Type FF3525	4 per leg
Bearing Pads	Carbon Steel	Hardened 60 Rc
Slewing Ring	Roballo Type 100-1400	$43\frac{1}{2}$" I.D.

BASE FRAME AND RAILS

Overall Dimensions		116½" x 55½"
Main Beams	R.S.J.	8" x 6" x 35lb
Secondary Beams	R.S.J.	6" x 3½" x 11lb
Wheel Centres		63½"
Wheel	Solid Steel Dry Bearing	10"dia flanged
Rail	Bull Head	45lb
Track	Tubular Tie Bars	4' 11"
Radius of Curvature		25ft min

HEATERS

Internal

Flanges	2 elements flange	4
Heater Rating (element)		1¾ kw
Form		Immersion Type Inconel Sheathed
Supply		2 - 30 Amp Single Phase

External

Elements		15
Rating (element)		2 kw
Form		Rod Inconel Sheathed
Supply		60 Amp 3 phase 4 wire

THERMAL NEUTRON CYLINDERS

Material	30% B_4C in Al	$\frac{1}{8}$" plate
Cladding	EN58B	22 gauge Sheet
Welding	Argon Arc	Parent filler rod
Fixtures	EN58B or equivalent	

DUMP TANK

Size			4ft x 4ft x 4ft
Material	Sheet	EN58B	14 Gauge
	Top Rim	EN58B	$1\frac{1}{2}$ x $1\frac{1}{2}$ x $\frac{1}{4}$ Angle
	Bracing Structure	Mild Steel	"